

**An investigation of the sensory and motor innervation of extraocular  
muscles in monkey and rat with combined tract-tracing and  
immunofluorescence methods:  
Evidence for a dual motor innervation as common concept in mammals.**

Dissertation

zur Erlangung des Grades eines Doktors

der Naturwissenschaften

der Fakultät für Biologie

der Ludwig-Maximilians-Universität München

vorgelegt von

**Andreas Christian Eberhorn**

aus Garmisch-Partenkirchen

17. März 2005

1. Gutachter: PD Dr. Anja Horn-Bochtler

2. Gutachter: Prof. Dr. Gerd Schuller

Tag der mündlichen Prüfung: 19.07.2005

*to Nicola and Luis*

## Table of contents

<b>ABSTRACT .....</b>	<b>2</b>
<b>ZUSAMMENFASSUNG .....</b>	<b>4</b>
<b>ABBREVIATIONS .....</b>	<b>7</b>
<b>INTRODUCTION .....</b>	<b>8</b>
<b>Extraocular muscles (EOM).....</b>	<b>8</b>
<i>Participation of each EOM in eye movement .....</i>	<i>9</i>
<i>Muscle pulleys .....</i>	<i>10</i>
<i>Functional types of eye movements .....</i>	<i>11</i>
<i>Fine anatomy of EOMs .....</i>	<i>12</i>
<i>Characterization of the six EOM fibre types .....</i>	<i>14</i>
<i>Molecular properties of EOM .....</i>	<i>15</i>
<b>Motor innervation of eye muscles .....</b>	<b>16</b>
<b>Sensory innervation of EOM.....</b>	<b>17</b>
<i>Muscle spindles, Golgi tendon organs, and palisade endings.....</i>	<i>17</i>
<i>Palisade endings and their role in proprioception.....</i>	<i>18</i>
<b>Motoneurons of eye muscles.....</b>	<b>20</b>
<i>Anatomy of motoneurons .....</i>	<i>20</i>
<i>A revision of the organization of the oculomotor nuclei .....</i>	<i>24</i>
<b>The dual motor control of EOM and its possible role in proprioception .....</b>	<b>25</b>
<b>AIMS OF THIS PHD-PROJECT .....</b>	<b>27</b>
<b>RESULTS.....</b>	<b>29</b>
<b>Paper 1: Motoneurons of multiply-innervated muscle fibres in extraocular muscles have different histochemical properties than motoneurons of singly-innervated muscle fibres.....</b>	<b>29</b>
<b>Paper 2: Identification of MIF and SIF motoneurons innervating the extraocular muscles in the rat.....</b>	<b>67</b>
<b>Paper 3: Palisade endings in extraocular eye muscles revealed by SNAP-25 immunoreactivity .....</b>	<b>102</b>
<b>DISCUSSION .....</b>	<b>112</b>
<b>FINAL CONSIDERATIONS .....</b>	<b>118</b>
<b>LITERATURE CITED.....</b>	<b>119</b>
<b>ACKNOWLEDGEMENTS.....</b>	<b>129</b>
<b>CURRICULUM VITAE .....</b>	<b>130</b>

## **Abstract**

The oculomotor system is one of the best studied motor systems. Afferents from a variety of premotor areas converge on the motoneurons in the three oculomotor nuclei to produce the different types of eye movements. All oculomotor motoneurons participate in all types of eye movements, and it was generally accepted, that these motoneurons form a relative homogenous group which provides the final common pathway for extraocular muscle (EOM)-motor innervation. The EOM in mammals, the effector organs of the oculomotor system, are fundamentally different from skeletal muscle. They have two functionally different layers, global and orbital layer, and are composed of two major muscle fibre classes, singly-innervated (SIF) and multiply innervated fibres (MIF). Previous studies in monkey revealed that SIF and MIF motoneurons are anatomically separated and have different premotor inputs, which support the idea of a dual motor innervation of EOM rather than a final common pathway from motoneuron to EOM. Up to date, neither motoneuron type has been further characterized nor has any study proven their presence in other species to support the hypothesis of the dual motor innervation as a common concept in mammals. The functional implication of this system remains speculative, though a role of MIFs together with their motoneurons in a sensory feedback system controlling the EOMs is quite possible and heavily debated. However, the lack of a common proprioceptor in eye muscles does not support this theory.

In monkeys SIF and MIF motoneurons of extraocular muscles were identified by tracer injections into the belly or the distal myotendinous junction of the medial or lateral rectus muscle and further characterized by combined tracer detection and immunohistochemical methods. The experiments revealed that the MIF motoneurons in the periphery of the motor nuclei lack non-phosphorylated neurofilaments, parvalbumin and perineuronal nets, whereas SIF motoneurons intensively express all three markers. In addition to the histochemical

differences, the MIF motoneurons are on average significantly smaller in size than the SIF motoneurons.

Analogous to the study in monkey, the SIF and MIF motoneurons of the medial and lateral rectus muscle of rats were identified with tracer injections and further characterized by immunolabelling. For the first time it was shown that both motoneurons types are present in rat as well. The MIF motoneurons lie mainly separated from the SIF motoneurons, and are different in size and histochemical properties. As in monkey, the smaller MIF motoneurons lack non-phosphorylated neurofilaments and perineuronal nets, both of which are definite markers for the larger SIF motoneurons.

A possible proprioceptive control of eye movements requires the presence of proprioceptive structures. The palisade endings represent the best candidate for an EOM-proprioceptor. They were analysed using antibody stains against the synaptosomal associated protein of 25kDA, SNAP-25. With this robust method palisade ending-like structures were identified for the first time in the extraocular muscles of the rat. Furthermore the rat palisade endings show characteristics of sensory structures thereby supporting their role in proprioception.

In conclusion, the EOM of both monkey and rat are innervated by two sets of motoneurons which differ in localization, morphology and molecular components. These findings further support the presence of a dual motor control of EOM that may apply widely to mammals, since it was verified in monkey and rat. Palisade endings are a ubiquitous feature of mammal EOM and most likely provide sensory information used for the proprioceptive control of eye movements.

## **Zusammenfassung**

Das okulomotorische System ist eines der am besten untersuchten motorischen Systeme. Eingänge aus unterschiedlichen prämotorischen Zentren konvergieren auf die Motoneurone der drei okulomotorischen Kerne, welche die verschiedenen Arten von Augenbewegungen generieren. Da alle okulomotorischen Motoneurone an allen Augenbewegungen beteiligt sind, war man bisher der Ansicht, dass es sich hierbei um eine einheitliche Gruppe handelt, welche gemeinsam den letzten Abschnitt der motorischen Innervation der Augenmuskulatur darstellt. Die Augenmuskeln der Säugetiere unterscheiden sich grundsätzlich von der Skelettmuskulatur. Sie bestehen aus zwei funktionell unterschiedlichen Schichten, der globalen und der orbitalen Schicht, und setzen sich aus zwei Hauptklassen von Muskelfasern zusammen, den einfach innervierten Fasern (SIF) und den multipel innervierten Fasern (MIF). In früheren Studien an Affen fand man heraus, dass SIF- und MIF-Motoneurone anatomisch voneinander getrennt liegen und unterschiedliche prämotorische Eingänge erhalten, was eher die Idee einer dualen motorischen Innervation der Augenmuskulatur unterstützt, als die einer uniformen Endstrecke. Bisher wurden weder die beiden Motoneuron-Typen weitergehend charakterisiert, noch wurden Studien unternommen, die deren Vorhandensein in anderen Spezies nachweisen, um so die Hypothese der dualen motorischen Innervation als gemeinsames Konzept aller Säugetiere zu bestärken. Die sich aus diesem System ergebenden funktionellen Folgerungen bleiben spekulativer Art. Wenn auch heftig debattiert, erscheint es durchaus möglich, dass die MIFs zusammen mit ihren Motoneuronen in einem sensorischen Feedback-System zur Kontrolle der Augenmuskulatur involviert sind. Da jedoch den Augenmuskeln ein gemeinsamer Propriozeptor fehlt, erscheint diese Theorie unwahrscheinlich.

In Affen wurden die SIF- und MIF-Motoneurone der Musculi recti medialis und lateralis mittels Tracer-Injektionen in den Muskelbauch oder den distalen Muskel-Sehnen-Übergang identifiziert und durch Kombination der Tracer-Darstellung mit immunhistochemischen

Methoden weiter charakterisiert. Dabei zeigte sich, dass den MIF-Motoneuronen in der Peripherie der Augenmuskelkerne unphosphorylierte Neurofilamente, Parvalbumin und perineuronale Netze fehlen. Im Gegensatz dazu exprimieren die SIF-Motoneurone diese drei Marker mit hoher Intensität. Zusätzlich zu den histochemischen Unterschieden sind die MIF-Motoneurone im Mittel signifikant kleiner als die SIF-Motoneurone.

Bei der Ratte wurden analog zu den Studien am Affen die SIF- und MIF-Motoneurone der Musculi recti medialis und lateralis mit Tracer-Injektionen identifiziert und mit Immunfärbungen charakterisiert. Dabei wurde zum ersten Mal gezeigt, dass auch die Ratte beide Motoneuron-Typen besitzt. Die MIF-Motoneurone liegen größtenteils anatomisch von den SIF-Motoneuronen getrennt, haben unterschiedliche Größe und histochemische Eigenschaften. Wie im Affen fehlen den kleineren MIF-Motoneurone unphosphorylierte Neurofilamente und perineuronale Netze, beides definitive Marker für die größeren SIF-Motoneurone.

Eine mögliche propriozeptive Kontrolle der Augenbewegung setzt das Vorhandensein propriozeptiver Strukturen voraus. Den besten Kandidaten für einen Augenmuskel-Propriozeptor stellen die Palisadenendigungen dar. Sie wurden mit Antikörperfärbungen gegen das synaptosomal-assoziierte Protein von 25kDa, SNAP-25, analysiert. Mithilfe dieser Methode konnten im Augenmuskel der Ratte zum ersten Mal Strukturen ähnlich den Palisadenendigungen identifiziert werden. Die Palisadenendigungen der Ratte weisen darüber hinaus Charakteristika sensorischer Strukturen auf und unterstützen damit ihre propriozeptive Funktion.

Zusammenfassend lässt sich sagen, dass die Augenmuskeln sowohl des Affen als auch der Ratte von zwei Typen von Motoneuronen innerviert werden, die sich in ihrer Lage, ihrer Morphologie und ihren molekularen Bestandteilen voneinander unterscheiden. Das Vorhandensein einer für viele Säugetiere zutreffenden dualen motorischen Kontrolle der Augenmuskulatur wird durch die Ergebnisse beim Affen und bei der Ratte zusätzlich

unterstützt. Die Palisadenendigungen sind ein allgemeiner Bestandteil der Augenmuskulatur von Säugetieren und liefern höchstwahrscheinlich die sensorische Information, die zur propriozeptiven Kontrolle der Augenbewegungen benutzt wird.

## **Abbreviations**

ChAT:	choline acetyltransferase
cMRF	central mesencephalic reticular formation
EOM:	extraocular muscles
INT:	abducens internuclear neuron
IO:	inferior oblique muscle
IR:	inferior rectus muscle
LP:	levator palpebrae muscle
LR:	lateral rectus muscle
MIF:	multiply-innervated muscle fibre
MLF:	medial longitudinal fascicle
MR:	medial rectus muscle
nIII:	oculomotor nucleus
nIV:	trochlear nucleus
nVI:	abducens nucleus
NIII:	oculomotor nerve
NMJ:	neuromuscular junction
NP-NF:	non-phosphorylated neurofilament
OKR:	optokinetic reflex
SC:	superior colliculus
SIF:	singly-innervated muscle fibre
SNAP-25:	synaptosomal associated protein of 25kDa
SO:	superior oblique muscle
SpV:	spinal trigeminal nucleus
SR:	superior rectus muscle
VOR:	vestibulo-ocular reflex

## **Introduction**

### Extraocular muscles (EOM)

The extraocular muscles (EOM) are the effector organs for voluntary and reflexive movements of the eyes. Among all vertebrates classes, the presence of six EOMs, four recti (superior, inferior, medial, and lateral) and two obliques (superior and inferior) is rather constant, despite some variation in arrangement and innervation (Isomura, 1981). An additional EOM, the levator palpebrae superioris, which elevates the upper eyelid, is present only in mammals. Many vertebrates possess accessory EOMs, such as the retractor bulbi muscle (Isomura, 1981). This muscle is correlated with the presence of a nictitating membrane and both structures act synergistically in reflex retraction of the globe in response to corneal stimulation. Since the levator palpebrae superioris and the retractor bulbi muscle do not contribute to eye movement, they will be not be considered further in this work. All these EOMs are relatively consistent across mammalian species in their general location and innervation pattern. However, individual muscle actions show interspecies variations, particularly in frontal-eyed (e.g., monkey, cat) versus lateral-eyed (e.g., rabbit, rat, mouse) animals. These variations are coincident with species differences in the forward extension of the maxillary process (Fink, 1953) and the relative angles of the visual axis and the semicircular canals (Simpson and Graf, 1981; Ezure and Graf, 1984).

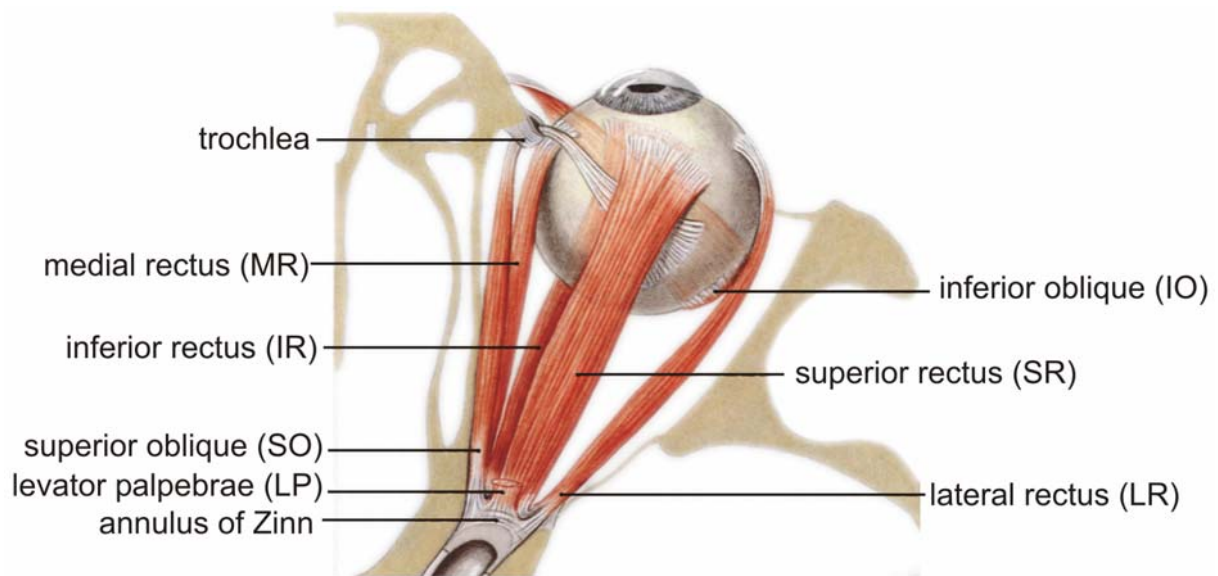


Figure 1: Schematic drawing of a right human eyeball viewed from dorsal. The surrounding tissue is removed to better visualize the extraocular muscles. The six extraocular muscles are shown from their origin of the annulus of Zinn to their insertion onto the globe. The levator palpebrae is cut at its origin. (Adapted, from Benninghoff, Anatomie Vol. 2, 15th edition 1993, Urban and Schwarzenberg).

#### *Participation of each EOM in eye movement*

The individual contribution of each of the four recti and two oblique eye muscles to eye movements depends on the point of rotation of the globe, the bony anatomy of the orbit, and the origin and insertion of each eye muscle. If one considers the eye rotating about a central point, the EOMs cause movement about three axes, x, y, and z. The four recti and the superior oblique muscle have their origin from the annulus of Zinn, a tendinous ring which surrounds the optic foramen and a portion of the superior orbital fissure, enveloping the optic nerve (Sevel, 1986). In contrast, the inferior oblique (IO) muscle arises from the maxillary bone in the medial wall of the orbit. The superior oblique (SO) muscle differs from all other EOMs by passing through the trochlea, a tendinous ring attached to the medial orbit, before reaching the globe. The trochlea is therefore regarded as the functional origin of the SO. Since the horizontal and vertical recti have symmetric origins and insertions on both sides of the globe,

they function relatively simple and act as antagonists: the medial rectus (MR) as the principal adductor, the lateral rectus (LR) as the principal abductor, the inferior rectus (IR) as the principal elevator, the superior rectus (SR) as the principal depressor. Since the vertical recti insert on the globe at angle of 23° laterally to the visual axis, they have more or less secondary roles in adduction for both muscles and intorsion for the SR and extorsion for the IR, depending on the direction of the visual axis. The principal action of superior oblique (SO) and inferior oblique (IO) muscle is intorsion and extorsion, respectively. Similar to the vertical recti, both oblique muscles have secondary functions: the SO additionally depresses and abducts the globe, the IO depresses and adducts. The primary actions of these six EOMs are similar in lateral-eyed mammals, though their secondary actions in eye movements differ from those of frontal-eyed mammals due to divergent insertion on the globe.

### *Muscle pulleys*

Connective tissue sheaths, the so-called 'pulleys', also influence muscle actions by coupling the extraocular muscles to the globe and orbit (Miller, 1989), thereby acting as peripheral mechanical support of the oculomotor system so that each EOM can exhibit its primary action in eye movement even in extreme positions of the globe. Pulleys consist of a ring of collagen located at above the globe equator of Tenon fascia (Demer et al., 1995). They are coupled to the orbital wall, adjacent EOMs, and equatorial Tenon fascia by slinglike bands containing densely woven collagen, elastin, and richly innervated smooth muscle (Demer et al., 1997). Their anatomy has been consistently demonstrated across diverse species like rat, rabbit, dog, horse, monkey, and human (Khanna and Porter, 2001; Oh et al., 2001). Functional MRI studies suggest that pulleys inflect rectus and inferior oblique EOM paths in a qualitatively similar manner as the inflection of the superior oblique tendon path by the trochlea. Recent studies verified that EOMs show a layered structure, an inner global layer that extends the full muscle length from the annulus of Zinn to the tendinous insertion on the sclera of the globe,

and an outer orbital layer, that ends before the muscle becomes tendinous, a consequence of its insertion into the muscle pulley (Demer et al., 2000; Miller et al., 2003). Thereby, the function of the orbital layer is, instead of rotating the globe along with the global layer, to position the pulley, as proposed by the “active pulley hypothesis” (Oh et al., 2001; Demer, 2002). Even though the detailed implications of pulleys for the control of eye movements is still controversially debated (Dimitrova et al, 2003), pulleys are in every aspect fundamental to understanding eye movements. New models of eye movements, like SEE-KID ([www.see-kid.at](http://www.see-kid.at)) implement, at least for some aspects, the role of pulleys.

### *Functional types of eye movements*

Stated simply, the need for eye movements is to permit the clear vision of objects, therefore creating the physiological basis for holding an image fairly steady on the retina. In primates one can distinguish between six distinct types of eye movements, the vestibulo-ocular reflex (VOR), the optokinetic reflex (OKR), saccades, smooth pursuit, vergence, and lastly gaze-holding. Since our eyes are attached to our heads, the disturbances that are most likely to affect vision are head perturbations, especially those that occur during locomotion (Miles, 1998; Grossman et al., 1988). Thus, to prevent blur during head/body movements, two reflexive oculomotor control systems evolved to stabilize images on the retina, the VOR and OKR. The VOR depends on the ability of the labyrinthine mechanoreceptors to sense head accelerations, whereas the OKR depends on the ability of the brain to determine the speed of image drift on the retina. Both types of eye movements are the phylogenetically old and can be found in all vertebrates, they function together to stabilize gaze. With the evolution of a specialized retinal area for precise vision (fovea, area centralis), it became now important to focus the desired targets, even without moving the head. This is done by a saccade, a rapid eye movement of the eyes that changes the line of sight and translates the image from an eccentric retinal position to the fovea. Since vision is blurred during saccades, they have very

short duration (e.g. in human for 20-150ms) and reach speeds up to 800°/s. Saccades include both voluntary and involuntary changes of fixation, the quick phases of vestibular and optokinetic nystagmus (that reset the eyes during prolonged rotation thus preventing extreme orbital positions of the eyes), and the rapid eye movements occurred during rapid eye movement (REM) sleep. Although compensatory eye movements (VOR and OKR) dominate in afoveate animals, they do show the same repertoire of saccadic eye movements, but voluntary saccades have to be always linked to voluntary head movements to override vestibular and optokinetic drives. In contrast, smooth pursuit movements and visual fixation are limited to foveate animals (Fuller, 1985). The smooth pursuit systems allows one to track small moving targets with the fovea in a fixed visual environment (or to hold the image of a near target on the fovea during self motion), by rotating the eyes at the same angular velocity as that of the target (Miles, 1998). Because other visually mediated eye movements have to be suppressed during smooth pursuit movements (e.g. VOR), the implication is that smooth pursuit depends on the ability to filter out visual motion inputs save for those at the focus of attention. This or a similar mechanism could even help to hold a stationary object steady on the fovea when the observer is stationary, thus enabling visual fixation. With the development of frontal vision and binocularity, disconjugate (in contrast the other eye movement types, that are conjugate) or vergence eye movements became also necessary, so that images of an object of interest could be placed on both foveas simultaneously. Loss of focus of images on the retina stimulates vergence movements that associated with accommodation of the lens and pupillary constriction.

### *Fine anatomy of EOMs*

The functional demands placed upon the extraocular eye muscles as shown above explains their complex organization. Already 1938, Kato showed that in mammals the six EOMs are characterized by a distinctive compartmentalized organization (Kato, 1938). Each has an outer

orbital layer adjacent to the orbital bone and an inner global layer close to the optic nerve and the eye. Sheep possess a distinct third muscle layer (Harker, 1972a). It lies mainly distally in a C-shape around the outside of the orbital layer, the peripheral patch layer. A similar layer, called the marginal layer was described in human (Wasicky et al., 2000). Its presence in other species remains unclear. The orbital layer is comprised of smaller diameter fibres and typically has a C-shaped appearance encompassing the global layer except for a small gap left in rectus muscles or completely encircles the global layer in oblique muscles (Oh et al., 2001). Whereas the global layer extends the full muscle length from the annulus of Zinn to the tendinous insertion on the sclera of the globe, the orbital layer ends before the muscle becomes tendinous, a consequence of its insertion into the muscle pulley, as shown by recent studies (Demer et al., 2000; Miller et al., 2003).

Skeletal muscles are characterized by the presence of four basic muscle fibre types that differ on the basis of biochemical (Moore and Schachat, 1985), histochemical (Brooke and Kaiser, 1970), immunocytochemical (Pierobon-Bormioli et al., 1980, 1981), ultrastructural (Schiaffino et al., 1970) and physiological (Burke, 1981) properties: 1. slow twitch, fatigue resistant; 2. fast twitch, fatigue resistant; 3. fast twitch, fatigable; 4. fast twitch, intermediate. These four fibre types are found in various proportions in virtually every mammalian skeletal muscle.

Early studies recognized that the myofibres in mammalian EOM were atypical. 1955, Siebeck and Kruger identified two basic EOM fibre types which were characterized as *Fibrillenstruktur* and *Feldernstruktur* on the basis of their histochemical appearance. The *Fibrillenstruktur* fibres are similar to the typical twitch fibres in skeletal muscle and are now designated as singly-innervated fibres, SIF. After stimulation, twitch fibres respond with a contraction in an all-or-none fashion. In contrast, *Feldernstruktur* fibres are unique to extraocular muscle and few other craniofacial muscles, e.g. tensor tympani and laryngeal muscles (Fernand and Hess, 1969). These fibres are multiply-innervated, now designated as

MIF, showing multiple nerve contacts along their length and are a regular component of the skeletal muscles of Amphibians, Reptiles and Fish (Morgan and Proske, 1984). Under the light microscope, these fibres show a characteristic broad Z-line. Beginning with the basic differences in innervation pattern of SIFs and MIFs in EOM, several studies have been carried out in various mammalian species to characterize the EOM fibre types in detail (mouse: Carry et al., 1982; rat: Pachter and Colbjornsen, 1983; rabbit: Reichmann and Srihari, 1983; sheep: Harker, 1972b; cat: Hanson et al., 1980; primates: Ringel 1978b; human: Ringel et al., 1978a). Even though these studies failed to develop a unitary classification, it is now generally accepted, that the EOMs contain six distinct fibre types with a broad spectrum of differences from other skeletal muscle fibre types.

#### *Characterization of the six EOM fibre types*

The most accepted scheme for EOM fibres type classification uses the obvious features of location (global or orbital), innervation pattern (SIF or MIF), and fatigue properties, or color (for a detailed review see: Porter et al., 1995; Spencer and Porter, 1988). Thus, the orbital layer contains two fibre types, one SIF and one MIF, and the global layer contains four fibre types, three SIF and one MIF, a pattern which is highly conserved within the mammalian species. The orbital singly-innervated fibre, the predominant fibre type (80%) of the orbital layer, has an extremely high content of mitochondria, high levels of oxidative enzymes, and a dense network of associated capillaries (much higher than in the global layer), implementing this fibre type to be among the most fatigue resistant mammalian skeletal muscle fibre types. Normal eye muscle tension never drops below 8-12 grams (Collins, 1975); this fibre type most likely is a major contributor to this force. The orbital layer MIFs are the remainder of fibres (20%) in the orbital layer. Physiologic studies indicate that these fibres change their properties along their length in a way that at the distal and proximal ends of the orbital layer they have the characteristics and innervation of a non-twitch muscle fibre, but in the central

region they have the characteristics and innervation of a twitch muscle fibre (Pachter, 1984; Jacoby et al., 1989). All of the SIFs in the global layer exhibit traits of fast-twitch fibres. The global red SIFs, which make up 30% of all global layer muscle fibres, show histochemical and ultrastructural features similar of that of the orbital SIF, suggesting that it is fast-twitch and highly fatigue resistant. The global intermediate and pale SIFs, each makes up of about 30% of the global layer fibres, differ mainly in their mitochondria content, with scattered clusters of mitochondria in the intermediate type, and few, small mitochondria in the pale type. Thus, the intermediate SIF has a profile of a fast-twitch fibre, with intermediate fatigue resistance, whereas the profile of the pale SIF is fast-twitch with low fatigue resistance. Global MIFs constitute the remaining 10% of fibres in the global layer. These fibres do not propagate action potentials like twitch-fibres, but undergo slow, local contractions at each synaptic site (Nelson et al., 1986; Chiarandini and Jacoby, 1987; Jacoby et al., 1989, 1990). Because of these functional differences among the six EOM fibre types, attempts were made to associate EOM fibre type with specific eye movement types (Jampel, 1967). Instead, it was shown that all motoneurons and all EOM fibre types participate in all eye movement classes. In addition, these studies demonstrated that orbital layer fibres are recruited before global layer fibres (Scott and Collins, 1973).

### *Molecular properties of EOM*

Recent studies on extraocular muscle fibres have focussed on myosin heavy chain expression and gave additional evidence for the outstanding properties of EOM. Myosin heavy chain is a key determinant of contractile properties of a muscle fibre. Multiple myosin genes encode proteins differing in contraction speed and energetic demands such that an individual skeletal muscle fibre typically expresses the one myosin isoform that is best suited for its workload. EOM expresses virtually all known striated muscle isoforms of myosin heavy chain, and shows additionally frequent heterogeneity in myosin expression within a single muscle fibre

(Wieczorek et al., 1985; McLoon et al., 1999; Wasicky et al., 2000; Rubinstein and Hoh, 2001; Briggs and Schachat, 2002). And even genetic approaches have further characterized EOM as fundamentally distinct from skeletal muscle (Porter et al., 2001; Cheng and Porter, 2002; Fischer et al., 2002), though the notion that EOM may be a distinct muscle tissue class has been rejected (Khanna et al., 2003).

Gene expression profiles of orbital versus global layer have been performed using DNA microarray analysis (Khanna et al., 2004). 181 transcripts with preferential expression in orbital or global layer have been identified. Among these, several slow/cardiac muscle markers were preferentially expressed in the orbital layer, suggesting that the orbital layer may be functionally slower than the global layer.

#### Motor innervation of eye muscles

In skeletal muscle, the signal from a motor nerve is transmitted onto the muscle fibre at the neuromuscular junction (NMJ). A presynaptic motoneuron axon enters the muscle, branches to innervate multiple muscle fibres, loses the myelin sheath adjacent to each fibre immediately, and finally forms a mitochondria and synaptic vesicle-filled bouton that closely contacts individual myofibres at one site only. The presynaptic boutons lie in deep synaptic gutters formed by invagination of the myofibre sarcolemma, thereby minimizing neurotransmitter distance and isolating the cell-cell interactions from the extracellular milieu. In addition, sarcolemmar postjunctional folds increase the surface area for synaptic interaction (for a review see Sanes and Lichtmann, 1999).

This idealized synaptic profile has considerable variations at the NMJs and demonstrates in extraocular eye muscle its extreme variability. Using acetylcholinesterase histochemistry and immunohistochemistry together with light and electron microscopy, two principal endplate types in EOM fibres have been identified (Mayr et al., 1975; Ringel et al, 1978; Oda, 1986;

Ogata, 1988). So-called 'en-plaque' endings, which are similar to the NMJs in skeletal muscle, are the characteristic type of ending in EOM SIFs. In longitudinal sections, they end as elongated or round cluster in the middle third of a single fibre. In human EOM, 'en-plaque' endings have a mean diameter of about 27 $\mu$ m, with only one ending per SIF. In contrast, the multiply-innervated fibres (MIFs) have so-called 'en-grappe' endings, which are irregularly distributed over the whole length of a single MIF. This type of ending is notably smaller in diameter, about 9.5 $\mu$ m in human EOM, and the boutons lie superficially on the fibre surface (Namba et al, 1968a; Ogata, 1988). In many cases, an unmyelinated nerve fibre runs along a MIF splitting up in several 'en-grappe' endings. Despite the morphologic differences of the 'en-grappe' endings compared to skeletal muscle endplates, they possess the molecular framework for the principal NMJ signal transduction (Khanna et al., 2003).

### Sensory innervation of EOM

#### *Muscle spindles, Golgi tendon organs, and palisade endings*

Three putative proprioceptors are found in eye muscles: muscle spindles, Golgi-tendon organs and palisade endings (called myotendinous cylinders when the collagen sheath is included) (Cilimbaris, 1910a; Maier, DeSantis et al., 1974; Büttner-Ennever et al., 2003). Whereas muscle spindles and Golgi tendon organs are the typical proprioceptors in skeletal muscles that generate sensory information used for motor control, the palisade endings are unique to EOMs. The term 'palisade endings' was first used by Dogiel (1906) who described a recurrent nerve entering the myotendinous junction from the tendon, which then split up into a "...whole bunch of small nerve branches of varying thicknesses, reaching the end of a muscle fibre and surrounding it from all sides like a palisade".

Searching for muscle spindles and Golgi tendon organs in EOM will be unrewarding in most cases. Accordingly, many species do not have muscle spindles, and in those that do (including

humans), the spindles have been described on morphological grounds to being incapable of any proprioceptive function, particularly those found in humans (Ruskell, 1999; Bruenech and Ruskell, 2001). Moreover, Golgi tendon organs are very rare and only found in artiodactyls (Abuel-Atta et al., 1997; Blumer et al., 2000; 2001; 2003). If present, both proprioceptors appear to be confined to a specific layer of the eye muscles (Büttner-Ennever et al., 2003): muscle spindles are predominantly in the orbital layer, Golgi tendon organs in sheep are found in the outermost peripheral patch layer, which surrounds the orbital layer distally (Blumer et al., 2000). This scheme can be extended to palisade endings, which are located exclusively at the myotendinous junction of the global layer (Dogiel, 1906; Cilimbaris, 1910b; Ruskell, 1999). Palisade endings form a cuff of fine vesicle-laden nerve terminals that insert only on the tip of the MIFs of the global layer, and, in the majority of cases, also on the adjacent collagen fibres of the tendon (Alvarado-Mallart and Pincon Raymond, 1979; Lukas et al., 2000). The palisade terminals arise from nerve fibres that enter the tendon from the central nerve entry zone, and then turn back 180°, to contact the tip of the muscle fibres (see figure 2).

#### *Palisade endings and their role in proprioception*

Several authors have suggested that palisade endings could be the source of sensory afferent signals (Ruskell, 1999; Weir et al., 2000; Donaldson, 2000; Büttner-Ennever et al., 2002); but there are still conflicting reports on the functional nature of palisade endings, whether they are sensory or motor structures, or both. The ultrastructural morphology of palisade endings in cat, rhesus monkey and sheep has been shown to be typical of a sensory structure (Ruskell, 1978; Alvarado-Mallart and Pincon Raymond, 1979; Blumer et al., 1998). However, in rabbit (Blumer et al., 2001), and for some part in human (Lukas et al., 2000) and cat (Konakci et al., 2005), the palisade terminals exhibit motor-terminal-like morphology.

The problem is compounded by the conflicting evidence for the location of the cell soma of the palisade ending. If the palisade endings are sensory their ganglion cell body should be in the trigeminal ganglion or in the mesencephalic trigeminal nucleus; whereas if the endings are of a motor origin then they would have cell bodies associated with the oculomotor nucleus. Tozer and Sherrington (1970) as well as Sas and Schab (1952) provided evidence for their location in the oculomotor nerve or nucleus, a result more compatible with a motor role for the palisade endings (Gentle and Ruskell, 1997; Ruskell, 1999): whereas the results of other studies point to the trigeminal ganglion as the location of palisade ending soma, and imply a sensory function (Billig et al., 1997). Thus, up to now the function of palisade endings remains unclear.

Palisade endings have been found in almost all investigated species, with the exception of the rat (Daunicht, 1983; Daunicht et al., 1985). So far, it cannot be assumed that all mammals have palisade endings in the global layer of their eye muscles.

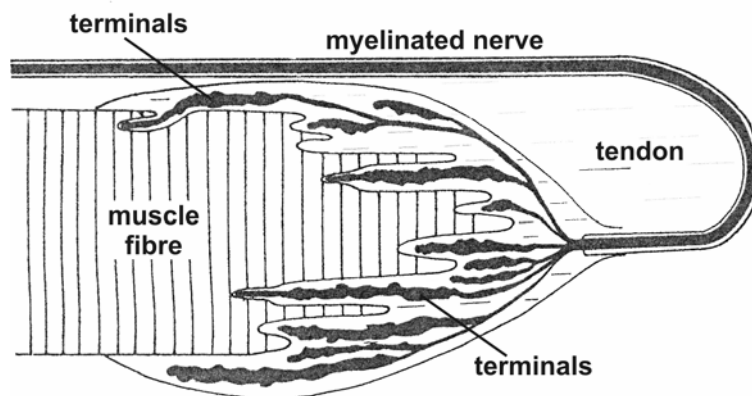


Figure 2: Schematic drawing illustrating the relationship of a palisade ending and the myotendinous junction of the global layer MIF. A myelinated nerve runs parallel a MIF, then loops back in the tendon and divides to form terminal branches which terminate on the collagen fibrils and on the muscle fibre. (Adapted from Alvarado-Mallart and Pincon Raymond, 1979)

### Motoneurons of eye muscles

The increased interest in the motor control of eye muscles in the late 1960's was stimulated mainly by the vestibular studies of Bernard Cohen, and the recording-modelling approach of David A. Robinson and his colleagues. This resulted in the development of a thorough understanding of many aspects of the oculomotor system (Cohen, 1974; Büttner and Büttner-Ennever, 1988; Leigh and Zee, 1991; Leigh and Zee, 1999). Several relatively independent premotor circuits carrying vestibular, saccadic, smooth pursuit or vergence signals, have been discovered, modelled and shown to converge on the motoneurons in the oculomotor, trochlear or abducens nuclei. The motoneurons generate motor responses, some with more tonic, others with a more phasic properties, but all of the motoneurons respond with every type of eye movement (Keller and Robinson, 1972; Fuchs et al., 1985; Dean, 1996). This concept of a final common pathway has become widely accepted but remains incomplete (Ling et al., 1999; Miller, Bockisch et al., 2001).

### *Anatomy of motoneurons*

The motoneurons innervating the eye muscles lie in three separate nuclei: the oculomotor (nIII) and trochlear nucleus (nIV) in the mesencephalon, and further caudal, the abducens nucleus (nVI) in the pons (figure 3).

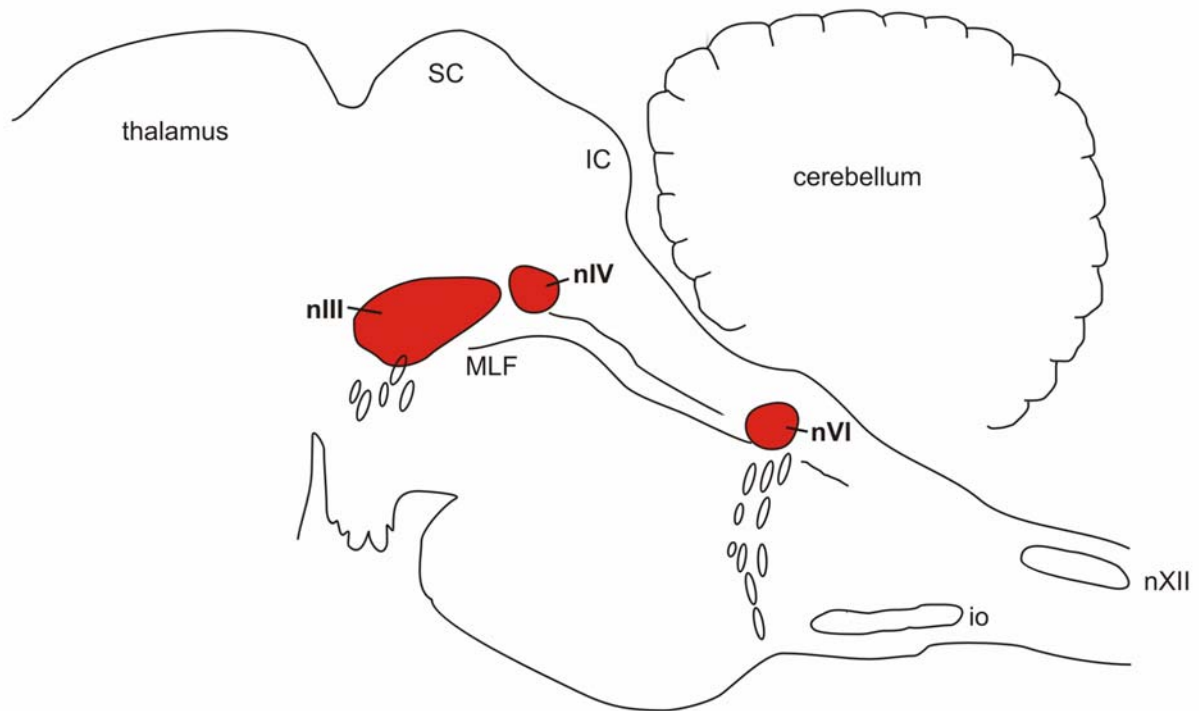


Figure 3: Illustration of a monkey brainstem and midbrain, sagittal view, showing the anatomic localization of the oculomotor (nIII), trochlear (nIV), and abducens nucleus (nVI). SC: superior colliculus, IC: inferior colliculus, MLF: medial longitudinal fascicle, io: inferior olive, nXII: hypoglossal nucleus.

The oculomotor nucleus (nIII) is located as compact paired nucleus in the tegmental area of the midbrain, ventral to the aqueduct and dorsal to the fibres of the medial longitudinal fascicle (MLF) and innervates via the oculomotor nerve (NIII) ipsilaterally the medial (MR) and inferior rectus (IR), and the inferior oblique (IO) muscle, and contralateral the superior rectus muscle (SR). As early as 1878, Henson and Völckers showed by stimulation experiments, that motoneurons within the oculomotor nucleus innervating the same eye muscle are bundled. The localization of these subgroups has been the issue of many studies and was described in monkey (Warwick, 1953; Büttner-Ennever and Akert, 1981; Porter et al., 1983), cat (Naito et al., 1974; Gacek, 1974; Akagi, 1978), rabbit (Akagi, 1978; Murphy et al., 1986), rat (Glicksman, 1980; Labandeira-Garcia et al., 1983), and guinea pig (Gomez-Segade and Labandeira-Garcia, 1983). The motoneuron subgroups within nIII show a topographic organization. From rostral to caudal, the motoneuron populations in all species

follow an IR, MR, IO, and SR sequence (Evinger, 1988). One apparent difference in the organization between primates and non-primate mammals is the existence of three anatomically distinct subpopulations of MR motoneurons in primate (Büttner-Ennever and Akert, 1981). The greatest part of MR motoneurons form the A-group at the ventral portion of nIII, the B-group is located more dorsolaterally, and finally smaller diameter motoneurons form the C-group dorsomedially of nIII.

The oculomotor nucleus also contains internuclear neurons (INT) that project to the contralateral abducens nucleus (Highstein, 1977; Langer et al., 1986). In primates, on the dorsal pole at caudal planes of nIII, the motoneurons innervating the levator palpebrae (LP) form the central caudal nucleus, an unpaired nucleus embedded between the paired nIII. In lateral-eyed mammals like rat and rabbit, the LP-motoneurons lie laterally and occupy the ventrolateral part of the contralateral nIII at very caudal levels of this nucleus (Evinger et al., 1987). The distribution of the motoneurons subgroups in the monkey and rat nIII is summarized in figure 4.

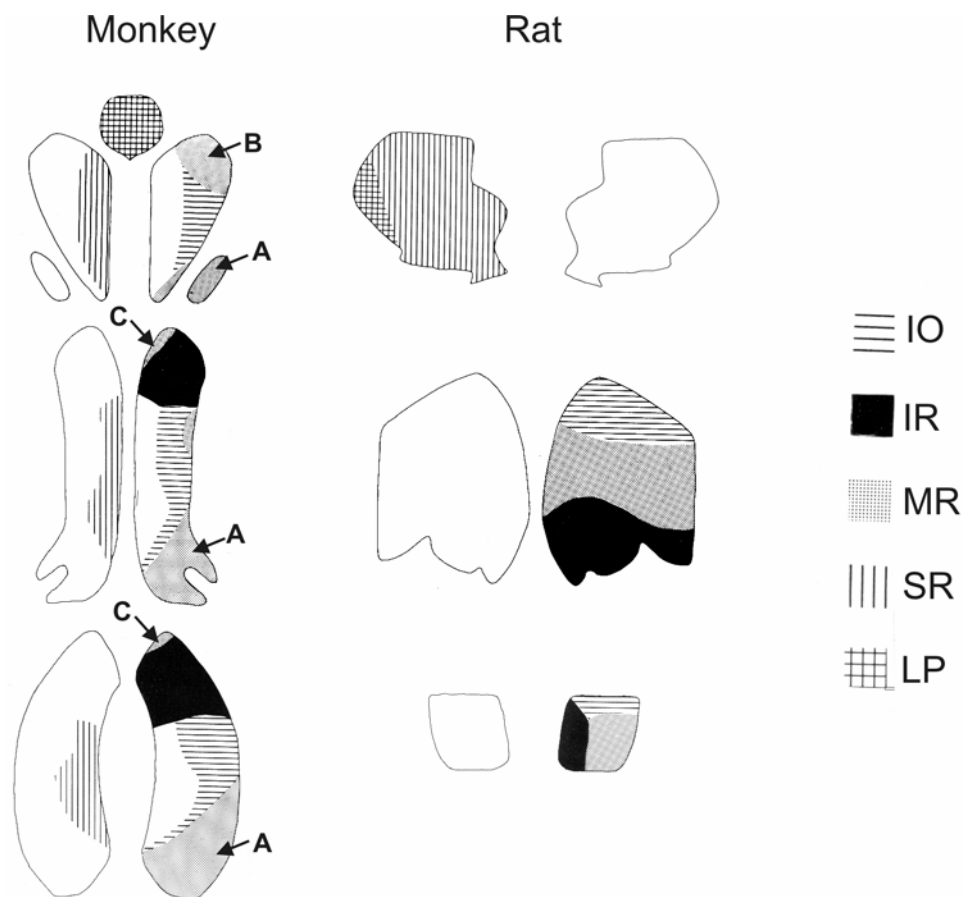


Figure 4: Coronal sections illustrating the location of motoneurons in the oculomotor nucleus of the monkey and rat. The rat sections are enlarged. (Adapted from Evinger, 1988)

Typically, the trochlear nucleus (nIV) occupies a region immediately caudal and slightly lateral to nIII. In mammals, it contains mainly (96-98%) motoneurons innervating the contralateral superior oblique (SO) muscle via the trochlear nerve (NIV). The remaining motoneurons project to the ipsilateral SO (Miyazaki, 1985; Evinger et al., 1987).

In mammals, the abducens nucleus (nVI) appears as rounded cluster of cells at the medullary-pontine junction at the bottom of the fourth ventricle, just below the facial genu. The majority of abducens motoneurons innervate the ipsilateral lateral rectus muscle (LR) via the abducens nerve, whereas only few innervate the accessory eye muscles, retractor bulbus (Spencer et al., 1980) or accessory LR, if present (Spencer and Porter, 1981). A second population within the

abducens nucleus is formed by the internuclear neurons (INT) that project rostrally via the MLF to the MR motoneurons in the contralateral oculomotor nucleus (Büttner-Ennever and Akert, 1981; McCrea et al., 1986). The exact location of INT in mammals is species-specific. In primates both neuron groups are not separated clearly, but tend to cluster in a band that extends from the dorsolateral to the ventromedial part of nVI at caudal planes and occupy the region lateral to the rootlets of nVI further rostrally (Büttner-Ennever, Horn et al., 1989). In contrast, in rat it was reported that they form a distinct cap at the lateral and ventral edges of nVI (Glicksman, 1980; Labandeira-Garcia et al., 1983). Both motoneurons and internuclear neurons form the anatomical basis for conjugated horizontal eye movements in mammals. In macaque monkey, a distinct group of neurons was identified in the rostral cap of nVI, extending even medial to the MLF, that projects to the floccular region of the cerebellum (Langer et al., 1985). Functionally these neurons are regarded as part of the paramedian tract neurons (PMT-cells) that receive afferent input from all premotor centres of the oculomotor system and project themselves to the floccular region of the cerebellum (Büttner-Ennever, 1992). Their function is still unclear. They may carry an eye-position signal to the cerebellum, which is in line with lesions in the PMT-system that resulted in deficits in gaze holding and smooth pursuit (Büttner et al., 1995).

#### *A revision of the organization of the oculomotor nuclei*

In all studies that examined the organization of the oculomotor nuclei in different species, it has not been possible to correlate the presence of two distinct fibre types, SIF and MIF, with different types of innervation in EOM, to different motoneuron populations. This issue was first dealt with by Büttner-Ennever 2001 (Büttner-Ennever et al., 2001) in a study in macaque monkey, where different location of the tracer injection sites resulted in the retrograde labelling of different motoneuron populations within a given oculomotor nucleus. Specifically, a tracer injection placed into the central endplate zone of an eye muscle labelled

large (SIF) motoneurons within nIII, nIV and nVI, and smaller motoneurons lying mainly around the periphery of these nuclei. In contrast, a tracer injection into the distal myotendinous junction of an EOM, where only 'en-grappe' endings of multiply-innervated muscle fibres (MIF) are found, labelled selectively the motoneurons (MIF motoneurons) that are distributed around the periphery of the classical oculomotor nuclei. In nIII, the MIF motoneurons of both IR and MR are grouped together mainly on the dorsomedial border and form the C-group (Büttner-Ennever et al., 2001). In contrast, the MIF motoneurons of the SR and IO are predominately located bilaterally around the midline, forming the S-group (Wasicky et al., 2004). In the trochlear nucleus, the MIF motoneurons lie almost exclusively like a cap at the dorsal border of the nucleus, whereas the MIF motoneurons of the abducens nucleus surround its medial half. Taken together, SIF and MIF motoneurons form two anatomical separated populations and are likely to have different functions.

#### The dual motor control of EOM and its possible role in proprioception

The recent tracer experiments in monkey EOM show that two sets of motoneurons, SIF and MIF motoneurons control the extraocular muscles (Büttner-Ennever et al., 2001). Subsequent studies of premotor inputs on both types of motoneurons revealed that MIF motoneurons (innervating the global layer MIFs) are associated with premotor areas for vergence, gaze holding, and visual fixation but in contrast to SIF motoneurons, *not* with premotor areas generating saccades or VOR (Büttner-Ennever et al., 2002; Wasicky et al., 2004). Thus, this dual motor control is in conflict with the theory of a single final common pathway from motoneuron to eye muscle. In the EOM of many mammals, the multiply-innervated non-twitch muscle fibres of the global layer and palisade endings form a unique unit. Considering the evidence that palisade endings most likely subserve a sensory function, has led to the propose of the following hypothesis: only the SIFs play a significant role in eye movement,

whereas the global layer MIFs adjust the tension on the eye muscle, possibly operating through the palisade endings. The palisade endings may provide an afferent signal to the CNS which is used to adjust eye-alignment (Büttner-Ennever et al., 2002).

## **Aims of this PhD-project**

1. SIF and MIF motoneurons of the oculomotor nuclei provide the dual motor innervation of the extraocular eye muscles in macaque monkey. Since the muscle fibre types innervated by SIF and MIF motoneurons show extreme different morphological and functional properties, and, in addition, both motoneuron populations receive a different premotor innervation, it is likely to assume that these differences are reflected in the properties of SIF and MIF motoneurons themselves.

Thus, in the primate model, both motoneuron populations will be characterized on a morphological, molecular, and functional level using combined tract tracing and immunohistochemical methods. The resulting characteristics should help to identify the complete population of MIF and SIF motoneurons in the oculomotor nuclei of the monkey and may provide the basis for the identification of similar populations in other species including human.

*The results are described and discussed in paper 1, pp 29-66*

2. The dual motor innervation of EOM may be regarded as a result of the visual demands placed upon the oculomotor system in highly developed frontal-eyed mammals like primates. According to this point of view, lateral-eyed mammals like the rat may differ in the organization of the motor control of their eye muscles. On the other hand, rat EOMs exhibit the same EOM fibre types as primates (Pachter, 1983; Pachter and Colbjornsen, 1983; Ringel et al., 1978; Spencer and Porter, 1988), and their eye movements include both fast and slow types (Delgado-Garcia, 2000).

To clarify if the dual motor control of EOM is a ubiquitous feature at least in mammals the organization of the motoneurons subserving the horizontal eye muscles in rat will be studied with similar methods used for the primate model.

*The results are described and discussed in paper 2, pp 67-102*

3. The hypothesis that EOM generate a proprioceptive signal focuses on the presence of palisade endings associated with the multiply-innervated non-twitch fibres of the global layer. Up to now, the function of palisade endings remains unclear. Conflicting results describe their properties as sensory (Ruskell, 1978; Alvarado-Mallart and Pincon Raymond, 1979) or motor (Blumer et al., 2001; Lukas et al., 2000). Further, palisade endings are not known to be a ubiquitous feature of all mammals, since in rat no such structure was described. In part these contradictions are based on the lack of a specific marker for palisade endings.

Thus, a staining technique should be developed which visualizes axon, branches and, most crucial of all, terminal boutons of the palisade endings. In addition, this marker should be simply combined with other immunohistochemical techniques to establish the functional properties of these putative receptors. Furthermore, this staining method should be suitable to look for similar structures in rat EOM.

*The results are described and discussed in paper 3, pp 103-112*

## **Results**

Paper 1: Motoneurons of multiply-innervated muscle fibres in extraocular muscles have different histochemical properties than motoneurons of singly-innervated muscle fibres

**Motoneurons of multiply-innervated muscle fibres in extraocular muscles  
have different histochemical properties than motoneurons of singly-  
innervated muscle fibres**

Andreas C. Eberhorn<sup>1</sup>, Patricia Ardeleanu<sup>1</sup>, Jean A. Büttner-Ennever<sup>1</sup>, Anja K.E. Horn<sup>1\*</sup>

<sup>1</sup>Institute of Anatomy, Ludwig-Maximilian University of Munich, D-80336 Munich Germany

Manuscript: 34 pages, 6 figures, 2 tables

Short title: Histochemistry of eye muscle motoneurons

Keyword: non-twitch muscle fibres, twitch muscle fibres, perineuronal net, non-phosphorylated neurofilament, parvalbumin, oculomotor, C-group, trochlear, abducens

\* Correspondence to: Institute of Anatomy III

Ludwig-Maximilians Universität

Pettenkofenstr. 11

D-80336 Munich

Germany

Phone: -49 89 5160 4880

Fax: -49 89 5160 4857

e-mail: Anja.Bochtler@anat.med.uni-muenchen.de

Grant sponsor: Deutsche Forschungsgemeinschaft (Ho 1639/4-1; GRK 267);

## Summary

The extraocular muscle fibres of vertebrates can be classified into two categories: singly-innervated fibres (SIFs) and multiply-innervated fibres (MIFs). In monkeys the motoneurons of SIFs lie within the oculomotor, trochlear, and abducens nucleus, whereas the motoneurons of MIFs appear in separate subgroups in the periphery of the classical nuclei borders. In the present study we investigated the histochemical properties of SIF and MIF motoneurons using combined tract-tracing and immunofluorescence techniques.

In monkeys SIF and MIF motoneurons of extraocular muscles were identified by tracer injections into the belly or the distal myotendinous junction of the medial or lateral rectus muscle. Alternatively the motoneurons were identified by choline acetyltransferase immunostaining. These techniques were combined with the detection of four histochemical markers: perineuronal nets, non-phosphorylated neurofilaments, parvalbumin and cytochrome oxidase.

The experiments revealed that the MIF motoneurons in the periphery of the motonuclei do not contain non-phosphorylated neurofilaments or parvalbumin and lack perineuronal nets. In contrast, SIF motoneurons express all markers at high intensity. Cytochrome oxidase immunostaining was found in both motoneuron populations. An additional population of motoneurons with 'MIF properties' was identified within the boundaries of the abducens nucleus, which could represent the motoneurons innervating MIFs in the orbital layer of lateral rectus muscle. Our data provide evidence that SIF and MIF motoneurons, which can be correlated with twitch motoneurons and presumed non-twitch motoneurons, differ in their histochemical properties. The absence of perineuronal nets, non-phosphorylated neurofilaments and parvalbumin may help to identify the homologous MIF motoneurons in other species, including humans.

## **Abbreviations**

CCN:	central caudal nucleus
ChAT:	choline acetyltransferase
Cox	cytochrome oxidase
CSPG:	chondroitin sulfate proteoglycan
CTb:	cholera toxin subunit B
EW:	Edinger-Westphal nucleus
IO:	inferior oblique muscle
LR:	lateral rectus muscle
MIF:	multiply-innervated muscle fibre
MR:	medial rectus muscle
nIII:	oculomotor nucleus
nIV:	trochlear nucleus
nVI:	abducens nucleus
NVII:	facial nerve
NP-NF:	non-phosphorylated neurofilament
PV:	parvalbumin
SIF:	singly-innervated muscle fibre
SO:	superior oblique muscle
SR:	superior rectus muscle
WFA:	Wisteria floribunda agglutinin
WGA-HRP	wheat germ agglutinin and horseradish peroxidase complex

## Introduction

The extraocular eye muscles are unique striated muscles, which differ in many respects from skeletal muscles. They consist of an outer orbital layer that is adjacent to the orbital bone, and an inner global layer adjacent to the eye globe. Only the global layer extends over the full muscle length from the annulus of Zinn to a well-defined tendon at the limbus of the globe (for review: see Porter et al., 1995). The orbital layer ends before the tendon (Oh et al., 2001) and is thought to insert on the collagenous pulleys, the Tenon's capsule (Demer et al., 2000; Oh et al., 2001; Demer, 2002). Based on morphological properties, three main categories of fibres can be identified in extraocular muscles: singly-innervated muscle fibres (SIFs) and two types of multiply-innervated muscle fibres (MIFs), one in the global and one in the orbital layer (for review: Mayr et al., 1975; Bondi and Chiarandini, 1983; Morgan and Proske, 1984; Spencer and Porter, 1988; Porter et al., 1995).

The SIFs correspond to the typical 'all-or-nothing' twitch muscle fibres of the skeletal muscles in mammals. In the eye muscles they are innervated by relatively thick axons, which terminate as large "en-plaque" endings within the middle third of the muscle. Upon electrical stimulation of the nerve they respond with propagated action potentials leading to a twitch, and are often called 'twitch muscle fibres' (Lennerstrand, 1974; Chiarandini and Stefani, 1979; Nelson et al., 1986; Jacoby et al., 1989; Lynch et al., 1994).

In mammals MIFs are rare, but are more common in skeletal muscles of amphibians and birds (Morgan and Proske, 1984). The MIFs of the *global layer* show a homogeneous morphology along their whole length, and they are innervated by multiple "en-grappe" endings throughout their extent (Pachter, 1984). After electrical stimulation MIFs respond with slow, graded potentials at each nerve ending, which are not propagated in an 'all-or-nothing' fashion, and resulting in the development of a tonic tension (Lennerstrand 1974; Chiarandini and Stefani, 1979). Therefore these global MIFs correlate with the 'non-twitch muscle fibres'.

In contrast, the MIFs of the *orbital layer* are more complex and show histochemical and morphological variation along their length (Pachter, 1984). Aside from the multiple innervation by “en-grappe” endings at their proximal and distal poles, they have a central endplate region typical for twitch muscle fibres (Davidowitz et al., 1982; Pachter, 1984; Jacoby et al., 1989). Accordingly, the orbital MIFs fibres have mixed physiological properties with a slow tonic and fast-twitch component (Lynch et al., 1994). Taken together it appears that only the global MIFs have pure non-twitch properties. These studies were carried out in rat, but the same basic morphology is present in all mammals, including primates (Spencer and Porter, 1988; Porter et al., 1995).

#### Motoneurons of multiply-innervated muscle fibres (MIFs)

Recently, we have identified the location of motoneurons that innervate the MIFs in the extraocular eye muscles of the macaque monkey (Büttner-Ennever et al., 2001). Injections of retrograde tracers into the distal tip of eye muscles resulted in uptake at the endplates of mainly global MIFs, since the orbital MIFs do not insert into the distal tendon. Therefore in these experiments predominantly the motoneurons of the *global* MIFs were retrogradely labelled; these motoneurons are assumed to be mainly global non-twitch motoneurons. The location of the MIF motoneurons of the orbital layer is unknown. The motoneurons of SIFs - the twitch motoneurons - were found to lie within the classical oculomotor nuclei, whereas the motoneurons of the MIFs - the presumed non-twitch motoneurons - were found in the periphery of the oculomotor nuclei (Büttner-Ennever et al., 2001). The largest and most compact population of MIF motoneurons are those of the medial and inferior rectus muscles that form the C-group at the dorsomedial border of the oculomotor nucleus (Büttner-Ennever and Akert, 1981; Spencer and Porter, 1981; Büttner-Ennever et al., 2001). The C-group has been identified in several species (Clarke et al., 1987; Sun and May, 1993; Shall et al., 2003). It is clearly separated from the SIF motoneurons of the oculomotor nucleus (nIII) and lies

close to the Edinger-Westphal nucleus (EW), which contains the preganglionic neurons for pupil constriction and accommodation (Akert et al., 1980; Burde and Williams, 1989; Ishikawa et al., 1990).

The MIF motoneurons of the superior rectus and inferior oblique eye muscles are located around the midline between the oculomotor nuclei forming the S-group (Büttner-Ennever et al., 2001; Wasicky et al. 2004). The MIF motoneurons of the superior oblique muscle lie in a compact cluster in the dorsal cap of the trochlear nucleus. The MIF motoneurons of the lateral rectus muscle are arranged more loosely around the periphery of the abducens nucleus, whereas the SIF motoneurons are scattered within the nucleus (Büttner-Ennever et al., 2001).

In addition to motoneurons the motor nuclei contain several other functional cell groups: the non-cholinergic internuclear neurons (Baker and Highstein, 1975; Steiger and Büttner-Ennever, 1978; Büttner-Ennever and Akert, 1981, Maciewicz and Phipps, 1983; Spencer and Baker, 1986; Carpenter et al., 1992; Clendaniel and Mays, 1994), the paramedian tract-neurons at the rostral pole of the abducens nucleus projecting to the floccular region (Büttner-Ennever and Horn, 1996), as well as other physiological groups associated with vergence, which have not been identified anatomically, yet (Gamlin et al., 1989).

In the present paper we compared in the monkey the histochemical properties of the MIF motoneurons with those of the SIF motoneurons to find distinctive criteria, which allow us to identify them in other species, including human.

The histochemical markers that were tested included antibodies detecting the presence of cytochrome oxidase (Cox), the calcium-binding protein parvalbumin (PV) and perineuronal nets, that are cell coatings composed of large aggregating chondroitin sulfate proteoglycans (CSPG) (Celio and Blümcke, 1994). All these have proved useful markers for the identification of functional cell groups in the oculomotor system (Büttner-Ennever et al., 1988; Horn et al., 1994; Horn et al., 1995; Horn and Büttner-Ennever, 1998; Horn et al., 2003). Furthermore, we used SMI32, an antibody against non-phosphorylated neurofilament

protein (NP-NF) (Sternberger and Sternberger, 1983; Sternberger, 1986), which is present in all cranial nerve nuclei and virtually all cholinergic brainstem neurons (Tsang et al., 2000). We found that the motoneurons of extraocular muscles can be divided into two groups based on their staining properties, one group corresponds to SIF motoneurons and the other to MIF motoneurons. We propose that these populations correlate with twitch motoneurons and non-twitch motoneurons.

## **Materials and methods**

All experimental procedures conformed with the state and university regulations on Laboratory Animal Care, including the Principles of Laboratory Animal Care (NIH Publication 85-23, Revised 1985), and were approved by their Animal Care Officers and Institutional Animal Care and Use Committees.

SIF and MIF motoneurons of medial rectus (MR), lateral rectus (LR) and superior oblique (SO) muscle in the monkey were either identified by a retrograde tracer injection (wheat germ agglutinin horseradish peroxidase, WGA-HRP or non-toxic cholera toxin subunit B, CTb) into respective eye muscles or by immunocytochemical staining using antibodies against choline acetyltransferase (ChAT) (Oda, 1999; Büttner-Ennever et al., 2001). The visualization of the tracer or cholinergic marker was combined with the detection of four different markers: 1. perineuronal nets, either by binding of the lectin *Wisteria floribunda agglutinin* (WFA) or antibodies against chondroitin sulfate proteoglycans (CSPG), 2. non-phosphorylated neurofilaments (NP-NF) with a specific antibody (SMI32) (Sternberger and Sternberger, 1983), 3. the calcium-binding protein parvalbumin (PV), or 4. cytochrome oxidase (Cox).

### Retrograde tracing of motoneurons after eye muscle injections

In order to identify the motoneurons of the MR and LR four macaque monkeys received tracer injections. In one animal the tracer was placed in the belly of the MR (B61) to label both MIF and SIF motoneurons, in another animal into the belly of the LR (ZK-04). Two other animals were injected in the distal tip of either the MR (Y79) or LR (Y59), which labels predominantly global MIF motoneurons (Büttner-Ennever et al., 2001), since only the fibres of the global layer insert on the tendon and the fibres of the orbital layer end before the myotendinous junction (Demer et al., 2000; Oh et al., 2001). The tracers and the injection volumes are given in table 1. For the injection the macaque monkeys were anesthetized with sodium pentobarbital (30mg/kg). Under sterile conditions, the extraocular muscles were exposed and injected as described earlier (Büttner-Ennever et al., 2001).

After a survival time of three days, the animals were killed with an overdose of Nembutal (80mg/kg body weight) and transcardially perfused with 0.9% saline (35°C) followed by 2 liters of 4% paraformaldehyde in 0.1M phosphate buffer (PB; pH 7.4) and 1 liter 10% sucrose in 0.1M phosphate buffer (pH 7.4). The brain and the eye muscles were removed from the skull and equilibrated in 20% and 30% sucrose in 0.1M PB for 6 days. The eye muscles were shock frozen in isopentane (-60°C) and kept at -20°C until cutting. The brainstem was cut at 40µm on a freezing microtome in the transverse stereotaxic plane. In order to give an estimate of the injection size, all eye muscles of the injected side were cut at 20µm and thaw-mounted onto slides (Superfrost Plus). Every tenth eye muscle section was reacted for the detection of WGA-HRP or CTb.

### Combined tracer and immunocytochemical labelling

Free-floating brainstem sections of the WGA-HRP-injection case (B61) were reacted with 0.05% diaminobenzidine tetrahydrochloride (DAB) as chromogen, which yields a brown reaction product in retrogradely labelled motoneurons. This series underwent a second

protocol for the detection of perineuronal nets by lectin-binding with *Wisteria floribunda agglutinin* (WFA). Briefly, after suppressing endogenous peroxidase activity with 3% H<sub>2</sub>O<sub>2</sub>/10% Methanol in 0,1M PBS pH 7,4 the sections were incubated with WFA (Sigma: L1766) 1:1000 for 2 hours at room temperature, followed by Extravidin-Peroxidase (1:1000) for 1 hour. The lectin was visualized with a DAB-reaction enhanced with ammonium nickel sulfate resulting in a black reaction product.

### Double-fluorescence labelling

#### *CTb and marker*

Free floating sections of all CTb-injection cases (ZK-04, Y79, Y59) were first processed for the immunofluorescent detection of the tracer. After blocking with 5% normal donkey serum in 0,1M PBS pH 7,4 containing 0,3% Triton X-100 for 1 hour, sections were incubated with goat anti-CTb (1:5000, List) overnight. Rinsed sections were then reacted with Cy<sup>2</sup>-anti-goat (1:200; Dianova) for 2 hours. After rinsing, the sections were incubated with one of the following antibodies overnight: anti-chondroitin sulfate proteoglycans (mouse anti-CSPG; 1:100; Chemicon) as a label for perineuronal nets, SMI32 (mouse SMI32, 1:900; Sternberger Monoclonals) for non-phosphorylated neurofilaments (NP-NF), anti-parvalbumin (mouse anti-PV, 1:1000; Swant), and anti-cytochrome oxidase (mouse anti-Cox, 1:100; Molecular Probes). The sections were subsequently reacted with Cy<sup>3</sup>-anti-mouse (1:200; Dianova) for two hours.

#### *ChAT and marker*

In brainstem sections from the retrograde tracing cases and three additional cases (B62, C97050, C96014), that had not received a tracer injection prior to the perfusion with 4% paraformaldehyde, all motoneurons in the oculomotor, trochlear and abducens nucleus were labelled by ChAT-immunocytochemistry (rabbit anti-ChAT, 1:500, Chemicon) and combined

with the subsequent immunofluorescent detection of perineuronal nets (with anti-CSPG), NP-NF (SMI32), PV or Cox.

### Triple-fluorescence-labelling

In order to make a judgement about the complete motoneuron population in the abducens nucleus, which must be distinguished from the intermingled non-cholinergic internuclear neurons, sections of the large LR muscle injection case (ZK-04) were stained with ChAT-antiserum in addition to the tracer detection. Sections were then treated with one of the other antibodies to show perineuronal nets, NP-NF, PV or Cox.

All triple-staining experiments on free floating sections were started by blocking with 5% normal donkey serum in 0,1M PBS pH 7,4 containing 0,3% Triton X-100 for 1 hour. Subsequently, the sections were processed with a mixture of goat anti-CTB (1:5000; List), rabbit anti-ChAT (1:500; Chemicon), and with mouse antibodies against either NP-NF (SMI32; 1:1000; Sternberger Monoclonals), PV (anti-PV; 1:1000, Swant), or mouse anti-Cox (1:100; Molecular Probes) overnight. For visualization of the applied antibodies, the sections were then reacted for 2 hours with a mixture of fluorochrome-tagged secondary donkey antibodies, namely Cy<sup>2</sup>-anti-rabbit (1:200; Dianova), Cy<sup>3</sup>-anti-mouse (1:200; Dianova), and AMCA (7-amino-4-methylcoumarin-3-acetyl)-anti-goat (1:100; Dianova). Table 2 gives an overview of the primary antibodies used in the experiments.

### Analysis of stained sections

All slides were examined with a Leica microscope DMRB (Bensheim, Germany) equipped with appropriate filters for red fluorescent Cy<sup>3</sup> (N2.1), green fluorescent Cy<sup>2</sup> or Alexa 488 (I3), and blue fluorescent AMCA (A).

Images of brightfield and fluorescence photographs were digitized by using the 3-CCD videocamera (Hamamatsu; C5810) mounted on a Leica DMRB microscope. The images were

captured on a computer with Adobe Photoshop 5 software. Sharpness, contrast, and brightness were adjusted to reflect the appearance of the labelling seen through the microscope. Overlays of double and triple fluorescent stains are produced by adding the signal of each different stain using the videocamera hardware control or by superimposing different fluorescence stains using Adobe Photoshop. The pictures were arranged and labelled with drawing software (CorelDraw 8 and 11). The labelled neurons of a series of transverse sections through the oculomotor, trochlear and abducens nucleus was plotted on the pictures taken with the 3-CCD videocamera and displayed on the computer screen using drawing software (CorelDraw 11). Each labelled neuron was analyzed for double-labelling by switching the filters of the fluorescence microscope.

#### Cell counts and cell size measurements

In order to estimate the proportion of MIF motoneurons within the complete motoneuron population, cell counts were performed on oculomotor, trochlear and abducens nucleus sections, double-immunostained for ChAT and SMI32. On every sixth section all ChAT-immunoreactive neurons with a clearly visible nucleus were counted giving the number of SIF and MIF motoneurons within the respective motor nuclei. The proportion of MIF motoneurons was calculated from cell counts of those ChAT-positive neurons, which do not express SMI32-immunoreactivity. In an attempt to relate the MIF motoneurons of the C-group in nIII to SIF motoneurons of the IR and MR, and those of the S-group to SIF motoneurons of the SR and IO, we counted these populations separately. Motoneuron subgroups within nIII of each individual eye muscle can be quite accurately outlined, because they form relatively separate cell clusters. Based on our previous study (Büttner-Ennever and Akert, 1981; Büttner-Ennever et al., 2001), we felt confident in outlining the combined SR and IO subgroup, and the combined MR (A and B group) and IR-subgroups (see Figure 2A dotted line).

Cell size measurements of SIF motoneurons (ChAT and NP-NF-staining) and presumed MIF motoneurons (ChAT without NP-NF- staining) were estimated from images captured with a 3-CCD videocamera (Hamamatsu; C5810) using an image analysis system (Optimas 6.1, Optimas Corp.). Cell sizes are given as mean diameters [(maximum cell diameter + minimum cell diameter)/2]. A two-tailed t test was used to compare cell sizes of MIF and SIF motoneurons of the three motor nuclei.

## **Results**

### Perineuronal nets and non-phosphorylated neurofilaments (NP-NF)

#### *Oculomotor nucleus*

The tracer injection into the distal tip of the medial rectus muscle (MR) resulted in the retrograde labelling of MR MIF motoneurons almost exclusively in the C-group, dorsomedial to the oculomotor nucleus (nIII) that contains the (Büttner-Ennever et al., 2001). Our large injection into the belly of the MR labelled both MIF and SIF motoneurons, in the C-group and the A- and B-group within the nIII.

The combined identification of the tracer (WGA-HRP) and perineuronal nets by WFA-lectin binding revealed that all motoneurons within the A- and B-group (brown DAB) were ensheathed by strongly labelled perineuronal nets (black DAB-Ni) (Fig. 1A, C), whereas all retrogradely labelled motoneurons of the C-group dorsomedial to the oculomotor nucleus lack perineuronal nets (Fig. 1A-B). At rostral sections, the neurons of the C-group were bordered medially by scattered neurons with prominent perineuronal nets, which form a ventral continuation of the Edinger-Westphal nucleus (EW) (Fig. 1A-B arrowheads). Some of these neurons with perineuronal nets adjacent to the C-group are cholinergic. Dorsal to the rostral part of nIII only a few neurons with perineuronal nets are intermingled with ChAT-positive, presumed preganglionic neurons in the EW, which lack perineuronal nets (Fig. 1A-B; 5A-C).

A systematic investigation of the properties of EW neurons versus MIF motoneurons of the C-group will be subject of a separate publication.

As with perineuronal net labelling, combined tract-tracing from the MR and immunostaining for NP-NFs revealed that all retrogradely labelled motoneurons within the classical oculomotor nucleus, including the A- and B-group of MR-motoneurons were strongly labelled with the SMI32-antibody (Fig. 4C-D; 6A-C). In contrast, retrogradely labelled MIF motoneurons in the C-group lack NP-NFs (Fig. 4A-B; 6A-C).

#### *Trochlear nucleus*

No tracer injections into the superior oblique muscle have been performed in this study. All data on SIF and MIF motoneurons in the trochlear nucleus are taken from double-immunolabelling experiments described below.

#### *Abducens nucleus*

After a small tracer injection into the myotendinous junction of the LR muscle (Fig. 3), retrogradely labelled motoneurons were predominantly located in an outer shell around the medial and ventromedial aspect of the abducens nucleus (nVI), as seen earlier (Büttner-Ennever et al., 2001). In addition, few retrogradely labelled neurons were found scattered within the nVI confirming occasional observations in earlier experiments (Fig. 4b in Büttner-Ennever et al., 2001).

Combined detection of perineuronal nets with CSPG-antibodies in this distal injection case revealed that all retrogradely labelled neurons including those scattered cells within nVI lack perineuronal nets. The combination of perineuronal net labelling in a tracer case with a large belly injection into the LR muscle showed that the vast majority of retrogradely labelled motoneurons within the nucleus are surrounded by prominent perineuronal nets. In addition a ‘new’ group of retrogradely labelled neurons that were not ensheathed by perineuronal nets

was detected within the nucleus. This set of motoneurons was previously unrecognized, and in tracer experiments assumed to belong to the SIF motoneuron population.

The combined detection of the tracer and non-phosphorylated neurofilaments (NP-NFs) resembled the findings with perineuronal nets: the retrogradely labelled MIF motoneurons in the periphery of nVI do not contain NP-NFs, whereas the tracer-labelled SIF motoneurons within nVI exhibit a distinct NP-NF-expression shown by the strong SMI32-immunolabelling (Fig. 4O-P). As seen with perineuronal nets, a population of retrogradely labelled motoneurons within the nucleus was detected that did not express NP-NF-labelling.

#### Parvalbumin (PV)

All motor nuclei of the extraocular muscles are highlighted by their high PV content. PV is concentrated within the cell bodies, and shows a strong neuropil labelling as well. Double-labelling of the tracer cases involving large muscle injections into the MR and LR, respectively, revealed that the PV-immunoreactivity was found at high intensity in the motoneurons of oculomotor and abducens nuclei (Fig. 4G-H). These observations were confirmed by additional triple-staining for ChAT in the abducens nucleus in order to label the complete population of SIF motoneurons. The analysis of the tracer cases with small injections into the myotendinous junction of the MR and LR revealed that the vast majority of retrogradely labelled MIF motoneurons in the C-group and in the abducens nucleus lack PV (Fig. 4E-F). However, a small number of MIF motoneurons in the C-group did exhibit a weak PV-immunoreactivity.

#### Cytochrome oxidase (Cox)

The least distinction between SIF and MIF motoneurons was seen with Cox-immunolabelling. All neurons within the oculomotor (nIII) and abducens nucleus (nVI) exhibit a strong Cox-immunoreactivity (Fig. 4M-N), as well as the EW. In contrast to immunostaining for

perineuronal nets or NP-NFs, the combined tracer-labelling experiments with distal injections into the LR and MR revealed that virtually all MIF motoneurons in the C-group and in nVI exhibit a more or less weak Cox-immunoreactivity, too (Fig. 4K-L). Internuclear neurons were presumed to be the ChAT and tracer-negative cells ensheathed by perineuronal nets. The analysis of triple-immunofluorescent staining for perineuronal nets and ChAT or tracer, revealed that Cox is present in internuclear neurons of nIII and nVI as well.

#### Complete populations of MIF motoneurons

Unlike tracer injections, which usually label only parts of the motoneuron populations, ChAT-immunolabelling visualized the complete motoneuron population, including both, SIF and MIF motoneurons in the oculomotor, trochlear and abducens nucleus. With the combined staining for ChAT and perineuronal nets or NP-NFs the complete population of MIF motoneurons in each nucleus was identified.

#### *Oculomotor nucleus (nIII)*

Using ChAT-immunolabelling additional cell groups associated with the oculomotor nucleus were labelled, such as the central caudal nucleus (CCN) containing motoneurons of the levator palpebrae muscle on caudal sections, and more rostrally the medium-sized neurons of the EW proper, presumably representing parasympathic preganglionic neurons of the pupil (Fig. 2A; 5A-C, E) (Burde and Williams, 1989; Sun and May, 1993). The combined labelling with either CSPG or SMI32 antiserum revealed clearly that all ChAT-positive MIF motoneurons in the C-group (IR and MR) lack perineuronal net and NP-NF labelling (Fig. 2A; 5A-C; 6A-C). The same was found for another population of ChAT-positive neurons more ventrally at the midline between the oculomotor nuclei, which presumably represents the MIF motoneurons of the inferior oblique (IO) and superior rectus (SR) muscle in the S-group (Fig. 2A; 5A-C; 6A-C) (Wasicky et al., 2004). In addition few scattered ChAT-positive

neurons within the oculomotor nucleus lacked perineuronal nets and NP-NF. In contrast, the vast majority of ChAT-positive neurons within the oculomotor nucleus, representing SIF motoneurons of the medial rectus (MR), inferior rectus (IR), superior rectus (SR) and inferior oblique (IO) muscles, were ensheathed by distinct perineuronal nets and were strongly labelled by SMI32 (Fig. 2A; 5A-C; 6A-C).

Whereas a small number of ChAT-negative neurons with strong perineuronal net labelling was found scattered within the oculomotor nucleus (Fig. 5A-C, asterisks), NP-NF-expression was always confined to cholinergic neurons (Fig. 6A-C). Therefore the combined detection of ChAT and NP-NFs with the SMI32-antibody was found to be well suited to identify the complete populations of SIF and MIF motoneurons in the oculomotor nucleus. The cell counts of the double-labelled sections revealed that the MIF motoneurons (SMI32-negative) of MR and IR within the C-group make up 20% of the total motoneuron population of the MR and IR (1454 cells were counted on every sixth section). Similarly, MIF motoneurons of the IO and SR within the S-group make up 21% of the total motoneuron population of the IO and SR (811 cells were counted on every sixth section). The morphometric analysis revealed that the mean cell diameters of MIF motoneurons in the C-group, ranging from 19.3 $\mu$ m – 38.2 $\mu$ m (mean = 27.1 $\mu$ m; SD = 3.9; N=57), were significantly smaller ( $p < 0.001$ ) than those of MR and IR SIF motoneurons, which ranged from 24.8 $\mu$ m – 45.5 $\mu$ m (mean = 35.1 $\mu$ m; SD = 4.0; N = 108). Similarly, the mean cell diameters of MIF motoneurons in the S-group, ranging from 20.3-40.3 $\mu$ m (mean = 29.0 $\mu$ m; SD = 3.8; N=58), were significantly smaller ( $p < 0.001$ ) than those of SR and IO SIF motoneurons, which ranged from 25.9 $\mu$ m – 46.6 $\mu$ m (mean = 34.9 $\mu$ m; SD = 3.6; N = 120).

#### *Trochlear nucleus (nIV)*

In the trochlear nucleus (nIV) no retrograde tracer labelling, but only ChAT-immunolabelling was used for the identification of motoneurons. All neurons within nIV are ChAT-

immunoreactive and delineate the nucleus clearly within the mesencephalic tegmentum. On caudal and central planes, combined immunolabelling for the presence of perineuronal nets or NP-NFs, with CSPG- or SMI32-antibodies, respectively, revealed that all motoneurons in nIV are double-labelled with CSPG and SMI32 except a small cell cluster in the dorsal cap, which lacks perineuronal nets and NP-NF expression (Fig. 2B; 5D; 6D). This dorsal group corresponds exactly to the population of retrogradely labelled neurons seen after a tracer injection into the myotendinous junction of the superior oblique muscle, and is therefore assumed to be MIF motoneurons (Büttner-Ennever et al., 2001). On further rostral planes, the MIF motoneurons were more scattered (Fig. 5E; 6E). The cell counts within nIV revealed that NP-NF-lacking MIF motoneurons make up 19% of all motoneurons (426 cells were counted on every sixth section). The mean cell diameters of MIF motoneurons in the dorsal cap ranged from 26.9 $\mu$ m – 41.4 $\mu$ m (mean = 31.4 $\mu$ m; SD = 3.; N = 47) and were significant smaller ( $p < 0.001$ ) compared to those of superior oblique SIF motoneurons, which ranged from 27.8 $\mu$ m – 50.6 $\mu$ m (mean = 37.6 $\mu$ m; SD = 4.0; N = 122).

#### *Abducens nucleus (nVI)*

With ChAT-immunolabelling the complete population of motoneurons (SIF motoneurons and MIF motoneurons) was visualized and could be distinguished from internuclear neurons, which are as large as motoneurons and lie intermingled with motoneurons, but are not cholinergic (Spencer and Baker, 1986; Carpenter et al., 1992). As shown by tracer-labelling, a small population of ChAT-immunoreactive neurons that were not ensheathed by perineuronal nets and being devoid of NP-NF-labelling was located in the periphery of the abducens nucleus identifying them as MIF motoneurons (Fig. 2C; 5F-G; 6F-G). In contrast to the MIF motoneurons in the C- and S-group of the oculomotor nucleus and the dorsal cap of the trochlear nucleus, those of the LR are not clustered within a compact cell group, but are rather scattered around the periphery of the abducens nucleus. As in the muscle belly tracer-case, a

considerable portion of ChAT-positive neurons, which lack perineuronal nets and NP-NFs, are located within the nucleus as well (Fig. 4Q-R; 5F-H; 6F-H). These neurons with “MIF properties” within the abducens nucleus do not differ morphologically from those in the periphery, both consisting of predominantly small, fusiform neurons, rarely medium-sized neurons as described earlier for the peripheral group (Büttner-Ennever et al., 2001). The mean cell diameters of LR MIF motoneurons around the periphery of nVI ranged from 27.1 $\mu$ m – 45.4 $\mu$ m (mean 34.6 $\mu$ m; SD = 4.7; N = 52). The mean diameter of the central ‘MIF-like’ motoneurons within nVI, which lack perineuronal nets and NP-NFs, ranged from 27.6 $\mu$ m – 50.5 $\mu$ m (mean = 37.8 $\mu$ m; SD = 4.9; N = 42). The LR SIF motoneurons were slightly larger (32.2 $\mu$ m – 50.8 $\mu$ m; mean = 40.7 $\mu$ m; SD = 4.0; N = 124). Both MIF motoneuron populations were significantly smaller than SIF motoneurons ( $p < 0.001$ ). Moreover, central ‘MIF-like’ motoneurons seem to be larger than peripheral MIF motoneurons ( $p = 0.002$ ).

The complete population of MIF motoneurons in the abducens nucleus lacking NP-NF make up 21% of all cholinergic motoneurons (606 cells were counted on every sixth section).

Whereas NP-NF expression was confined to ChAT-positive neurons, a major ChAT-negative neuron population with prominent perineuronal nets is present within the abducens nucleus - presumably representing internuclear and paramedian tract neurons (Fig. 4R, small arrows) (Baker and Highstein, 1975; Steiger and Büttner-Ennever, 1978; Büttner-Ennever and Akert, 1981; Büttner-Ennever and Horn, 1996). A systematic description of the histochemical properties and distribution of the other functional cell groups within the abducens nucleus will be reported separately.

## **Discussion**

The results demonstrate that identified motoneurons of extraocular MIFs differ from those of SIFs in their histochemical properties - a reflection of their differing physiology and function. The complete populations of these two different motoneuron types were identified by combined immunostaining for choline acetyltransferase (ChAT) and perineuronal nets or non-phosphorylated neurofilaments (NP-NFs). All motoneurons were cholinergic, but SIF motoneurons possessed perineuronal nets and contained NP-NFs, whereas motoneurons of the MIFs lacked both. In the following discussion we will first consider the basis of the histochemical differences of SIF and MIF motoneurons, and then we will discuss which functional motoneuron populations can be identified with these methods.

### **Histochemical properties of extraocular motoneurons**

#### *I. Cytochrome oxidase (Cox), parvalbumin (PV) and perineuronal net labelling (CSPG)*

It was not a surprising finding that SIF motoneurons are strongly Cox- and PV-immunoreactive, and that they are ensheathed by prominent perineuronal nets. Numerous studies in different neuronal systems have shown that the distribution of PV matches well that of Cox activity, both being concentrated in neurons with high metabolic energy consumption (e.g. Baimbridge et al., 1992; Blümcke and Celio, 1992). Furthermore, PV-immunoreactive neurons are often associated with perineuronal nets (Härtig et al., 1994; Horn et al., 2003), whereby the function of the perineuronal nets is still unclear (e.g. Hockfield et al., 1990; Okamoto et al., 1994; Brückner et al., 1999). One hypothesis suggests that perineuronal nets are preferably associated with highly active neurons (Brückner et al., 1993), such as those found in the rat medial septum and in functional neurons of the primate saccadic system (Morris and Henderson, 2000; Horn et al., 2003). In contrast, slow modulatory neurons lack perineuronal nets (Brückner et al., 1994; Hobohm et al., 1998).

Our work demonstrates that presumed MIF motoneurons are not ensheathed by perineuronal nets. This may reflect their different firing characteristics compared to SIF motoneurons. There is general agreement that twitch units innervate the SIFs, and the non-twitch units innervate global MIFs (Lennerstrand, 1975; Nelson et al., 1986). MIF (non-twitch) motoneurons have not been recorded in primates, but their firing characteristics may be deduced from studies in frog and cat, where non-twitch units were described (Dieringer and Precht, 1986; Goldberg et al., 1981; Nelson et al., 1986; Shall and Goldberg, 1992). In frog non-twitch units were shown to fire tonically at around 50 Hz (Dieringer and Precht, 1986). Therefore the relative lack of PV and complete absence of perineuronal nets around MIF motoneurons fits well with their presumed slow firing pattern. Our findings correspond to the observations of May and Fratkin (2002), who did not detect PV-immunoreactivity in the C-group of the primate.

The "burst-tonic" pattern of activity recorded from motoneurons in behaving animals probably arises from SIF motoneurons, although in none of these studies has a distinction been made between SIF and MIF motoneurons (Robinson, 1970; Keller and Robinson, 1972; Delgado-Garcia et al., 1986a). Recording of lateral rectus motoneurons in monkey demonstrated that most abducens motoneurons had maximal burst firing rates of 300-400 Hz, some of which could reach rates as high as 800 Hz (Fuchs and Luschei, 1971; Fuchs et al., 1988), which requires a remarkable high level of metabolic activity and could explain our histochemical findings, the presence of Cox, PV and perineuronal nets in SIF motoneurons.

The immunocytochemical detection of cytochrome oxidase (Cox) in our study has not proved a suitable marker for the distinction between both motoneuron groups, since all motoneurons including MIF motoneurons were more or less labelled. These findings differ from the observations made by May and Fratkin (2002), who showed that Cox activity is absent from the neurons of the C-group, whereas the motoneurons within the oculomotor nucleus are labelled. These discrepancies are likely due differences in the detection methods for Cox. We

used the immunocytochemical detection of Cox, whereas May and Fratkin (2002) visualized the enzymatic activity of Cox. It is likely that the enzyme activity, rather than the presence of the enzyme, correlates better with the firing characteristics of the motoneurons, and would explain the different picture seen for MIF motoneurons.

Finally, in spite of the various histochemical differences seen between SIF and MIF motoneurons, no staining differences could be found between the two seemingly independent A- and B-subgroups of MR in the present study. Many animals have a dorsal B- and a ventral A-group of MR motoneurons, but in the monkey the A-group is particularly evident, and its neurons tend to be smaller than those of the B-group (Büttner-Ennever and Akert, 1981; McClung et al., 2001). Up to now, no difference in afferent projections or efferent targets has been found between the A- and B-groups.

## *II. Non-phosphorylated neurofilaments (NP-NFs)*

The NP-NF labelling with the SMI32-antibody was surprisingly specific for the SIF motoneuron population, and was not detected in any other cell type in the ocular motor nuclei. NP-NF labelling was reported as a reliable marker for motoneurons, but that it is not restricted to this cell type (Tsang et al., 2000). The lack of NP-NF labelling in MIF motoneurons in our study demonstrates, that NP-NF cannot be used as a marker for all motoneurons.

The presumed internuclear neurons, identified as being ChAT-negative but with perineuronal nets (see Fig. 5), also lacked NP-NFs. Since internuclear and motoneurons have a similar cell size profile and similar firing patterns (McCrea et al., 1986; Delgado-Garcia et al., 1986a; Delgado-Garcia et al., 1986b; Fuchs et al., 1988), the presence of NP-NFs cannot be correlated with unit activity or cell size as suggested by Campell and Morrison (1989).

Taken together, the present results indicate that within the motoneuronal populations of the extraocular muscles, the presence of NP-NFs shown by SMI32-immunoreactivity serves as a selective marker for SIF motoneurons and does not include MIF motoneurons.

*Are there two populations of MIF motoneurons?*

With combined ChAT and perineuronal nets, or NP-NF-labelling, the MIF motoneurons of all eye muscles could be identified simultaneously, whereas in tracing experiments, which are always confined to one muscle, far fewer MIF motoneurons are seen.

It was a consistent observation in the present and previous study (Büttner-Ennever et al., 2001) that a distal tracer injection into the myotendinous junction of extraocular muscles, which targets primarily the global layer in primates (Demer et al., 2000; Oh et al., 2001), labelled mainly the MIF motoneurons around the periphery of the classical motor nuclei, in the C-, S-groups, dorsal cap of nIV and the medial aspect of nVI. However a few scattered neurons could often be found within the boundaries of the motor nuclei as well. Our experiments demonstrate that these central motoneurons share the histochemical properties of MIF motoneurons in the periphery, suggesting that both groups share physiological characteristics. Since the tracer uptake area did not involve the central endplate zones of global or orbital muscle fibres (see Fig. 3), these central motoneurons with histochemical ‘MIF properties’ are more likely to be MIF motoneurons, rather than atypical SIF motoneurons as suggested by their location.

Large tracer injections involving the global and orbital layer, or our combined histochemical methods, revealed a surprisingly large population of central motoneurons with ‘MIF properties’, most obvious in nVI (Fig. 5F-H; 6F-H). These central cells with ‘MIF properties’ could be ‘displaced’ global MIF motoneurons, but it seems more probable that they are the MIF motoneurons innervating the orbital layer, whose location is up to now unknown. If the central ‘MIF-like’ motoneurons are considered as an individual cell group, than they appear to be slightly larger than peripheral MIF motoneurons.

Tracing experiments with selective injections into the orbital layer combined with histochemical stains are necessary to conclusively resolve this question.

### Quantitative aspects of MIF motoneurons

Although the MIF motoneurons of all motor nuclei were found to be smaller than SIF motoneurons (see also Büttner-Ennever et al., 2001; McClung et al., 2001), the different histochemical properties for both populations is far more striking than their morphological differences. Our estimates on the complete populations of MIF motoneurons indicated that the proportion of approximately 20% MIF motoneurons within the total motoneuron population is constant for abducens, trochlear and oculomotor nuclei. Cell counts for each individual eye muscle within the oculomotor nucleus could not be performed with our methods, but the estimates of 20% hold true for the muscle pairs with synergistic actions: IR and MR in vergence, IO and SR in upgaze. Apart from this restriction, we found a noteworthy consistency in the proportion of SIF to MIF motoneurons for individual eye muscles. In some ways these figures resemble the data of 20% MIFs to 80% SIFs for whole muscle fibre counts (for review: Porter et al., 1995). However the relationship between these percentages is unclear because of the complexities of motor unit structure (Shall and Goldberg, 1992) and polyneuronal innervation of MIFs (Jacoby et al., 1989).

### **Conclusion**

The present work provides more evidence that the MIF motoneurons of extraocular muscles, innervating presumed non-twitch muscle fibres, are a specialized cell group and have different histochemical properties than SIF motoneurons. The best marker for MIF motoneurons within the complete motoneuron population is the lack of perineuronal nets and non-phosphorylated neurofilaments. On the other hand, the labelling of NP-NFs with SMI32 is a selective marker for SIF motoneurons. Perineuronal nets are present around SIF motoneurons and internuclear neurons within the oculomotor and abducens nucleus, and alone are not suited for the specific identification of SIF motoneurons. These histochemical properties of SIF motoneurons and MIF motoneurons appear to be a general feature in mammals as seen in preliminary

observations in rat and human (Eberhorn et al., 2003). A possible segregation of orbital and global MIF motoneuron populations must be investigated by further studies.

### **Acknowledgements**

The authors thank Drs. Sergej Yakushin (Mount Sinai Hospital, New York) and Bernhard Hess (Dept. Neurology, University of Zürich) for the collaboration and generous supply of primate muscle and brain tissue. We are grateful to Prof. Lange for his continuous support and to Ahmed Messoudi and Christina Glombik for their excellent technical expertise.

## Literature cited

- Akert K, Glicksman MA, Lang W, Grob P, Huber A. 1980. The Edinger-Westphal nucleus in the monkey. A retrograde tracer study. *Brain Res* 184:491-498.
- Baimbridge KG, Celio MR, Rogers JH. 1992. Calcium-binding proteins in the nervous system. *Trends Neurosci* 15:303-308.
- Baker R, Highstein SM. 1975. Physiological identification of interneurons and motoneurons in the abducens nucleus. *Brain Res* 91:292-298.
- Blümcke I, Celio MR. 1992. Parvalbumin and calbindin D-28k immunoreactivities coexist within cytochrome oxidase-rich compartments of squirrel monkey area 18. *Exp Brain Res* 92:39-45.
- Bondi AY, Chiarandini DJ. 1983. Morphologic and electrophysiologic identification of multiply-innervated fibers in rat extraocular muscles. *Invest Ophthalmol Vis Sci* 24:516-519.
- Brückner G, Brauer K, Härtig W, Wolff JR, Rickmann MJ, Derouiche A, Delpech B, Girard D, Oertel WH, Reichenbach A. 1993. Perineuronal nets provide a polyanionic, glia-associated form of microenvironment around certain neurons in many parts of the rat brain. *Glia* 8:3183-3200.
- Brückner G, Hausen D, Härtig W, Drlicek M, Arendt T, Brauer K. 1999. Cortical areas abundant in extracellular matrix chondroitin sulphate proteoglycans are less affected by cytoskeletal changes in Alzheimer's disease. *Neurosci* 92:791-805.
- Brückner G, Schütz A, Härtig W, Brauer K, Paulke BR, Bigl V. 1994. Projection of non-cholinergic basal forebrain neurons ensheathed with perineuronal nets to rat mesocortex. *J Chem Neuroanat* 8:11-18.
- Burde RM, Williams F. 1989. Parasympathetic nuclei. *Brain Res* 498:371-375.
- Büttner-Ennever JA, Akert K. 1981. Medial rectus subgroups of the oculomotor nucleus and their abducens internuclear input in the monkey. *J Comp Neurol* 197:17-27.
- Büttner-Ennever JA, Cohen B, Pause M, Fries W. 1988. Raphe nucleus of the pons containing omnipause neurons of the oculomotor system in the monkey, and its homologue in man. *J Comp Neurol* 267:307-321.
- Büttner-Ennever JA, Horn AKE. 1996. Pathways from cell groups of the paramedian tracts to the floccular region. *N Y Acad Sci* 781:532-540.
- Büttner-Ennever JA, Horn AKE, Scherberger H, D'Ascanio P. 2001. Motoneurons of twitch and nontwitch extraocular muscle fibers in the abducens, trochlear, and oculomotor nuclei of monkeys. *J Comp Neurol* 438:318-335.
- Campbell MF, Morrison JH. 1989. Monoclonal antibody to neurofilament protein (SMI-32) labels a subpopulation of pyramidal neurons in the human and monkey neocortex. *J Comp Neurol* 282:191-205.
- Carpenter MB, Periera AB, Guha N. 1992. Immunocytochemistry of oculomotor afferents in the squirrel monkey (*Saimiri Sciureus*). *J Hirnforsch* 33:151-167.

- Celio MR, Blümcke I. 1994. Perineuronal nets – a specialized form of extracellular matrix in the adult nervous system. *Brain Res Rev* 19:1128-1145.
- Chiarandini DJ, Stefani E. 1979. Electrophysiological identification of two types of fibres in rat extraocular muscles. *J Physiol* 290:453-465.
- Clarke RJ, Alessio ML, Pessoa VF. 1987. Distribution of motoneurons innervating extraocular muscles in the brain of the marmoset (*Callithrix jacchus*). *Acta Anat* 130:191-196.
- Clendaniel RA, Mays LE. 1994. Characteristics of antidromically identified oculomotor internuclear neurons during vergence and versional eye movements. *J Neurophysiol* 71:1111-1127.
- Davidowitz J, Chiarandini DJ, Philips G, Breinin GM. 1982. Morphological variation along multiply-innervated fibers of rat extraocular muscles. In: *Functional Basis of Ocular Motility Disorders*. Lennerstrand G, Zee DS, Keller EL, New York: Pergamon, pp. 17-26.
- Delgado-Garcia JM, Del Pozo F, Baker R. 1986a. Behavior of neurons in the abducens nucleus of the alert cat. I. Motoneurons. *Neurosci* 17:929-952.
- Delgado-Garcia JM, Del Pozo F, Baker R. 1986b. Behavior of neurons in the abducens nucleus of the alert cat. II. Internuclear neurons. *Neurosci* 17:953-973.
- Demer JL. 2002. The orbital pulley system: A revolution in concepts of orbital anatomy. *Ann N Y Acad Sci* 956:17-32.
- Demer JL, Yeul Oh S, Poukens V. 2000. Evidence for active control of rectus extrocular muscle pulleys. *Invest Ophthal Vis Sci* 41:1280-1290.
- Dieringer N, Precht W. 1986. Functional organization of eye velocity and eye position signals in abducens motoneurons of the frog. *J Comp Physiol* 158:179-194.
- Eberhorn, A., Horn, A., Messoudi, A., Büttner-Ennever, J (2003). Twitch and non-twitch motoneurons of extraocular muscles have different histochemical properties. *Soc Neurosci Abstr*.33:391.18.
- Fuchs AF, Luschei ES. 1971. Development of isometric tension in simian extraocular muscle. *J Physiol* 219:155-166.
- Fuchs AF, Scudder CA, Kaneko CR. 1988. Discharge patterns and recruitment order of identified motoneurons and internuclear neurons in the monkey abducens nucleus. *J Neurophysiol* 60:1874-1895.
- Gamlin PDR, Gnadt JW, Mays LE. 1989. Abducens internuclear neurons carry an inappropriate signal for ocular convergence. *J Neurophysiol* 62:70-81.
- Goldberg SJ, Clamann HP, McClung JR. 1981. Relation between motoneuron position and lateral rectus motor unit contraction speed: an intracellular study in the cat abducens nucleus. *Neurosci Lett* 23:49-54.
- Härtig W, Brauer K, Bigl V, Brückner G. 1994. Chondroitin sulfate proteoglycan-immunoreactivity of lectin-labeled perineuronal nets around parvalbumin-containing neurons. *Brain Res* 635:307-311.

- Hobohm C, Härtig W, Brauer K, Brückner G. 1998. Low expression of extracellular matrix components in rat brain stem regions containing modulatory aminergic neurons. *J Chem Neuroanat* 15:135-142.
- Hockfield S, Kalb RG, Zaremba S, Fryer H. 1990. Expression of neural proteoglycans correlates with the acquisition of mature neuronal properties in the mammalian brain. *Cold Spring Harbor Symp Quant Biol* 55:505-514.
- Horn AKE, Brückner G, Härtig W, Messoudi A. 2003. Saccadic omnipause and burst neurons in monkey and human are ensheathed by perineuronal nets but differ in their expression of calcium-binding proteins. *J Comp Neurol* 455:341-352.
- Horn AKE, Büttner-Ennever JA. 1998. Premotor neurons for vertical eye-movements in the rostral mesencephalon of monkey and man: the histological identification by parvalbumin immunostaining. *J Comp Neurol* 392:413-427.
- Horn AKE, Büttner-Ennever JA, Suzuki Y, Henn V. 1995. Histological identification of premotor neurons for horizontal saccades in monkey and man by parvalbumin immunostaining. *J Comp Neurol* 359:350-363.
- Horn AKE, Büttner-Ennever JA, Wahle P, Reichenberger I. 1994. Neurotransmitter profile of saccadic omnipause neurons in nucleus raphe interpositus. *J Neurosci* 14:2032-2046.
- Ishikawa S, Sekiya H, Kondo Y. 1990. The center for controlling the near reflex in the midbrain of the monkey: a double labelling study. *Brain Res* 519:217-222.
- Jacoby J, Chiarandini DJ, Stefani E. 1989. Electrical properties and innervation of fibers in the orbital layer of rat extraocular muscles. *J Neurophysiol* 61:116-125.
- Keller EL, Robinson DA. 1972. Abducens unit behavior in the monkey during vergence movements. *Vision Res* 12:369-382.
- Lennerstrand G. 1974. Electrical activity and isometric tension in motor units of the cat's inferior oblique muscle. *Acta Physiol Scand* 91:458-474.
- Lennerstrand G. 1975. Motor units in eye muscles. In Lennerstrand G and Bach-Y-Rita P, editors. *Basic mechanisms of ocular motility and their clinical implications*. Oxford; New York; Toronto; Sidney; Paris; Braunschweig: Pergamon Press. p 119-143.
- Lynch GS, Frueh BR, Williams DA. 1994. Contractile properties of single skinned fibres from the extraocular muscles, the levator and superior rectus, of the rabbit. *J Physiol* 475:337-46.
- Maciewicz R, Phipps BS. 1983. The oculomotor internuclear pathway: a double retrograde labeling study. *Brain Res* 262:1-8.
- May PJ, Fratkin JD. 2002. Identification of the Edinger-Westphal nucleus in primates by means of multiple markers. *Invest Ophthalmol Vis Sci* 43: 1488
- Mayr R, Gottschall J, Gruber H, Neuhuber W. 1975. Internal structure of cat extraocular muscle. *Anat Embryol* 148:25-34.

- McClung JR, Shall MS, Goldberg J. 2001. Motoneurons of the lateral and medial rectus extraocular muscles in squirrel monkey and cat. *Cell Tiss Org* 168:220-227.
- McCrea RA, Strassman A, Highstein SM. 1986. Morphology and physiology of abducens motoneurons and internuclear neurons intracellularly injected with horseradish peroxidase in alert squirrel monkeys. *J Comp Neurol* 243:291-308.
- Morgan DL, Proske U. 1984. Vertebrate slow muscle: its structure, pattern of innervation, and mechanical properties. *Physiol Rev* 64:103-138.
- Morris NP, Henderson Z. 2000. Perineuronal nets ensheath fast spiking, parvalbumin-immunoreactive neurons in the medial septum/diagonal band complex. *Eur J Neurosci* 12:828-838.
- Nelson JS, Goldberg SF, McClung JR. 1986. Motoneuron electrophysiological and muscle contractile properties of superior oblique motor units in cat. *J Neurophysiol* 55:715-726.
- Oda Y. Choline acetyltransferase: The structure, distribution and pathologic changes in the central nervous system. *Pathol Internat* 49, 921-937. 1999.
- Oh SY, Poukens V, Demer JL. 2001. Quantitative analysis of rectus extraocular muscle layers in monkey and human. *Invest. Ophthalmol Vis Sci* 42:10-16.
- Okamoto M, Mori S, Endo H. 1994. A protective action of chondroitin sulphate proteoglycans against neuronal cell death induced by glutamate. *Brain Res* 637:57-67.
- Pachter BR. 1984. Rat extraocular muscle. 3. Histochemical variability along the length of multiply-innervated fibers of the orbital surface layer. *Histochem* 80:535-538.
- Porter JD, Baker RS, Ragusa RJ, Brueckner JK. 1995. Extraocular muscles: basic and clinical aspects of structure and function. *Surv Ophthalmol* 39:451-484.
- Robinson DA. 1970. Oculomotor unit behavior in the monkey. *J Neurophysiol* 38:393-404.
- Shall MS, Goldberg SJ. 1992. Extraocular motor units - type classification and motoneuron stimulation frequency-muscle unit force relationships. *Brain Res* 587:291-300.
- Shall MS, Dimitrova DM, Goldberg SJ. 2003. Extraocular motor unit and whole-muscle contractile properties in the squirrel monkey. *Exp Brain Res* 151:338-345.
- Spencer RF, Baker R. 1986. Histochemical localization of acetylcholinesterase in relation to motor neurons and internuclear neurons of the cat abducens nucleus. *J Neurocytol* 15:137-154.
- Spencer RF, Porter JD. 1981. Innervation and structure of extraocular muscles in the monkey in comparison to those of the cat. *J Comp Neurol* 198:649-665.
- Spencer RF and Porter JD. 1988. Structural organization of the extraocular muscles. In Büttner-Ennever JA, editor. *Neuroanatomy of the oculomotor system*. Amsterdam; New York; Oxford; Elsevier. p 33-79.

Steiger HJ, Büttner-Ennever JA. 1978. Relationship between motoneurons and internuclear neurons in the abducens nucleus: a double retrograde tracer study in the cat. *Brain Res* 148:181-188.

Sternberger LA. 1986. *Immunocytochemistry*. New York: Wiley.

Sternberger LA, Sternberger NH. 1983. Monoclonal antibodies distinguish phosphorylated and non-phosphorylated forms of neurofilaments in situ. *Proc Natl Acad Sci* 80:6126-6130.

Sun WS, May PJ. 1993. Organization of the extraocular and preganglionic motoneurons supplying the orbit in the lesser galago. *Anat Rec* 237:89-103.

Tsang YM, Chiong F, Kuznetsov D, Kasarskis E, Geula C. 2000. Motor neurons are rich in non-phosphorylated neurofilaments: cross-species comparison and alterations in ALS. *Brain Res* 861:45-58.

Wasicky R, Horn AKE, Büttner-Ennever JA. 2004. Twitch and non-twitch motoneuron subgroups of the medial rectus muscle in the oculomotor nucleus of monkeys receive different afferent projections. *J Comp Neurol* 479: 117-129

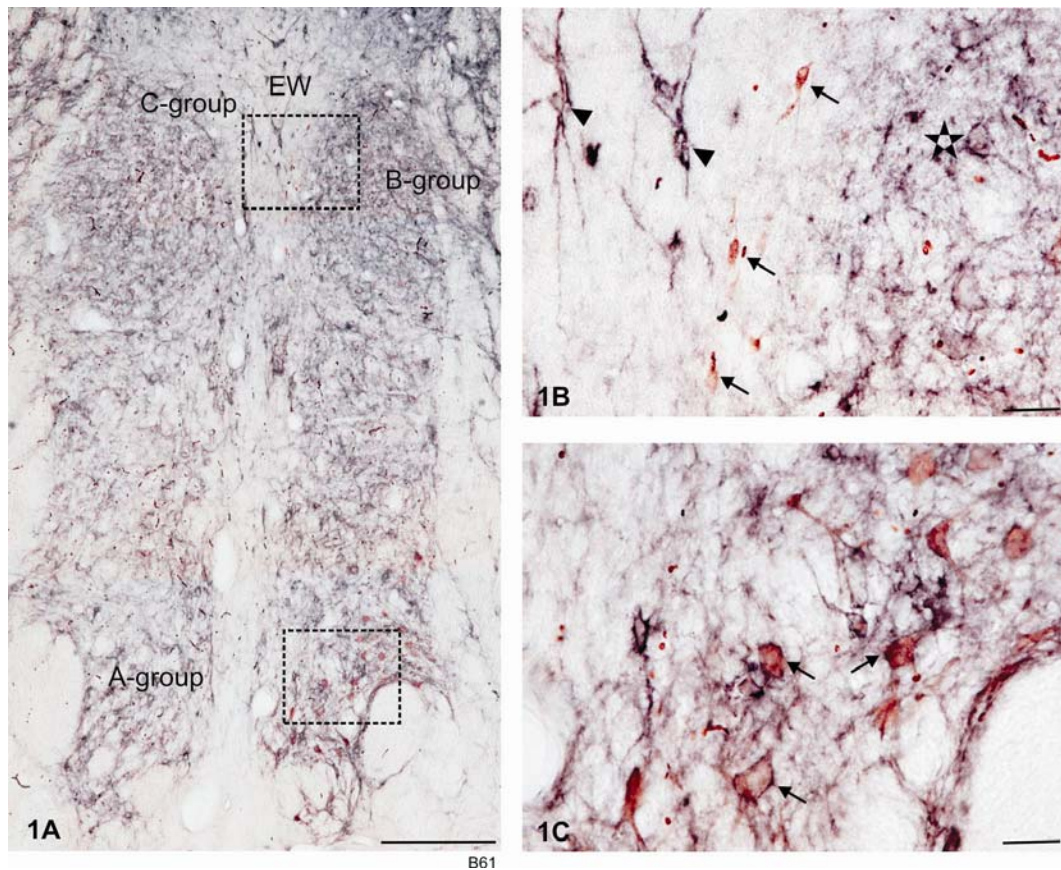


Fig. 1. A-C: Transverse section through nIII with the combined labelling of the retrograde tracer (WGA-HRP, brown) and perineuronal nets (WFA, black) after a large tracer injection into the belly of MR. A: Low-power photomicrograph of nIII showing the retrogradely labelled neurons (brown) within the A-, B- and C-group. B: Detailed view of the upper rectangle in A demonstrating that tracer-labelled motoneurons in the C-group (brown, arrows) lack perineuronal nets. Note that the C-group is medially bordered by neurons that are continuous with the Edinger-Westphal nucleus (EW) and are ensheathed by prominent perineuronal nets (arrowhead) and laterally by the twitch motoneurons of nIII displaying strong perineuronal labelling (asterisk). C: Detailed view of the lower rectangle in A showing the tracer-labelled twitch motoneurons of the A-group, which are all ensheathed by black perineuronal net (arrows). Scale bar in 1A is 500 $\mu$ m, in 1B and 1C 50 $\mu$ m.

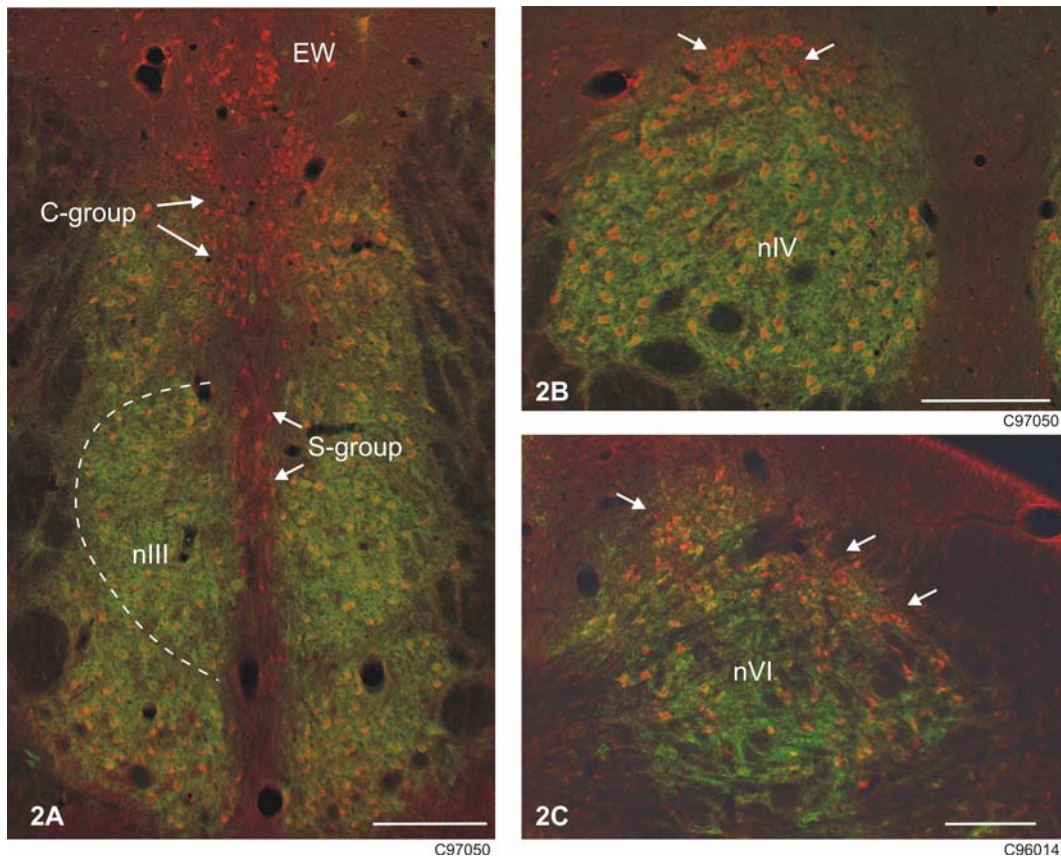


Fig. 2. Photomicrographs of transverse sections at the level of the oculomotor (A), trochlear (B) and abducens nucleus (C) that were double-labelled for ChAT (red) and perineuronal nets (green). A: All motoneurons and the preganglionic neurons in the Edinger-Westphal are ChAT-positive (red). Only the SIF motoneurons within the nucleus are ensheathed by perineuronal nets (green), whereas MIF motoneurons in the C-group lack perineuronal nets. Note that an additional group of ChAT-positive neurons on the midline is not ensheathed by perineuronal nets at the location of the S-group. B: Left trochlear nucleus. MIF motoneurons that lack perineuronal nets are located in a dorsal cap of the trochlear nucleus (arrows) in this plane of section. C: Left abducens nucleus. The MIF motoneurons lacking perineuronal nets are not located in a compact group, but lie scattered around the periphery of the nucleus (arrows). Scale bar is 500µm.

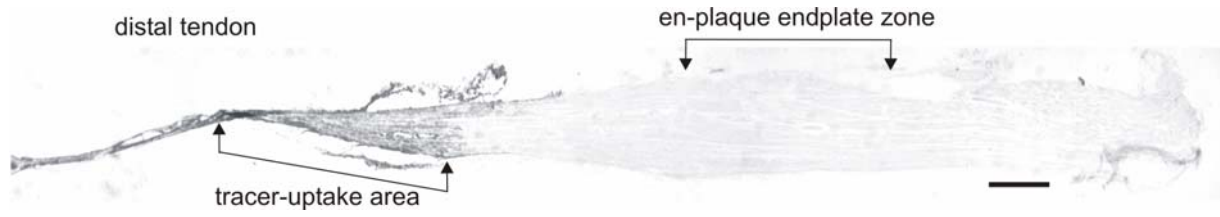
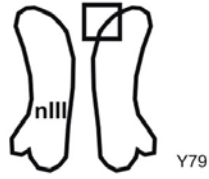
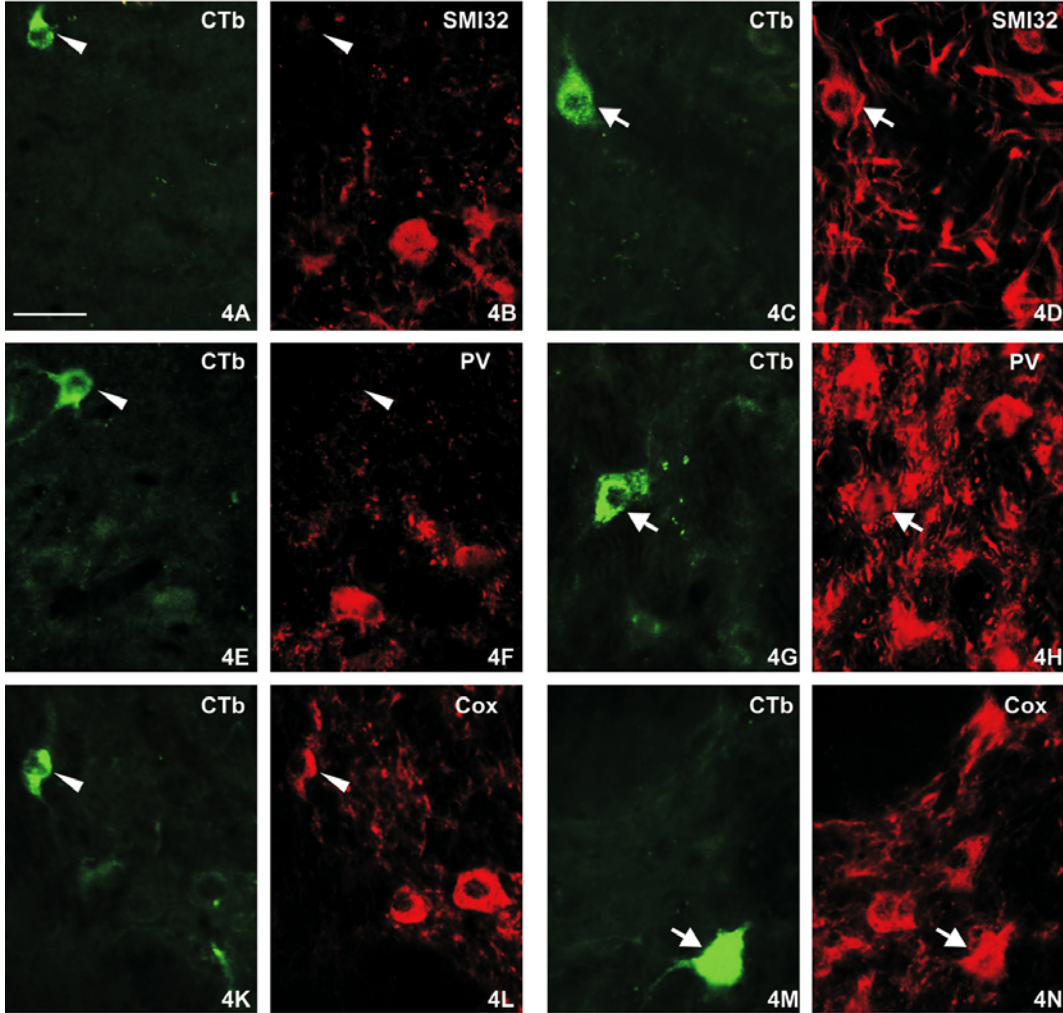


Fig. 3. Photomicrograph of the CTb-injected LR. The tracer-uptake area after the CTb-injection into the myotendinous junction is confined to the distal part of the muscle, whereas the central 'en-plaque' endplate zone shows no tracer labelling. Scale bar is 100 $\mu$ m.

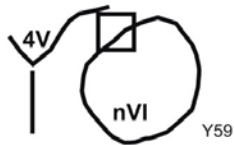
MIF motoneurons



SIF motoneurons



MIF motoneurons



SIF and MIF motoneurons

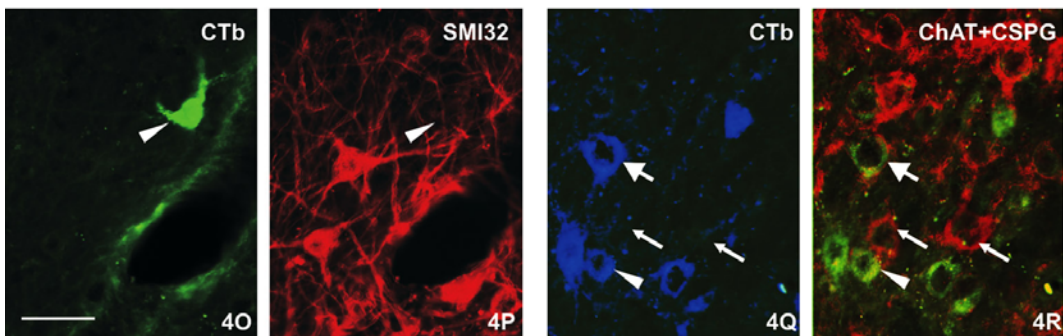
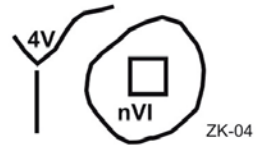


Fig. 4. A-N: High magnifications of transverse sections through the oculomotor nucleus (nIII) demonstrating the retrogradely labelled MIF motoneurons (green) after a small CTb-injection into the distal MR combined with immunofluorescence for one of the following antibodies (red): SMI32-staining for NP-NF (B), PV (F), and Cox (L). Each pair of neighbouring photographs shows the same section illustrated to demonstrate for different antigens. Note that the tracer-positive MIF motoneurons (green) lack SMI32- and PV-immunoreactivity (A-B, E-F), whereas the tracer-positive SIF motoneurons (green) within the oculomotor nucleus are SMI32- and PV-positive (C-D, G-H). In contrast both, MIF motoneurons (K) and SIF motoneurons (M) are Cox-positive (L, N). 4 O-R: High magnifications of transverse sections through the abducens nucleus (nVI). The CTb-positive MIF motoneurons (O; green; arrowhead) from a distal tracer injection into the LR lacks non-phosphorylated neurofilaments (P; SMI32; red; arrowhead). It is located in the periphery of the classical nVI. After a large CTb-injection into the muscle belly of LR both, MIF motoneurons (Q-R; arrowheads) and SIF motoneurons (Q-R; arrows) in the central part of nVI are CTb-positive (Q). The small arrows indicate internuclear neurons, which lack both, the tracer and ChAT-immunoreactivity (Q-R), but are surrounded by prominent red perineuronal nets (R). Scale bar is 30 $\mu$ m.

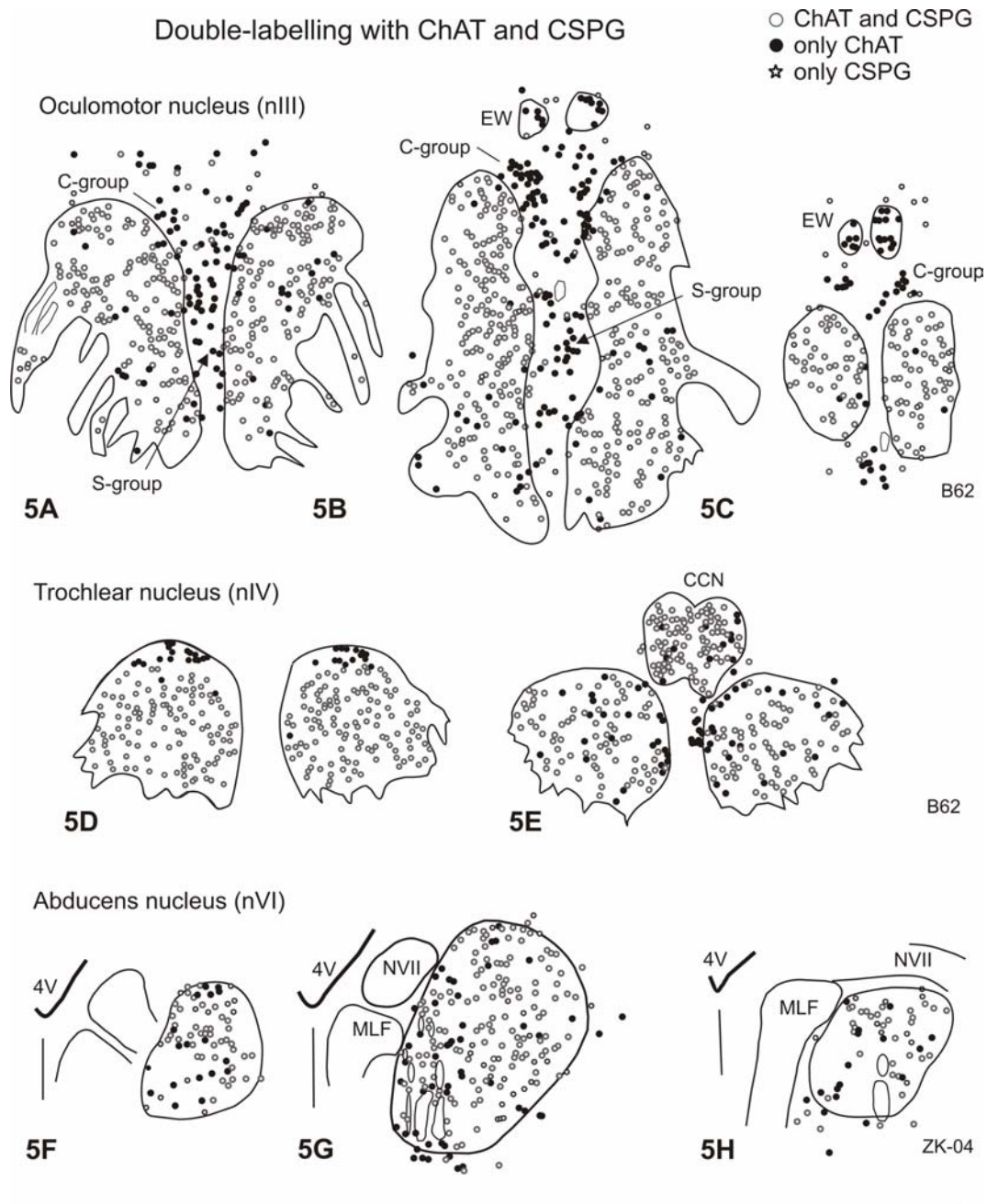


Fig. 5. Plots of transverse sections of nIII (A-C), nIV (D-E) and nVI (F-H), the outlines are drawn after subsequently treating the sections with Nissl stain. The sections were double-labelled for ChAT and perineuronal nets (CSPG). SIF motoneurons (open circle) are both, ChAT- and CSPG-positive, whereas MIF motoneurons (filled circle) lack CSPG. In nIII (F-H), the SIF motoneurons form the classical nucleus, whereas the MIF motoneurons are grouped together into the C-group at the mediadorsal border and more ventrally the S-group. The ChAT-positive and CSPG-negative EW-neurons lie dorsally to the C-group (G-H). In nIV the CSPG-negative MIF motoneurons are clustered at the dorsal border (D). At the rostral pole of nIV (E), the MIF motoneurons show a broader distribution. In nVI (F-H), the MIF motoneurons are not clustered together, but lie scattered around the borders of the nucleus and a considerable portion within the nucleus as well. Neurons (indicated by asterisks) that lack ChAT-immunoreactivity, but show strong CSPG-labelling are presumably internuclear neurons. Scale bar is 500 $\mu$ m.

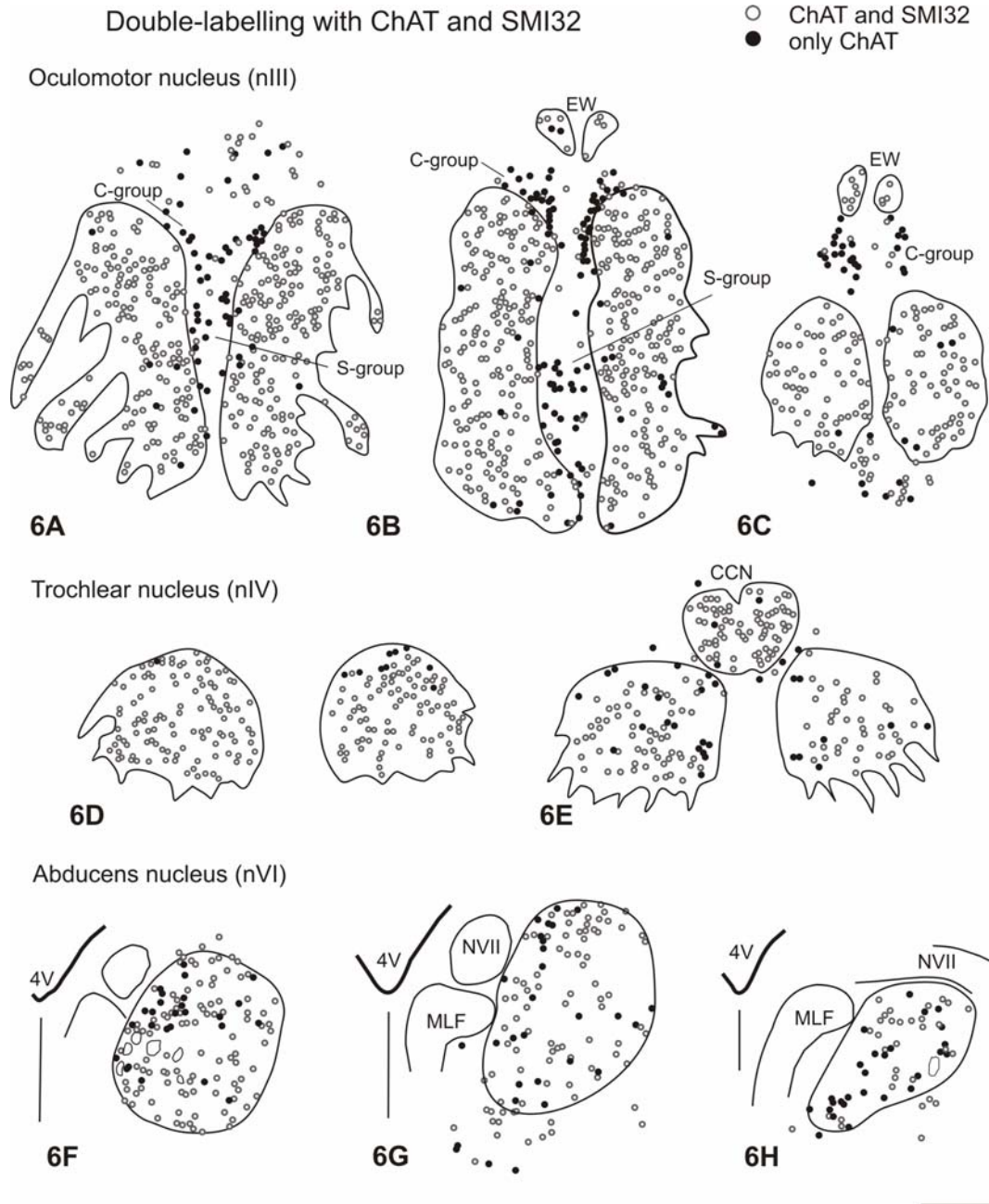


Fig. 6. Plots of transverse sections of nIII (A-C), nIV (D-E) and nVI (F-H), the outlines are drawn after subsequently treating the sections with Nissl stain. The sections were double-labelled for ChAT and NP-NFs with SMI32 antibody. SIF motoneurons (open circle) are both ChAT- and SMI32-positive, whereas MIF motoneurons (filled circle) lack SMI32-immunoreactivity. The SIF motoneurons in all three nuclei are ChAT- and SMI32-positive. Note, that most of the EW-neurons (A-C) are SMI32-positive, which helps to delineate the MIF motoneurons of the C-group from the EW. MIF motoneurons in the dorsal cap of nIV (D, E) and the C- and S-group in nIII lack SMI32 (A-C). As with double-labelling for ChAT and perineuronal nets (CSPG), the MIF motoneurons in nVI lie scattered around the borders, and centrally within the nucleus (F-H). Scale bar is 500 $\mu$ m.

Table 1:

Case	Injection site	Tracer	Volume	Survival time	Tracer detection
B61	belly of MR	2.5% WGA-HRP	25 $\mu$ l	3 days	DAB
Y79	distal MR	1% CTB	8 $\mu$ l	3 days	immunofluorescence
ZK-04	belly of LR	1% CTB	30 $\mu$ l	3 days	immunofluorescence
Y59	distal LR	1% CTB	15 $\mu$ l	3 days	immunofluorescence

Table 2:

Antibody	Host	Antigen	Manufacturer	Dilution
ChAT	rabbit	Choline acetyltransferase	Chemicon, Temecula CA	1:500
Cox	mouse	Cytochrome oxidase	Molecular Probes Inc, Eugene OR	1:100
CSPG	mouse	Chondroitin sulfate proteoglycan	Chemicon, Temecula CA	1:100
CTb	goat	Cholera toxin subunit B	List Biological Lab. Inc., Campbell CA	1:5000
PV	mouse	Parvalbumin	Swant, Bellizona CH	1:1000
SMI32	mouse	Non-phosphorylated neurofilament	Sternberger Monoclonals Inc., Lutherville MD	1:900

Paper 2: Identification of MIF and SIF motoneurons innervating the extraocular muscles  
in the rat.

# **Identification of MIF and SIF motoneurons innervating the extraocular muscles in the rat**

Andreas C. Eberhorn<sup>1</sup>, Jean A. Büttner-Ennever<sup>1</sup>, Anja K.E. Horn<sup>1</sup>

<sup>1</sup>Institute of Anatomy, Ludwig-Maximilian University of Munich, D-80336 Munich Germany

Manuscript: 34 pages, 4 figures, 4 tables

Short title: Localizations of eye muscle motoneurons

Keyword: non-twitch muscle fibres, twitch muscle fibres, perineuronal net, non-phosphorylated neurofilament, oculomotor, C-group, trochlear, abducens, internuclear

Correspondence to: Institute of Anatomy III

Ludwig-Maximilians Universität

Pettenkoferstr. 11

D-80336 Munich

Germany

Phone: -49 89 5160 4880

Fax: -49 89 5160 4857

e-mail: [andreas.eberhorn@med.uni-muenchen.de](mailto:andreas.eberhorn@med.uni-muenchen.de)

Grant sponsor: Deutsche Forschungsgemeinschaft (Ho 1639/4-1; GRK 267);

## Summary

In mammals, the extraocular muscle fibres can be categorized in singly-innervated (SIF) and multiply-innervated (MIF) muscle fibres. In the monkey oculomotor (nIII), trochlear (nIV) and abducens nucleus (nVI) the motoneurons of MIFs lie separated from those innervating SIFs and show different histochemical properties. In the present study we investigated the location of SIF and MIF motoneurons in the rat using combined tract-tracing and immunohistochemical techniques.

SIF and MIF motoneurons of the medial (MR) and lateral rectus (LR) muscle were identified by retrograde tracer injections into the muscle belly or the distal myotendinous junction. The belly injections labelled the MR subgroup of the nIII and the greatest part of nVI, including some cells outside the medial border of nVI. In contrast, the distal injections labelled only a subset of the MR motoneurons and exclusively cells outside the medial border of nVI. The tracer detection was combined with immunolabelling using antibodies for perineuronal nets (CSPG) and non-phosphorylated neurofilaments (NP-NF). In monkeys both antibodies allowed to distinguish between SIF and MIF motoneurons. The experiments revealed that neurons labelled from a distal injection lack both markers and thus assumed to represent MIF motoneurons, whereas those labelled from a belly injection are CSPG- and NP-NF-immunopositive, assumed to represent SIF motoneurons. The overall identification of MIF and SIF motoneurons within nIII, nIV, and nVI revealed that the smaller MIF motoneurons tend to lie separated from the bigger SIF motoneurons.

Our data provide evidence that rat extraocular muscles are innervated by two sets of motoneurons that differ in their molecular, morphologic, and anatomic properties.

## Abbreviations

4V:	fourth ventricle
ChAT:	choline acetyltransferase
CSPG:	chondroitin sulfate proteoglycan
CTb:	cholera toxin subunit B
g7:	genus of facial nerve
INT:	abducens internuclear neuron
IO:	inferior oblique muscle
IR:	inferior rectus muscle
LR:	lateral rectus muscle
MIF:	multiply-innervated muscle fibre
MLF:	medial longitudinal fascicle
MR:	medial rectus muscle
nIII:	oculomotor nucleus
nIV:	trochlear nucleus
nVI:	abducens nucleus
NP-NF:	non-phosphorylated neurofilament
SIF:	singly-innervated muscle fibre
SO:	superior oblique muscle
SR:	superior rectus muscle
WGA-HRP:	wheat germ agglutinin and horseradish peroxidase complex
TMR:	tetramethyl rhodamine

## **Introduction**

The eye of vertebrates is rotated by six principal extraocular muscles (EOM). These unique striated muscles differ in many aspects from the classical skeletal muscle. Accordingly, they do not show uniform morphology but consist of an outer orbital layer adjacent to the orbital bone, and an inner global layer adjacent to the eye globe. The global layer extends over the full muscle length from its origin at the annulus of Zinn to a well-defined tendon at the limbus of the globe (for review see: Porter et al., 1995). In contrast, the orbital layer ends before the tendon (Oh et al., 2001) and is thought to insert on the collagenous pulleys, the Tenon's capsule (Demer et al., 2000; Oh et al., 2001; Demer, 2002). The extraocular muscles consist of three main categories of fibre types: singly-innervated muscle fibres (SIFs) and two types of multiply-innervated muscle fibres (MIFs), one in the global and one in the orbital layer (for review: (Mayr et al., 1975; Bondi and Chiarandini, 1983; Morgan and Proske, 1984; Spencer and Porter, 1988; Porter et al., 1995). Whereas the SIFs are similar to the twitch muscle fibres in the skeletal muscles of mammals - with one single 'en-plaque' ending in the middle third of the muscle and an 'all-or-nothing' twitch upon electrical stimulation – the MIFs are rare in mammals (Morgan and Proske, 1984). The global layer MIFs are innervated by multiple 'en-grappe' endings throughout their extent (Pachter, 1984) and respond after stimulation with slow, graded potentials at each nerve ending, which are not propagated in an 'all-or-nothing' fashion, and resulting in the development of a tonic tension (Lennerstrand, 1974; Chiarandini and Stefani, 1979). Therefore these global MIFs correlate with the 'non-twitch muscle fibres'. In contrast, the orbital layer MIFs show mixed properties, 'non-twitch'-like at the proximal and distal ends and twitch-like at the middle third of the fibre (Pachter, 1984; Jacoby et al., 1989; Lynch, Frueh et al., 1994).

The basic anatomical organization of the oculomotor nuclei controlling the six principal extraocular eye muscles shows a very constant pattern across various vertebrate classes (for a

review, see: Evinger, 1988). Motoneurons of the oculomotor nucleus (nIII) innervate the medial (MR), inferior (IR), superior (SR) rectus muscles, and the inferior oblique (IO) muscle, motoneurons of the trochlear nucleus (nIV), namely the superior oblique (SO) muscle, and motoneurons of the abducens nucleus (nVI) and the lateral rectus (LR) muscle. In addition to the motoneurons of LR, the abducens nucleus contains the internuclear neurons (INT) that project to the contralateral oculomotor nucleus and are used for conjugated horizontal eye movements (Evinger, 1988).

Electrophysiological studies showed that all extraocular motoneurons participate in all types of eye movements (vergence, saccades, smooth pursuit, vestibulo-ocular and optokinetic nystagmus) (Robinson, 1970; Mays and Porter, 1984) and that motor unit discharges are tightly linked to eye-position (Keller and Robinson, 1972; Keller, 1973). This led to the current assumption that oculomotor commands convert at the level of motoneurons and innervate the muscle fibres through a final common pathway.

A reconsideration of this view is forced by recent studies in monkey EOM. Büttner-Ennever et al. (2001) showed by tracer injections into the belly or the distal myotendinous junction (thereby tracing only the 'en-grappe' endplates of global MIFs) of the EOM that two anatomically separated sets of motoneurons control the EOM: motoneurons of SIFs were found within the classical oculomotor nuclei, whereas the motoneurons of (global) MIFs were located in the periphery of these nuclei. Subsequent studies of premotor inputs on both types of motoneurons revealed that global MIF motoneurons are associated with premotor areas for vergence, smooth pursuit and gaze holding, but in contrast to SIF motoneurons, *not* with premotor areas generating saccades or VOR (Büttner-Ennever et al., 2002; Wasicky et al., 2004). Furthermore, both types of motoneurons differ in their morphology and histochemical properties (Eberhorn et al., 2005). Accordingly, the smaller MIF motoneurons do not contain non-phosphorylated neurofilaments or parvalbumin and lack perineuronal nets whereas the larger SIF motoneurons express all markers at high intensity. Taken together, all these

differences between both motoneuron populations contradict the theory of a single final common pathway from motoneuron to eye muscle but point out for a dual motor control (Büttner-Ennever et al., 2002).

The dual motor innervation of monkey EOM may be regarded as a result of the visual demands placed upon the oculomotor system in highly developed frontal-eyed mammals like primates. According to this point of view, lateral-eyed mammals like the rat may differ in the organization of the motor control of their eye muscles. On the other hand, rat EOMs exhibit the same EOM fibre types like primates (Pachter, 1983; Pachter and Colbjornsen, 1983; Ringel et al., 1978b; Spencer and Porter, 1988), and their eye movements include both fast and slow types (Delgado-Garcia, 2000). Previous studies on the localization of EOM motoneurons in the rat (Glicksman, 1980; Labandeira-Garcia et al., 1983) achieved only the identification of the overall distribution of motoneurons innervating individual EOMs, but did not distinguish between SIF and MIF motoneurons.

In the present study we identified the motoneurons innervating the MIFs of the horizontal recti, MR and LR, in rat using a similar tract-tracer injection approach as in a previous study on monkeys (Büttner-Ennever et al., 2001). We further combined the tracing with immunolabelling for markers which were to differentiate between SIF and MIF motoneurons in monkey, non-phosphorylated neurofilaments (NP-NF; SMI32) and perineuronal nets (CSPG) (Eberhorn et al., 2005).

## **Materials and methods**

All experimental procedures conformed with the state and university regulations on Laboratory Animal Care, including the Principles of Laboratory Animal Care (NIH Publication 85-23, Revised 1985), and were approved by their Animal Care Officers and Institutional Animal Care and Use Committees. Eight approximately one year old male

pigmented rats (Charles River) with a weight range of 280 to 350 grams were used in this study. SIF and MIF motoneurons of medial rectus (MR) and lateral rectus (LR) muscle were either identified by a retrograde tracer injection (wheat germ agglutinin horseradish peroxidase, WGA-HRP, or non-toxic cholera toxin subunit B, CTb) into respective eye muscles or by immunocytochemical staining using antibodies against choline acetyltransferase (ChAT) (Oda, 1999; Büttner-Ennever et al., 2001). The visualization of the tracer or cholinergic marker was combined with the detection of two different markers: 1. perineuronal nets with antibodies against chondroitin sulfate proteoglycans (CSPG), and 2. non-phosphorylated neurofilaments (NP-NF) with a specific antibody (SMI32) (Sternberger and Sternberger, 1983). In addition, the abducens internuclear neurons were identified with tracer injections into the oculomotor nucleus and characterized using the antibodies described above.

#### Retrograde tracing of motoneurons after eye muscle injections

In order to identify the motoneurons of the MR and LR three pigmented rats underwent tracer injections. In one animal (AII-99) the LR and MR were injected into the belly to label both MIF and SIF motoneurons (LR: WGA-HRP; MR: CTb, List, Campbell, CA). Three other animals were injected into the distal tip of either the MR (R12-03) or LR (AIV-99), which labels predominantly global MIF motoneurons (Büttner-Ennever et al., 2001). For the injection the rats were anesthetized with Equitesin (2.5ml/kg). The extraocular muscles were exposed by retracting the eyelid and incising the conjunctiva. In order to minimize tracer spread a small piece of plastic film was slipped between the eyeball and the muscle to be injected. The tracer was injected using a sharp glass pipette mounted on a Hamilton micro syringe. After a survival time of three days, the animals were killed with an overdose of Nembutal (80mg/kg body weight) and transcardially perfused with 0.9% saline (35°C) followed by 0.5 litres of 4% paraformaldehyde in 0.1M phosphate buffer (PB; pH 7.4) and 0.5

litre 10% sucrose in 0.1M phosphate buffer (pH 7.4). The brain and the eye muscles were removed from the skull and equilibrated in 20% and 30% sucrose in 0.1M PB for 3 days. The eye muscles were shock frozen in isopentane ( $-60^{\circ}\text{C}$ ) and kept at  $-20^{\circ}\text{C}$  until cutting. The brainstem was cut at  $40\mu\text{m}$  on a freezing microtome in the transverse stereotaxic plane. In order to give an estimate of the injection size, all eye muscles of the injected side were cut at  $20\mu\text{m}$  and thaw-mounted onto slides (Superfrost Plus). Every tenth eye muscle section was reacted for the detection of WGA-HRP or CTb.

#### Anterograde tracing of abducens internuclear neurons after injections into the oculomotor nucleus

In two animals (R13-03, R1-04), tetramethyl-rhodamine dextran (TMR-Dextran, Molecular Probes, Eugene, OR) was injected into the oculomotor nucleus. With animals under general anaesthesia and placed in a stereotaxic frame, a small hole was trephined in the skull according to the coordinates of an atlas (Paxinos: The rat brain in stereotaxic coordinates, 3<sup>rd</sup> edition 1997). The tracer was injected using a fine glass pipette mounted on a Hamilton syringe that was attached to the stereotaxic frame. After a five day survival, the animals were perfused and histological processing was carried out as described above.

The tracer cases and the injection volumes are given in table 1.

#### Visualization of the tracer

Free-floating brainstem sections of the WGA-HRP-injection case (AII-99) were reacted with 0.005% tetramethylbenzidine (TMB) as chromogen, which yields a black reaction product in retrogradely labelled motoneurons. Briefly, after rinsing in ice-cold 0.1M PBS, the sections were incubated in an acetic acid buffered solution (pH 3.3) containing ethanolic TMB and sodium-ferroprusside and an additional mixture of  $\beta$ -D-glucose, ammonium chloride, and

glucoseoxidase, then stabilized with ammonium heptamolybdate and counterstained with neutral-red (Mesulam, 1978).

In three CTb-injection cases (AII-99, AIV-99, R12-03), and the two TMR-Dextran cases, the tracer was visualized with antibodies against CTb or TMR using the DAB method. All sections were pretreated with 3% H<sub>2</sub>O<sub>2</sub>/10% Methanol in 0.1M PB pH 7.4 for 15min to suppress endogenous peroxidase activity and then thoroughly washed. For the detection of CTb immunoreactivity, the sections were blocked with 5% rabbit serum in 0.1M PB pH 7.4 containing 0.3% Triton X-100 for 1h and subsequently processed with goat anti-CTb antibodies (1:5000, List) overnight at room temperature. The TMR-sections were blocked with 5% goat serum in 0.1M PB pH 7.4 containing 0.3% Triton X-100 for 1h and processed with rabbit anti-TMR antibodies (1:5000, Molecular Probes) overnight at room temperature. After several buffer washes the sections were treated either with biotinylated rabbit-anti goat antibody (1:200; Alexis) in the CTb-cases, or biotinylated goat-anti rabbit antibody (1:200; Alexis) in the TMR-cases, for 1h at room temperature, then washed and incubated in extravidin-horseradish peroxidase (1:1000; Sigma) again for 1h. Diaminobenzidin served as chromogen for the detection of CTb- and TMR-immunoreactivity. The sections were then counterstained with cresyl violet.

Alternatively, TMR-Dextran can be directly examined using a fluorescent microscope equipped with filters for red fluorescent Cy<sup>3</sup> (N2.1).

### Double-fluorescence labelling

#### *CTb and marker*

Free floating sections of all CTb-injection cases were first processed for the immunofluorescent detection of the tracer. After blocking with 5% normal donkey serum in 0,1M PBS pH 7,4 containing 0,3% Triton X-100 for 1 hour, sections were incubated with goat

anti-CTb (1:5000, List) overnight. Rinsed sections were then reacted with AMCA-anti-goat (1:200; Dianova) for 2 hours. After rinsing, the sections were incubated with anti-chondroitin sulfate proteoglycans (mouse anti-CSPG; 1:100; Chemicon) as a label for perineuronal nets, or SMI32 (mouse SMI32, 1:900; Sternberger Monoclonals) for non-phosphorylated neurofilaments (NP-NF) overnight. The sections were subsequently reacted with Cy<sup>2</sup>-anti-mouse (1:200; Dianova) for two hours at room temperature in the dark.

#### *TMR-Dextran and marker*

Sections with TMR-Dextran labelled cells were blocked with 5% normal donkey serum in 0,1M PBS pH 7,4 containing 0,3% Triton X-100 for 1 hour and subsequently processed with a mixture of rabbit anti-ChAT (1:500) and mouse anti CSPG (1:100) overnight. For visualization of the applied antibodies, the sections were then reacted for 2 hours with a mixture of fluorochrome-tagged secondary donkey AMCA-anti-rabbit (1:200; Dianova) and Cy<sup>2</sup>-anti-mouse (1:200; Dianova) at room temperature in the dark.

#### *ChAT and marker*

In brainstem sections from two additional cases (R6-03 and R3-04), that had not received a tracer injection prior to the perfusion with 4% paraformaldehyde, all motoneurons in the oculomotor, trochlear and abducens nucleus were labelled by ChAT-immunocytochemistry (rabbit anti-ChAT, 1:500, Chemicon) and combined with the subsequent immunofluorescent detection of perineuronal nets (with anti-CSPG) and NP-NF (SMI32).

Table 2 summarizes the antibodies used.

### Analysis of stained sections

All slides were examined with a Leica microscope DMRB (Bensheim, Germany) equipped with appropriate filters for red fluorescent Cy<sup>3</sup> (N2.1), green fluorescent Cy<sup>2</sup> or Alexa 488 (I3), and blue fluorescent AMCA (A).

Images of brightfield and fluorescence photographs were digitized by using the 3-CCD videocamera (Hamamatsu; C5810) mounted on a Leica DMRB microscope. The images were captured on a computer with Adobe Photoshop 5 software. Sharpness, contrast, and brightness were adjusted to reflect the appearance of the labelling seen through the microscope. Overlays of double and triple fluorescent stains are produced by adding the signal of each different stain using the videocamera hardware control or by superimposing different fluorescence stains using Adobe Photoshop. The pictures were arranged and labelled with drawing software (CorelDraw 8 and 11). The labelled neurons of a series of transverse sections through the oculomotor, trochlear and abducens nucleus was plotted on the pictures taken with the 3-CCD videocamera and displayed on the computer screen using drawing software (CorelDraw 11). Each labelled neuron was analyzed for double-labelling by switching the filters of the fluorescence microscope.

### Cell counts and cell size measurements

In order to estimate the proportion of MIF motoneurons within the complete motoneuron population, cell counts were performed on oculomotor, trochlear and abducens nucleus sections (R6-03, R3-04), double-immunostained for ChAT and CSPG or NF-NP, respectively. All ChAT-immunoreactive neurons with a clearly visible nucleus were counted giving the number of SIF and MIF motoneurons within the respective motor nuclei. The proportion of MIF motoneurons was calculated from cell counts of those ChAT-positive neurons, which do not express CSPG- or NP-NF-immunoreactivity. Motoneuron subgroups within nIII of each individual eye muscle are difficult to outline and were therefore not counted separately.

Cell size measurements of SIF motoneurons (ChAT and CSPG-staining or NP-NF-staining) and presumed MIF motoneurons (ChAT without CSPG- or NP-NF-staining) were estimated from images captured with a 3-CCD videocamera (Hamamatsu; C5810) using an image analysis system (Optimas 6.1, Optimas Corp.). Cell sizes are given as mean diameters  $[(\text{maximum cell diameter} + \text{minimum cell diameter})/2]$ . A two-tailed t test was used to compare cell sizes of MIF and SIF motoneurons of the three motor nuclei.

## **Results**

### Tracer injection cases

#### *Oculomotor nucleus*

The tracer injection into the belly of the medial rectus muscle (MR) resulted in the retrograde labelling of MR motoneurons, which are located predominantly in the medial and rostral part of the ipsilateral oculomotor nucleus (Fig.1A and adjacent plot). At mediorostral levels, the tracer positive MR motoneurons form a band of cells at the medial border extending from ventral to dorsal. Inside this band, some labelled motoneurons appear fusiform. In addition, tracer positive MR motoneurons are scattered within the nucleus. Hence, a few marked neurons were found in the contralateral oculomotor nucleus. They might resemble SR and LP motoneurons which were labelled due to some tracer spread after the injection into the MR.

The tracer injection into the distal tip of the MR labelled motoneurons exclusively in the ipsilateral oculomotor nucleus. Their distribution within the nucleus is similar to those obtained after a big injection into MR, though less motoneurons are labelled. A certain amount of tracer positive motoneurons is located at the medial border, for the greatest part in the ventral half of the nucleus. Additional labelled motoneurons can be found scattered within the nucleus, most of them tend to be located dorsally (Fig. 1B and adjacent plot).

In accordance to the results which our group obtained from experiments performed on monkey oculomotor neurons (Eberhorn et al., 2005) we combined the detection of the tracer after injections into the MR belly or myotendinous junction with antibodies for perineuronal nets (CSPG) or non-phosphorylated neurofilaments (NP-NF) in order to identify SIF and MIF motoneurons by their immunohistochemical differences. After a big tracer injection the majority of labelled motoneurons in the oculomotor nucleus is surrounded by strong perineuronal nets (Fig. 1E, F) and is NF-NP immunoreactive (Fig. 1J, K). Few labelled motoneurons differ in their histochemical properties and lack both, perineuronal net and NF-NP immunolabelling. In contrast, virtually all MR motoneurons labelled after a tracer injection into the distal myotendinous junction lack perineuronal net (Fig. 1G, H) and NF-NP immunoreactivity (Fig. 1L, M).

#### *Trochlear nucleus*

No tracer injections into the superior oblique muscle have been performed in this study. All data on SIF and MIF motoneurons in the trochlear nucleus are taken from double-immunolabelling experiments described below.

#### *Abducens nucleus*

A big tracer injection into the muscle belly of the LR muscle filled the whole ipsilateral abducens nucleus (Fig. 1C and adjacent plot). Some marked cells could even be found lateral to the facial genu. In addition, few cells were labelled outside the medial border of abducens nucleus just as far medial as the MLF (Fig. 1C, arrows).

After a small tracer injection into the myotendinous junction of the LR muscle, only few retrogradely labelled motoneurons were found (Fig. 1D and adjacent plot). They were located clearly separated from the classical abducens motoneurons outside the medial border of

abducens nucleus, with some being intermingled in the MLF. No labelled motoneurons were found within the borders of the nucleus.

In monkey, a major ChAT-negative neuron population with prominent perineuronal nets is present within the abducens nucleus and presumably represents internuclear neurons (Eberhorn et al., 2005). To verify these results tracer injections of TMR-Dextran were placed into the oculomotor nucleus in order to retrogradely label internuclear neurons (Glicksman, 1980). The tracer uptake area was confined to the medial to rostral planes of both nIII and extended ventrally into the MLF just between the red nuclei (Fig. 2A). TMR labelled neurons were observed in the ventrolateral part of both abducens nuclei at caudal to medial planes (Fig. 2B, arrows), identifying them as internuclear neurons (Glicksman, 1980). Additional double-labelling with ChAT and CSPG revealed that the INTs in rat are not cholinergic, but unlike in monkey show only weak CSPG-immunoreactivity compared to the SIF motoneurons (Fig. 2C, D).

#### Complete populations of MIF motoneurons

Unlike tracer injections, which usually label only parts of the motoneuron populations, ChAT-immunolabelling visualized the complete motoneuron population, including both, SIF and MIF motoneurons in the oculomotor, trochlear and abducens nucleus. With the combined staining for ChAT and perineuronal nets or NP-NFs the complete population of MIF motoneurons in each nucleus was identified.

#### *Oculomotor nucleus (nIII)*

Using ChAT-immunolabelling in the oculomotor nucleus, the motoneuron subgroups of MR, IR, SR and IO muscle were labelled, and in addition those of the LP muscle (LP has only SIF motoneurons, which are located at caudal planes at the ventrolateral border of nIII). A

separation of the subgroups within the nucleus is not possible using the double-labelling, but was shown by tracing experiments in other studies (Glicksman, 1980; Gomez-Segade and Labandeira, 1980).

The cholinergic neurons being ensheathed by perineuronal nets, representing the SIF motoneurons of MR, IR, IO, SR and LP, clearly fill up the whole oculomotor nucleus from the caudal to the rostral planes. Within the nucleus, a certain amount of cholinergic neurons can be found which lack perineuronal nets and lie intermingled with the SIF motoneurons. These neurons, which presumably resemble the MIF motoneurons of MR, IR, IO and SR, are not evenly distributed throughout the nucleus, but tend to cluster at some regions. The most obvious cluster is located at the medial aspect of nIII where the MIF motoneurons form a band which extends from ventral to the dorsal half of nIII, and is present at medial to rostral planes. The remaining MIF motoneurons either lie close to the ventral, lateral and dorsal borders or concentrate at the center of III (Fig. 3A, 4A).

The same overall distribution of SIF and MIF motoneurons was found using double-labelling with ChAT and NF-NP. The NF-NP positive SIF motoneurons clearly outline the oculomotor nucleus, whereas the population of cholinergic neurons, which lack NF-NP immunoreactivity, tend to group at certain spots of nIII. Similar to the results from the double-labelling with ChAT and perineuronal nets, the NF-NP lacking neurons, presumably the MIF motoneurons of MR, IR, IO and SR, cluster at the medial border forming a band, and are additionally located close to the ventral, lateral and dorsal border or at the center of nIII (Fig. 4D).

The cell counts of the double-labelled sections revealed that the MIF motoneurons within the oculomotor nucleus make up 21% of the total motoneuron population (2410 cells were counted on all sections). The morphometric analysis revealed that the mean cell diameters of MIF motoneurons, ranging from 11.2 $\mu$ m – 18.4 $\mu$ m (mean = 14.5 $\mu$ m; SD = 1.7; N=100), were

significantly smaller ( $p < 0.0001$ ) than those of the SIF motoneurons, which ranged from  $14.5\mu\text{m} - 24.1\mu\text{m}$  (mean =  $19.4\mu\text{m}$ ; SD = 2.3; N = 100) (Fig. 3B).

#### *Trochlear nucleus (nIV)*

In the trochlear nucleus (nIV) no retrograde tracer labelling, but only ChAT-immunolabelling was used for the identification of motoneurons. All neurons within nIV are ChAT-immunoreactive and delineate the nucleus clearly within the mesencephalic tegmentum. Combined immunolabelling for the presence of perineuronal nets or NP-NFs, with CSPG- or SMI32-antibodies, respectively, revealed that all motoneurons in nIV are double-labelled with CSPG and SMI32 except few neurons at the dorsal, medial and ventral border of the nucleus, which lack perineuronal nets (Fig. 3C, 4B) and NP-NF expression (Fig. 4E). These neurons share the same properties than the MIF motoneurons of oculomotor nucleus and are therefore designated as MIF motoneurons of trochlear nucleus. The cell counts within nIV revealed that CSPG- and NP-NF- lacking MIF motoneurons make up 15% of all motoneurons (392 cells were counted on every section). The mean cell diameters of MIF motoneurons ranged from  $10.0\mu\text{m} - 16.1\mu\text{m}$  (mean =  $12.9\mu\text{m}$ ; SD = 1.4; N = 50) and were significant smaller ( $p < 0.0001$ ) compared to those of superior oblique SIF motoneurons, which ranged from  $11.8\mu\text{m} - 23.0\mu\text{m}$  (mean =  $17.9\mu\text{m}$ ; SD = 2.4; N = 100) (Fig. 3D).

#### *Abducens nucleus (nVI)*

With ChAT-immunolabelling the complete population of motoneurons (SIF motoneurons and MIF motoneurons) was visualized and could be distinguished from internuclear neurons, which are not cholinergic (Spencer and Baker, 1986; Carpenter et al., 1992).

As shown by tracer-labelling, the largest population of ChAT-immunoreactive neurons that are not ensheathed by perineuronal nets and lack NP-NF-labelling was located in a separate group, clearly outside the medial border of the classical abducens nucleus identifying them as

presumed MIF motoneurons. This medial population of MIF motoneurons extends from the caudal to the very rostral level and forms a sort of cap which shelters the medial aspect of abducens nucleus. In addition a small subset of neurons sharing the same properties (>20) lie at the dorsal border or inside the abducens nucleus and were not labelled by distal tracer injections. The mean cell diameters of LR MIF motoneurons of nVI ranged from 9.9  $\mu\text{m}$  – 20.3 $\mu\text{m}$  (mean 13.2 $\mu\text{m}$ ; SD = 2.0; N = 100) and are significantly smaller ( $p < 0.0001$ ) than those of the LR SIF motoneurons, which range from 12.2 $\mu\text{m}$  – 21.9 $\mu\text{m}$  (mean = 17.3 $\mu\text{m}$ ; SD = 2.3; N = 100).

On every section of the abducens nucleus the cholinergic motoneurons (SIF and MIF motoneurons) were counted which resulted in a total of 628 motoneurons. The complete population of MIF motoneurons in the abducens nucleus lacking perineuronal nets and NP-NF was 139 and make up 22% of all cholinergic motoneurons.

The cell counts are summarized in Table 3, the cell size measurements in Table 4.

## **Discussion**

Our results demonstrate that in rat the extraocular muscles are innervated by two sets of motoneurons, SIF and MIF motoneurons, which differ in size and histochemical properties, and tend to lie separate from each other. We identified the two motoneuron populations by tracer injections into the belly (SIF and MIF) or the distal myotendinous junction (MIF) of the horizontal recti, medial and lateral rectus muscle. A combination of the tracer experiments with immunolabelling for perineuronal nets (CSPG) and non-phosphorylated neurofilaments (NP-NF) revealed that only the SIF motoneurons stain positive for both markers. In addition, we combined CSPG and NP-NF staining with choline-acetyltransferase (ChAT) immunostaining to visualize the complete population of SIF and MIF motoneurons in all three oculomotor nuclei. Since all motoneurons are cholinergic (ChAT-positive), MIF motoneurons could easily be depicted by their lack of CSPG and NP-NF.

In the following discussion, we compare our results with the observations made in previous studies in rat and monkey oculomotor system and further discuss the functional implications for all mammals.

### Localization of SIF and MIF motoneurons in rat

Up to now, the detailed localization of MIF and SIF motoneurons has only been studied in monkey (Büttner-Ennever et al., 2001; Eberhorn et al., 2005). In this animal, the largest and most compact population of MIF motoneurons are those of the medial and inferior rectus muscles that form the C-group at the dorsomedial border of the oculomotor nucleus (Spencer and Porter, 1981; Büttner-Ennever and Akert, 1981; Büttner-Ennever et al., 2001). The C-group has been identified in several species (Clarke et al., 1987; Sun and May, 1993; Shall et al., 2003). It is clearly separated from the SIF motoneurons of the oculomotor nucleus (nIII) and lies close to the Edinger-Westphal nucleus (EW), which contains the preganglionic neurons for pupil constriction and accommodation (Akert et al., 1980; Burde and Williams,

1989; Ishikawa et al., 1990). The MIF motoneurons of the superior rectus and inferior oblique eye muscles are located around the midline between the oculomotor nuclei forming the S-group (Büttner-Ennever et al., 2001; Wasicky et al., 2004).

Compared to the monkey the MIF and SIF motoneurons in rat are not clearly separated in the oculomotor nucleus. Regarding the MR subgroup in the oculomotor nucleus, one major difference between monkey and rat is the existence of three anatomically distinct subpopulations of MR motoneurons in primates (Büttner-Ennever and Akert, 1981). The SIF motoneurons form the A-group and the B-group, whereas the MIF motoneurons form the C-group. Though a similar division of MR motoneurons in rat was not found in this study or by other authors (Glicksman, 1980; Labandeira-Garcia et al., 1983), the MIF motoneurons tend to cluster at or close to the medial border of nIII (Fig. 3A, 4A, D). This is in line with previous studies on the localization of motoneurons innervating the EOM in rat (Glicksman, 1980; Labandeira-Garcia et al., 1983). Although both studies were focussed on the identification of the complete motoneuron population of each EOM and did not incorporate a possible difference between motoneurons innervating 'en-grappe' and 'en-plaque' endplates in the EOM, one can find several indices for the presence and localization of MIF motoneurons. In one tracer injection case of the MR, Glicksman (1980) found only few motoneurons that were labelled. Those were located predominantly at the medial border of nIII, a finding very similar to the results obtained from a tracer injection into the myotendinous junction in our study. The combined detection of the tracer with immunolabelling for CSPG or NP-NF revealed that majority of these neurons lack both markers, identifying them as MIF motoneurons. Furthermore, Landeira Garcia et al. (1983) measured the size of tracer-positive motoneurons and found that in the MR subgroup the smallest neurons appear along the medial border of nIII, where they are intermingled with similar small motoneurons labelled from tracer injections into the IR. The visualization of the overall population of MIF motoneurons in nIII, showed their localization exactly at the medial

border. Thus, the medial cluster of MIF motoneurons may be considered as homologue to the C-group found in monkey. Accordingly, the additional MIF motoneurons inside and at the dorsal border of nIII may be homologue to the S-group. Hence, a more detailed study involving the SR, IO, and IR muscle has to clarify this issue. In monkey the MIF motoneurons of the superior oblique muscle lie in a compact cluster in the dorsal cap of the trochlear nucleus. Our results in the rat reveal an analogous pattern, though the MIF motoneurons form rather an envelope than a cap. The MIF motoneurons of the lateral rectus muscle in monkey are arranged more loosely around the periphery of the abducens nucleus, whereas the SIF motoneurons are scattered within the nucleus (Büttner-Ennever et al., 2001). In addition, a certain amount of motoneurons with MIF properties can be found within the abducens nucleus, possibly representing the MIF motoneurons of the orbital layer of LR (Eberhorn et al., 2005). In the rat, the MIF motoneurons of abducens nucleus are predominantly located outside its medial border, intermingled within the fibres of MLF. Again, this finding is supported by Labandeira Garcia et al., (1983) who found the smallest motoneurons of nVI localized exactly at the same position as the MIF motoneurons. A comparable group of central MIF motoneurons was not found in the rat nVI.

The rat is most likely not the only lateral-eyed animal showing two types of motoneurons that innervate the EOM. In both rabbit (Akagi, 1978) and guinea pig (Gomez-Segade and Labandeira-Garcia, 1983) some smaller sized neurons were found (and referred to as gamma-motoneurons) intermingled with the classical motoneurons in the oculomotor, trochlear, and abducens nucleus. These gamma-motoneurons are similar to those described in rat (Labandeira-Garcia et al., 1983), where they occupy the position of our identified MIF motoneurons. Thus, it is very tempting to speculate that these gamma-motoneurons represent MIF motoneurons in the rabbit and the guinea pig.

Our demonstration, that identified abducens internuclear neurons (INT) are not cholinergic confirms the findings in monkey (Carpenter et al., 1992; Spencer and Baker, 1986) and prevented us from a possible misinterpretation of these neurons as MIF or SIF motoneurons.

A second group of motoneurons which are often found close to or within the abducens nucleus are those innervating the retractor bulbi muscle. The occurrence of this muscle, which pulls the eye back into the orbit, is coupled to the presence of a nictitating membrane. In rats, the retractor bulbi motoneurons form the accessory abducens nucleus (nVIa). This nucleus is present at levels just caudal to the nVI, medial to the lower part of the facial root fibres (refs: Oda, 1981; Szekely et al., 1982). Thus the relatively great distance of nVIa to nVI makes it very unlikely that retractor bulbi motoneurons may have been mistaken for LR motoneurons.

As in monkey (Eberhorn et al., 2005), we found that in rat MIF motoneurons are smaller than SIF motoneurons. Looking at the overall number of MIF motoneurons, we found that their proportion is about 21% within the total motoneuron population in the oculomotor and abducens nucleus, and about 15% in the trochlear nucleus, thus a little more invariant than in monkey (about 20% for all three nuclei) (Eberhorn et al., 2005). These percentages of MIF and SIF motoneurons may be a common feature, since the 'gamma-motoneurons' found in the guinea pig (and which we rather call MIF motoneurons), made up about 20% of the total motoneuron number within the oculomotor and abducens nuclei, and about 10% within the trochlear nucleus. It is difficult to deduct a relationship between these percentages, since motor unit structure is rather complex (Shall and Goldberg, 1992) and in addition MIFs are thought to receive a polyneuronal innervation (Jacoby et al., 1989). However, the number of MIF and SIF motoneurons could somehow resemble the data of 20% MIFs to 80% SIFs for whole muscle fibre counts (Porter et al., 1995).

### Functional implications

Compared to the monkey, the rat shows a strikingly analogous organization of MIF and SIF motoneurons in its oculomotor nuclei based on anatomical, molecular, and quantitative respects. But what is the function of MIF motoneurons, if a lateral-eyed animal like the rat with a limited repertoire of eye movements shows a similar system like the highly visual oriented monkey? In monkeys, the premotor innervation of the MIF motoneurons imply a role in tension feedback, which could involve gaze holding, eye alignment and vergence (Büttner-Ennever et al., 2002; Wasicky et al., 2004).

Rats are functionally afoveate animals, whose eye movements differ in many respects from those of foveate animals like primates (Fuller, 1985; Collewijn, 1981; Delgado-Garcia, 2000). Compensatory eye movements, vestibulo-ocular reflex (VOR) and optokinetic reflex (OKN), are more important than voluntary eye movements like saccades, vergence, or gaze holding. Smooth pursuit movements are not present at all (Delgado-Garcia, 2000). Although rats have a smaller binocular field and their gaze holding ability is much poorer than in monkey (Chelazzi et al., 1989), the MIF motoneurons in this species may function similar to those in monkey, being involved in gaze holding and vergence. The less obvious separation of MIF and SIF motoneurons observed in rat (especially in the oculomotor nucleus) may be due to its limits in eye movements. Since there are no studies yet on the premotor inputs of the MIF motoneurons in rats, their function remains speculative.

In the EOM of mammals, the MIFs of the global layer and palisade endings form a unique unit (Alvarado-Mallart and Pincon Raymond, 1979; Blumer et al., 1998, 2001; Lukas et al., 2000; Eberhorn et al., 2005). This unit may function as inverted muscle spindle, as once suggested by Robinson (1991). A view which is supported by the finding that global MIFs have the same heavy-chain myosin as the nuclear bag<sub>1</sub> intrafusal fibres of muscle spindles (Pedrosa-Domellof et al., 1991). Accordingly the global MIF motoneurons then may resemble gamma motoneurons, a notion which was pointed out by several authors for the small

motoneurons found in the oculomotor nuclei of the rabbit, and guinea pig, and rat (Akagi, 1978; Gomez-Segade and Labandeira-Garcia, 1983; Labandeira-Garcia et al., 1983).

## **Conclusion**

In this study on the rat oculomotor system, we showed for the first time that the dual motor control of extraocular muscles is not an adoption to the visual needs of highly developed animals like primates, but is also present in lateral-eyed, afoveate animals like the rat. The less elaborate separation of MIF and SIF motoneurons in the rat compared to the monkey, together with the more rudimentary palisade endings in its EOM possibly reflects the simpler demands placed upon the dual motor control system in the rat.

## **Acknowledgements**

The authors thank Prof. Lange for his continuous support and Ahmed Messoudi and Christina Glombik for their excellent technical expertise.

## Literature cited

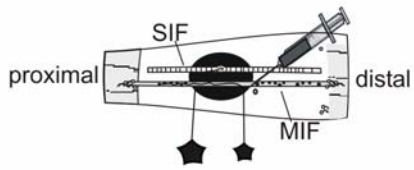
- Akagi Y. 1978. The localization of the motor neurons innervating the extraocular muscles in the oculomotor nuclei of the cat and rabbit, using horseradish peroxidase. *J Comp Neurol* 181:745-761.
- Akert K, Glicksman MA, Lang W, Grob P, and Huber A. 1980. The Edinger-Westphal nucleus in the monkey. A retrograde tracer study. *Brain Res* 184:491-498.
- Alvarado-Mallart RM and Pincon Raymond M. 1979. The palisade endings of cat extraocular muscles: a light and electron microscope study. *Tissue Cell* 11:567-584.
- Blumer R, Lukas JR, Wasicky R, and Mayr R. 1998. Presence and structure of innervated myotendinous cylinders in sheep extraocular muscle. *Neurosci Lett* 248:49-52.
- Blumer R, Wasicky R, Hötzenecker W, and Lukas JR. 2001. Presence and structure of innervated myotendinous cylinders in rabbit extraocular muscle. *Exp Eye Res* 73:787-796.
- Bondi AY and Chiarandini DJ. 1983. Morphologic and electrophysiologic identification of multiply innervated fibers in rat extraocular muscles. *Invest Ophthal Vis Sci* 24:516-519.
- Burde RM and Williams F. 1989. Parasympathetic nuclei. *Brain Res* 498:371-375.
- Büttner-Ennever JA and Akert K. 1981. Medial rectus subgroups of the oculomotor nucleus and their abducens internuclear input in the monkey. *J Comp Neurol* 197:17-27.
- Büttner-Ennever JA, Horn AKE, Graf W, and Ugolini G. 2002. Modern concepts of brainstem anatomy. *Ann N Y Acad Sci* 956:75-84.
- Büttner-Ennever JA, Horn AKE, Scherberger H, and D'Ascanio P. 2001. Motoneurons of twitch and nontwitch extraocular muscle fibers in the abducens, trochlear, and oculomotor nuclei of monkeys. *J Comp Neurol* 438:318-335.
- Carpenter MB, Periera AB, and Guha N. 1992. Immunocytochemistry of oculomotor afferents in the squirrel monkey (*Saimiri Sciureus*). *J Hirnforsch* 33:151-167.
- Chelazzi L, Rossi F, Tempia F, Ghirardi M, and Strata P. 1989. Saccadic eye movements and gaze holding in the head-restrained pigmented rat. *European Journal of Neuroscience* 1, 639-646.
- Chiarandini DJ and Stefani E. 1979. Electrophysiological identification of two types of fibres in rat extraocular muscles. *J Physiol* 290:453-465.
- Clarke RJ, Alessio ML, and Pessoa VF. 1987. Distribution of motoneurons innervating extraocular muscles in the brain of the marmoset (*Callithrix jacchus*). *Acta Anat* 130:191-196.
- Collewijn, H. 1981. The oculomotor system of the rabbit and its plasticity. *Studies of Brain Function* vol 5. Springer Verlag, Berlin, Heidelberg, New York
- Delgado-Garcia JM. 2000. Why move the eyes if we can move the head? *Brain Res Bull* 52:475-482.

- Demer JL. 2002. The orbital pulley system: A revolution in concepts of orbital anatomy. *Ann N Y Acad Sci* 956:17-32.
- Demer JL, Yeul Oh S, and Poukens V. 2000. Evidence for active control of rectus extrocular muscle pulleys. *Invest Ophthal Vis Sci* 41:1280-1290.
- Eberhorn AC, Ardelenanu P, Büttner-Ennever JA, and Horn AKE. 2005. Motoneurons of multiply-innervated muscle fibres in extraocular muscles have different histochemical properties than motoneurons of singly-innervated muscle fibres. *J Comp Neurol* (accepted).
- Eberhorn AC, Horn AKE, Eberhorn N, Fischer P, Boergen K-P, and Büttner-Ennever JA. 2005. Palisade endings in extraocular eye muscles revealed by SNAP-25 immunoreactivity. *J Anat* 205:307-315.
- Evinger C. 1988. Extraocular motor nuclei: location, morphology and afferents. In Büttner-Ennever JA, editor. *Neuroanatomy of the oculomotor system*. Amsterdam; New York; Oxford: Elsevier. p 81-117.
- Fuller JH. 1985. Eye and head movements in the pigmented rat. *Vision Res*. 25:1121-1128
- Glicksman MA. 1980. Localization of motoneurons controlling the extraocular muscles of the rat. *Brain Res* 188:53-62.
- Gomez-Segade LA and Labandeira JL. 1980. Location of proprioceptive neurons supplying the extraocular muscles in the rat; as revealed by horseradish peroxidase and fluorescent substances transport techniques. *Trab Inst Cajal LXXI*:293-299.
- Gomez-Segade LA and Labandeira-Garcia JL. 1983. Location and quantitative analysis of the motoneurons innervating the extraocular muscles of the guinea-pig, using horseradish peroxidase (HRP) and double or triple labelling with fluorescent substances. *J Hirnforsch* 24:613-626.
- Ishikawa S, Sekiya H, and Kondo Y. 1990. The center for controlling the near reflex in the midbrain of the monkey: a double labelling study. *Brain Res* 519:217-222.
- Jacoby J, Chiarandini DJ, and Stefani E. 1989. Electrical properties and innervation of fibers in the orbital layer of rat extraocular muscles. *J Neurophysiol* 61:116-125.
- Keller EL. 1973. Accommodative vergence in the alert monkey. motor unit analysis. *Vision Res* 13:1565-1575.
- Keller EL and Robinson DA. 1972. Abducens unit behavior in the monkey during vergence movements. *Vision Res* 12:369-382.
- Labandeira-Garcia JL, Gomez-Segade LA, and Nunez JMS. 1983. Localisation of motoneurons supplying the extra-ocular muscles of the rat using horseradish peroxidase and fluorescent double labelling. *J Anat* 137:247-261.
- Lennerstrand G. 1974. Electrical activity and isometric tension in motor units of the cat's inferior oblique muscle. *Acta Physiol.Scand.* 91, 458-474. 1974.

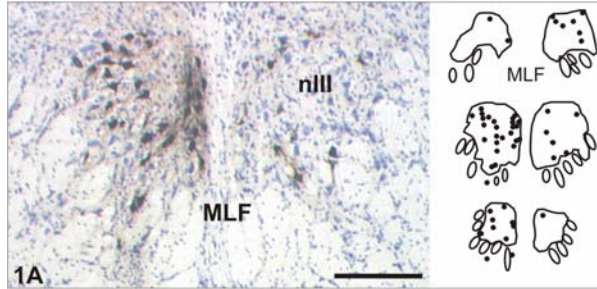
- Lukas JR, Blumer R, Denk M, Baumgartner I, Neuhuber W, and Mayr R. 2000. Innervated myotendinous cylinders in human extraocular muscles. *Invest Ophthalmol Vis Sci* 41:2422-2431.
- Lynch GS, Frueh BR, and Williams DA. 1994. Contractile properties of single skinned fibres from the extraocular muscles, the levator and superior rectus, of the rabbit. *J Physiol* 475:337-346.
- Mayr R, Gottschall J, Gruber H, and Neuhuber W. 1975. Internal structure of cat extraocular muscle. *Anat Embryol* 148:25-34.
- Mays LE and Porter JD. 1984. Neural control of vergence eye movements: activity of abducens and oculomotor neurons. *J Neurophysiol* 52:743-761.
- Mesulam, MM. 1978. Tetramethyl benzidine for horseradish peroxidase neurohistochemistry: a non-carcinogenic blue reaction-product with superior sensitivity for visualizing neural afferents and efferents. *J Histochem Cytochem* 26:106-117
- Morgan DL and Proske U. 1984. Vertebrate slow muscle: its structure, pattern of innervation, and mechanical properties. *Physiol Rev* 64:103-138.
- Oda Y. 1981. Extraocular muscles and their relationship to the accessory abducens nucleus in rats as studied by horseradish peroxidase method. *Okajimas Folia Anat Jpn* 58: 43-54.
- Oda Y. 1999. Choline acetyltransferase: The structure, distribution and pathologic changes in the central nervous system. *Pathology International* 49:921-937.
- Oh SY, Poukens V, Cohen MS, and Demer JL. 2001. Structure-function correlation of laminar vascularity in human rectus extraocular muscles. *Invest Ophthalmol Vis Sci* 42:17-22.
- Pachter BR. 1983. Rat extraocular muscle. 1. Three dimensional cytoarchitecture, component fibre populations and innervation. *J Anat* 137:143-159.
- Pachter BR. 1984. Rat extraocular muscle. 3. Histochemical variability along the length of multiply-innervated fibers of the orbital surface layer. *Histochem* 80:535-538.
- Pachter BR and Colbjornsen C. 1983. Rat extraocular muscle. 2. Histochemical fibre types. *J Anat* 137:161-170.
- Pedrosa-Domellof F, Soukup T, and Thornell LE. 1991. Rat muscle spindle immunocytochemistry revisited. *Histochem* 96:327-338.
- Porter JD, Baker RS, Ragusa RJ, and Brueckner JK. 1995. Extraocular muscles: basic and clinical aspects of structure and function. *Survey Ophthalmol* 39:451-484.
- Ringel SP, Engel WK, Bender AN, Peters ND, Yee RD. 1978. Histochemistry and acetylcholine receptor distribution in normal and denervated monkey extraocular muscles. *Neurology*. 28:55-63
- Robinson DA. 1970. Oculomotor unit behavior in the monkey. *J Neurophysiol* 38:393-404.
- Robinson DA. 1991. Overview, in vision and vision dysfunction. In: Carpenter RHS, editor. *Eye movements*. Boca Raton: CRC Press: 320-331

- Shall MS, Dimitrova DM, and Goldberg SJ. 2003. Extraocular motor unit and whole-muscle contractile properties in the squirrel monkey. *Exp Brain Res* 151:338-345.
- Shall MS and Goldberg SJ. 1992. Extraocular motor units - type classification and motoneuron stimulation frequency-muscle unit force relationships. *Brain Res* 587:291-300.
- Spencer RF and Baker R. 1986. Histochemical localization of acetylcholinesterase in relation to motor neurons and internuclear neurons of the cat abducens nucleus. *J Neurocytol* 15:137-154.
- Spencer RF and Porter JD. 1981. Innervation and structure of extraocular muscles in the monkey in comparison to those of the cat. *J Comp Neurol* 198:649-665.
- Spencer RF and Porter JD. 1988. Structural organization of the extraocular muscles. In Büttner-Ennever JA, editor. *Neuroanatomy of the oculomotor system*. Amsterdam; New York; Oxford; Elsevier. p 33-79.
- Sternberger LA and Sternberger NH. 1983. Monoclonal antibodies distinguish phosphorylated and non-phosphorylated forms of neurofilaments in situ. *Proc Natl Acad Sci* 80:6126-6130.
- Sun W and May PJ. 1993. Organization of the extraocular and preganglionic motoneurons supplying the orbit in the Lesser Galago. *The anatomical record* 237:89-103.
- Székely G, Matesz C. 1982. The accessory motor nuclei of the trigeminal, facial, and abducens nerves in rat. *J Comp Neurol* 210:258-264.
- Wasicky R, Horn AKE, and Büttner-Ennever JA. 2004. Twitch and non-twitch motoneuron subgroups of the medial rectus muscle in the oculomotor nucleus of monkeys receive different afferent projections. *J Comp Neurol* 479:117-129.

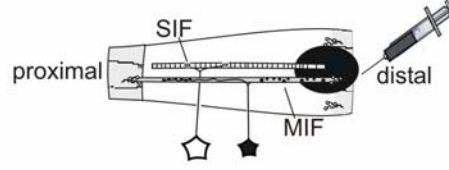
**Tracer injection into the muscle belly**



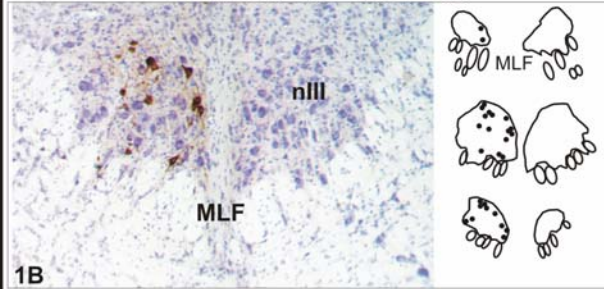
**Oculomotor nucleus**



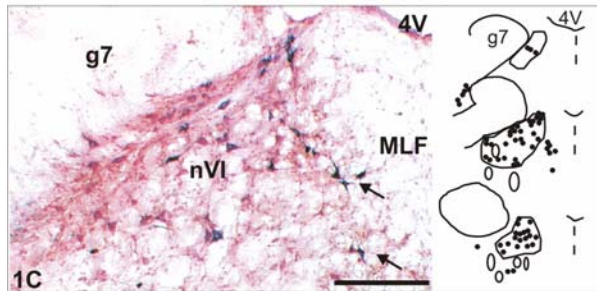
**Tracer injection into the distal myotendinous junction**



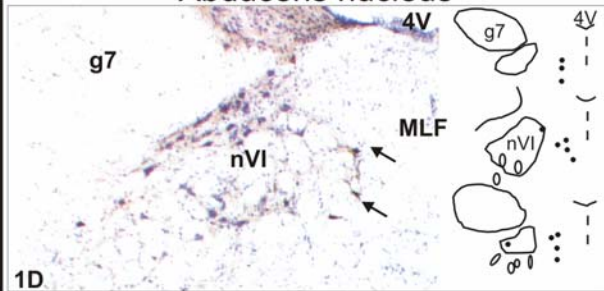
**Oculomotor nucleus**



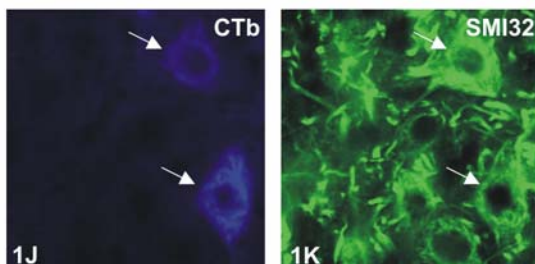
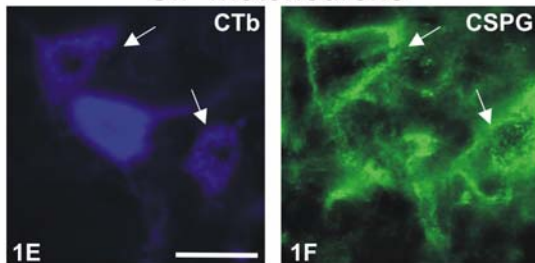
**Abducens nucleus**



**Abducens nucleus**



**SIF motoneurons**



**MIF motoneurons**

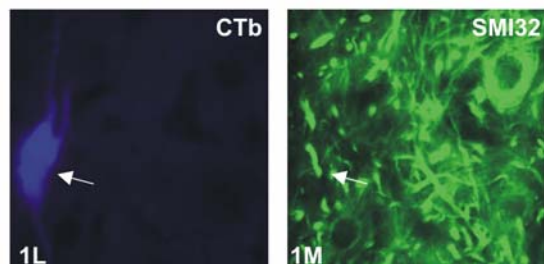
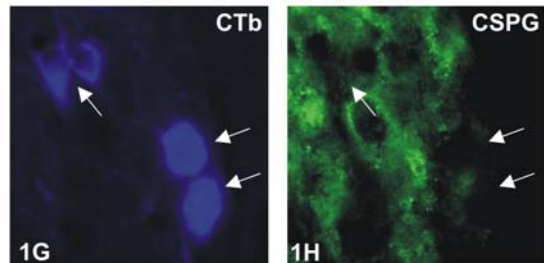


Figure 1: Comparison of tracer injections into the muscle belly (left column) or the distal myotendinous junction (right column) of medial (A, B) and lateral (C, D) rectus muscle in rat. The belly injection labels both SIF and MIF motoneurons, the distal injection only MIF motoneurons. A-D show transverse sections of oculomotor (A, B) and abducens (C, D) nucleus labelled for the tracer detection of CTb (A, B, D) or WGA-HRP (C). The adjacent plots to A-D represent 4 planes from caudal (top) to rostral (bottom) with tracer positive motoneurons.

In the oculomotor nucleus, a distal tracer injection (B) labels less neurons than obtained from a belly injection (A). Their overall localizations within the nucleus is more or less identical, with the greatest part grouped at the medial border and the dorsal third of nIII (A, B, and adjacent plots). In the abducens nucleus, a belly injection of LR fills up the whole nucleus. In addition a few labelled neurons are located outside the medial border (C, arrows). The latter are selectively labelled with a tracer injection into the distal myotendinous junction of the lateral rectus (D, arrows), whereas the motoneurons within the nucleus remain unstained (D). E-M show high magnifications of transverse sections through the oculomotor nucleus (nIII) demonstrating the different staining properties of retrogradely labelled MIF motoneurons (blue) after a small CTb-injection into the distal MR and retrogradely labelled SIF motoneurons after a CTb-injection into the belly of MR. The tracer detection is combined with immunofluorescence for NP-NF (SMI32-antibody) or perineuronal nets (CSPG-antibody) (green). Each pair of neighbouring photographs shows the same section illustrated to demonstrate for different antigens. Note that the tracer-positive MIF motoneurons (blue) lack SMI32- and CSPG-immunoreactivity (G-H, L-M; arrows), whereas the tracer-positive SIF motoneurons (blue) are SMI32- and CSPG-positive (E-F, J-K, arrows). Scale bar in A-D is 200 $\mu$ m, in E-M 40 $\mu$ m.

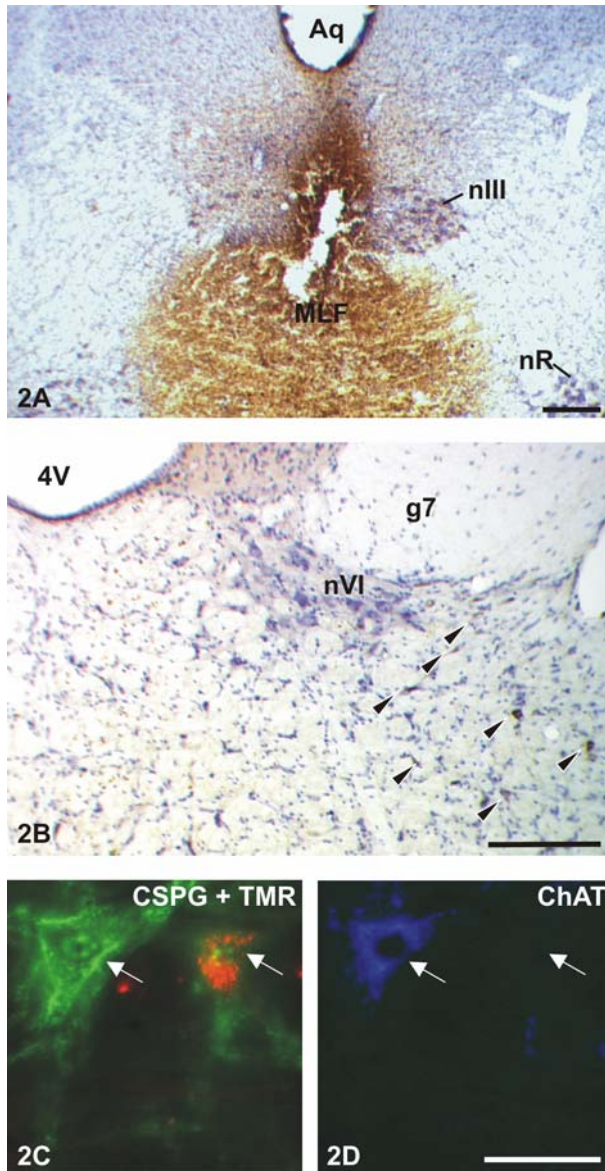


Figure 2: Tracer injection (TMR-dextran) into the oculomotor nucleus of the rat. (A) shows a transversal section of nIII at a mediorostral level labelled for tracer detection and counterstained with cresyl violet. The injection site is located at the midline between the nIIIs. The tracer uptake area involves the left and right nIII, fibres of the MLF and extends ventrally just in between the red nucleus (nR). In the transverse section of right abducens nucleus (B), tracer positive interneurons (arrowheads) are located ventral and lateral to the motoneurons of the abducens nucleus, identified by cresyl violet stain. Their distribution is similar to previous studies in rat by Glicksman (1980) and Labandeira-Garcia et al. (1983). C-D show high magnifications of transverse sections through nVI. C and D represent the same section stained for different antibodies. TMR positive interneuron (C, red fluorescence, arrow) is ChAT-negative (D, blue, arrow), and shows only weak perineuronal net labelling (with CSPG antibody, green, arrow) (C). In contrast, the ChAT positive motoneuron (D, arrow) is strongly CSPG-positive (C, arrow). Scale bar in A-B is 200 $\mu$ m, in C-D 40 $\mu$ m.

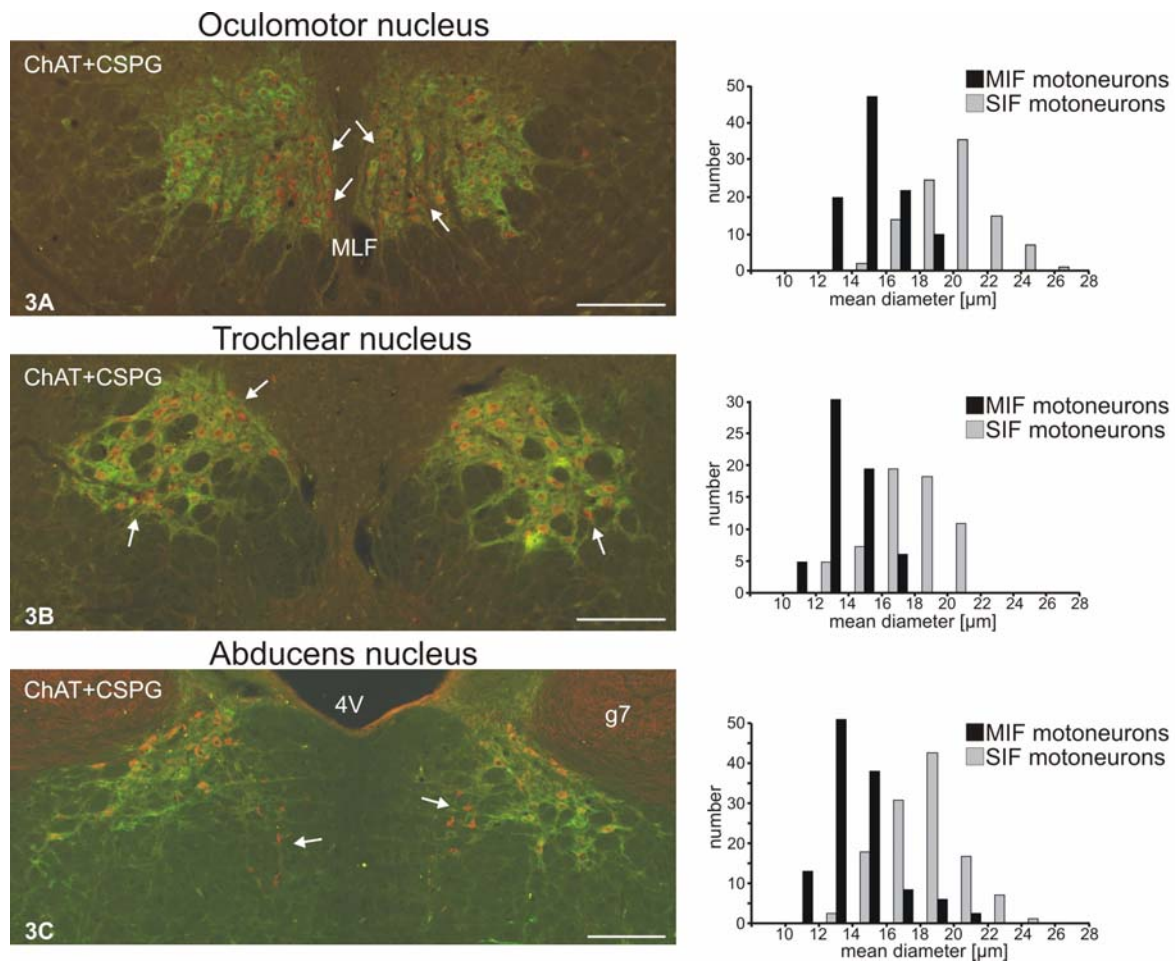
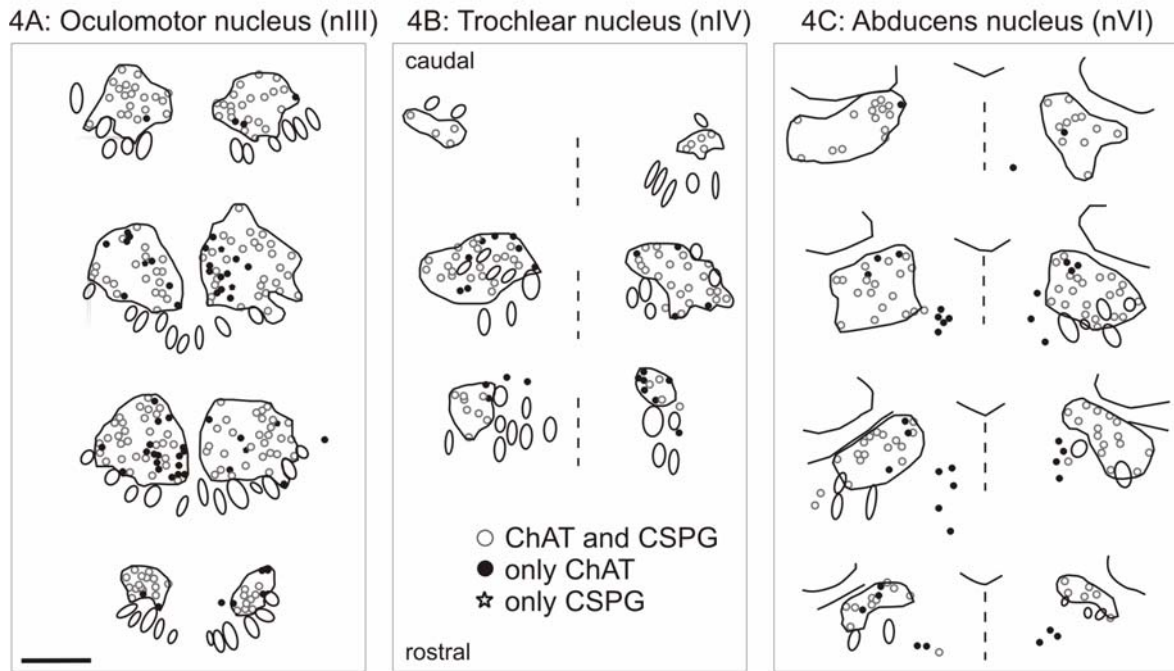


Figure 3: Transverse sections of the oculomotor (A), trochlear (B) and abducens nucleus (C) double labelled with ChAT (red fluorescence) and CSPG (green fluorescence). Whereas the majority of neurons in the three nuclei is positive for ChAT and CSPG representing SIF motoneurons, a certain amount of neurons show only ChAT immunolabelling (MIF motoneurons). In nIII, the MIF motoneurons are located for the greatest part at or close to the medial border (A, arrows), the remaining scattered within the nucleus. In nIV the MIF motoneurons are found at various positions close to the borders (B, arrows). In contrast to nIV, the MIF of nVI are located clearly separated outside the medial border (E, arrows), with additional few located at the dorsal border. Note: Since CSPG-labelling in nVI is not as strong as in nIII or nIV, the perineuronal nets are not clearly visible around some SIFs at the low magnifications shown here. Scale bar is 200 $\mu\text{m}$ .

The adjacent histograms to A-C demonstrate for each nucleus the size differences between MIF (only ChAT positive) and SIF (ChAT and CSPG- positive) motoneurons. In all of the three oculomotor nuclei, the MIF motoneurons are significantly smaller than SIF motoneurons ( $p < 0.001$ ). The detailed data is shown in Table 4.

### Double-labelling with ChAT and CSPG



### Double-labelling with ChAT and SMI32

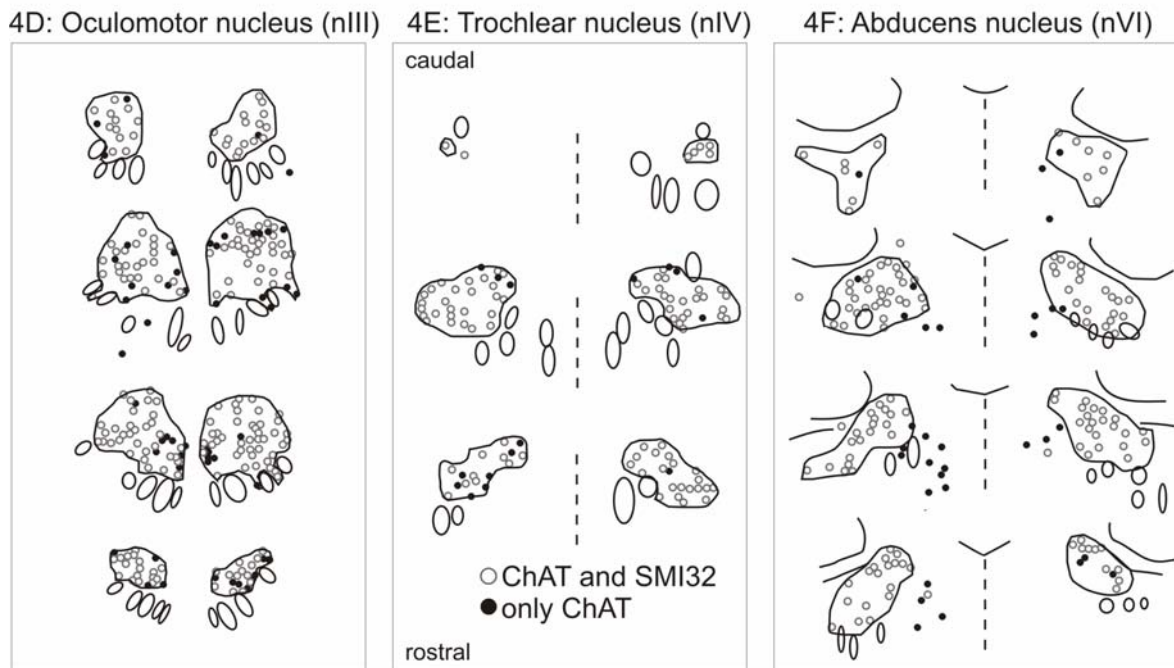


Figure 4: Plots of transverse sections of nIII (A, D), nIV (B, E) and nVI (C, F), the outlines are drawn after subsequently treating the sections with Nissl stain. The sections were double-labelled for ChAT and CSPG (A-C) or ChAT and NP-NFs with SMI32 antibody (D-F). SIF motoneurons (open circle) are both ChAT- and CSPG- or ChAT- and SMI32-positive, whereas MIF motoneurons (filled circle) lack CSPG- and SMI32-immunoreactivity. In nIII (A, D), the MIF motoneurons cluster at or close to the medial border. Additional MIF motoneurons are scattered within the nucleus and lie at the ventral and dorsal border. In nIV (B, E), the MIF motoneurons are found at the borders of the nucleus, whereas they lie clearly separated outside the medial borders in nVI (C, F). Additional MIF motoneurons are located at the dorsal tip of nVI. Scale bar is 200 $\mu$ m.

Table 1: Tracer cases

Case	Injection site	Tracer	Volume	Survival time	Tracer detection
AII-99	belly of MR	1% CTb	6 $\mu$ l	3 days	DAB
AII-99	belly of LR	2.5% WGA-HRP	5 $\mu$ l	3 days	TMB
R12-03	distal MR	1% CTB	1 $\mu$ l	3 days	DAB
AIV-99	distal LR	1% CTB	1 $\mu$ l	3 days	DAB
R13-03	oculomotor nucleus	TMR-Dextran	0.8 $\mu$ l	5 days	DAB
R1-04	oculomotor nucleus	TMR-Dextran	0.8 $\mu$ l	5 days	DAB

Table 2: Used antibodies

Antibody	Host	Antigen	Manufacturer	Dilution
ChAT	rabbit	Choline acetyltransferase	Chemicon, Temecula CA	1:500
CSPG	mouse	Chondroitin sulfate proteoglycan	Chemicon, Temecula CA	1:100
CTb	goat	Cholera toxin subunit B	List Biological Lab. Inc., Campbell CA	1:5000 1:20000
SMI32	mouse	Non-phosphorylated neurofilament	Sternberger Monoclonals Inc., Lutherville MD	1:900
TMR	rabbit	Tetramethyl-rhodamine-	Molecular Probes, Eugene OR	1:1000 1:5000

Table 3: cell counts of SIF and MIF motoneurons

Nucleus	motoneurons (ChAT)	SIF (ChAT+CSPG or +NF-NP)		MIF (ChAT)	
	number	number	percentage	Number	percentage
III	2410	1899	78.8%	511	21.2%
IV	392	333	84.9%	59	15.1%
VI	628	489	77.9%	139	22.1%

Table 4: average mean diameter and two tailed t-test

nucleus	Mean diameter [ $\mu\text{m}$ ]		t-test
	SIF	MIF	
III (100 SIF, 100 MIF)	19.41 +/- 2.31	14.53 +/- 1.65	P<0.0001
IV (100 SIF, 50 MIF)	17.91 +/- 2.45	12.91 +/- 1.42	P<0.0001
VI (100 SIF, 100 MIF)	17.33 +/- 2.27	13.24 +/- 2.01	P<0.0001

Paper 3: Palisade endings in extraocular eye muscles revealed by SNAP-25 immunoreactivity

# Palisade endings in extraocular eye muscles revealed by SNAP-25 immunoreactivity

Andreas C. Eberhorn,<sup>1</sup> Anja K. E. Horn,<sup>1</sup> Nicola Eberhorn,<sup>2</sup> Petra Fischer,<sup>1</sup> Klaus-Peter Boergen<sup>3</sup> and Jean A. Büttner-Ennever<sup>1</sup>

<sup>1</sup>Institute of Anatomy, and <sup>3</sup>Eye Clinic, Ludwig-Maximilian University of Munich, Germany

<sup>2</sup>Max-Planck-Institute of Neurobiology, Martinsried, Germany

---

## Abstract

Palisade endings form a cuff of nerve terminals around the tip of muscle fibres. They are found only in extraocular muscles, but no definite evidence for their role in eye movements has been established. Palisade endings have been reported in all species so far investigated except the rat. In this study we demonstrate that antibodies against SNAP-25, the synaptosomal associated protein of 25 kDa, reliably visualize the complete motor, sensory and autonomic innervation of the extraocular muscles in human, monkey and rat. The SNAP-25 antibody can be combined with other immunofluorescence procedures, and is used here to study properties of palisade endings. With SNAP-25 immunolabelling putative palisade endings are identified in the rat for the first time. They are not well branched, but fulfil several criteria of palisade endings, being associated with non-twitch fibres as shown by double labelling with 'myosin heavy chain slow-twitch' antibodies. The putative palisade endings of the rat lack  $\alpha$ -bungarotoxin binding, which implies that these synapses are sensory. If palisade endings are sensory then they could function as an eye muscle proprioceptor. They seem to be a general feature of all vertebrate eye muscles, unlike the other two extraocular proprioceptors, muscle spindles and Golgi tendon organs, the presence of which varies widely between species.

**Key words** human; monkey; myotendinous cylinders; oculomotor proprioception; rat.

## Introduction

Dogiel was one of the first scientists to describe palisade endings. He found them in the extraocular muscles of human, monkey, horse, oxen, dogs and cats, and referred to three previous reports of similar structures in rabbit, camel and cow (Dogiel, 1906). They were subsequently found in the eye muscles of many other species but, thus far, have not been reported in the rat (Dogiel, 1906; Ruskell, 1999). Palisade endings consist of a cuff, or 'palisade', of fine nerve terminals at the myotendinous junction. They arise from myelinated nerve fibres that enter the muscle at the central nerve entry zone, run to the distal or proximal tip of the muscle and into the tendon, then turning back 180° to

terminate around the tip of a muscle fibre. An alternative name for this type of terminal, plus its collagen capsule, is an 'innervated myotendinous cylinder' (Ruskell, 1978).

Palisade endings are thought to be confined to eye muscles, and they have not been found in any other vertebrate muscle up to now (Ruskell, 1999). Extraocular muscles have a particularly complex structure (reviewed by Spencer & Porter, 1988). They can be divided into an inner global and an outer orbital layer (Kato, 1938). The global layer is continuous from the annulus of Zinn to the tendinous insertion on the sclera of the globe, whereas the orbital layer terminates posterior to the scleral insertion on the fibroelastic capsule of Tenon (Porter et al. 1996; Demer, 2002; Miller et al. 2003). In contrast to skeletal muscles, which contain two main muscle fibre types, six fibre types can be distinguished in extraocular muscles. Spencer & Porter (1988) have reviewed their properties. Four of these fibre types are categorized as twitch muscle fibres (i.e. responding with an all-or-nothing response to stimulation), with a single 'en plaque' region of innervation similar to

---

### Correspondence

Dr Andreas Eberhorn, Institute of Anatomy, Ludwig-Maximilian University of Munich, Pettenkoferstr. 11, D-80336 Munich, Germany. T: +49 89 51604880; F: +49 89 51604857; E: [Andreas.Eberhorn@med.uni-muenchen.de](mailto:Andreas.Eberhorn@med.uni-muenchen.de)

Accepted for publication 17 December 2004

motor endplates found in skeletal muscles. The remaining two types are multiply innervated, one type lying in the orbital layer, the other in the global layer. The multiply innervated muscle fibres respond to stimulation with a slow tonic contraction, and are referred to here as non-twitch muscle fibres. The multiply innervated fibres of the orbital layer have mixed twitch and non-twitch properties (Pachter, 1984), whereas those of the global layer are 'pure' non-twitch fibres. Palisade endings innervate exclusively one specific type of extraocular muscle fibre, the multiply innervated non-twitch muscle fibres of the global layer.

The function of palisade endings has always been a highly controversial subject; and it is still unclear whether they have a sensory function, a motor function or perhaps a mixed function (Lukas et al. 2000). As early as 1910, Tozer and Sherrington showed that palisade endings in the monkey eye muscle did not degenerate when the sensory trigeminal nerve was sectioned (Tozer & Sherrington, 1910), but they did degenerate when the oculomotor nerves were cut. This result was confirmed by Sas & Schwab (1952), with similar methods. These findings imply that either the palisade endings do not have a sensory function and are therefore likely to have a motor function, or that the sensory afferents of palisade endings take a highly unusual route into the brain, for example via the oculomotor nerves.

The question of extraocular proprioception is also contentious, independent of the function of palisade endings. Both muscle spindles and Golgi tendon organs, the classical muscle proprioceptors, were only found in the extraocular muscles of cloven-hoofed species such as sheep (Harker, 1972), camel (Abuel-Atta et al. 1997), pig (Blumer et al. 2001a) and cow (Maier et al. 1974; Blumer et al. 2003). In contrast, some species, including humans, possessed only muscle spindles, but no Golgi tendon organs; by contrast, the eye muscles of numerous other species contained neither muscle spindles nor Golgi tendon organs (Cooper & Daniel, 1949; Lukas et al. 1994). No correlation could be established between the occurrence of proprioceptors and any other factor.

The results of physiological studies do not clarify the position. First, eye muscles do not show a stretch-reflex as skeletal muscles do, and the need for a sensory input from the eye muscles was often doubted, or considered not necessary, because the visual system exerts a constant feedback control over eye movements (Keller & Robinson, 1972). However, neural responses to stretching eye muscles have been reported in the superior

colliculus, the cerebellum and brainstem (Donaldson & Long, 1980; Ruskell, 1999; Donaldson, 2000). In addition, a variety of oculomotor deficits were found when sensory afferents from extraocular muscles were destroyed, manipulated or inactivated (Fiorentini & Maffei, 1977; Maffei & Fiorentini, 1976; Pettorossi et al. 1995). The problems of eye muscle proprioception were pushed aside in the 1970s and became unfashionable for several years, until the early 1980s when investigations of scientists such as Gordon Ruskell generated new interest in the complicated issue (reviewed by Ruskell, 1999).

We consider that palisade endings may provide a proprioceptive signal from eye muscles in the absence of muscle spindles and Golgi tendon organs (Büttner-Ennever et al. 2003). To support this hypothesis, the sensory nature of the palisade endings must be established. Any such study of palisade endings must depend on a staining technique that visualizes the axon, the branches of the palisade endings and, most crucial of all, the terminal boutons of the putative receptors. Classical silver stains (Richmond et al. 1984) may fulfil some of these criteria, but they cannot be combined with modern immunohistochemical techniques to determine the functional properties of the palisade terminals. For example, positive stains for synaptophysin at a presynaptic terminal indicate the presence of synaptic vesicles and thereby a functional synapse (Wiedenmann & Franke, 1985).

In this paper we describe a staining technique that uses antibodies against SNAP-25 to visualize motor axons and endplates, as well as sensory axons and their endings. It is suitable for the complete staining of palisade ending axons, their branches and terminals. The procedure can be simply combined with other immunohistochemical techniques to establish the functional properties of these endings. The synaptosomal associated protein SNAP-25 is a t-SNARE (i.e. a target receptor associated with the presynaptic plasma membrane), involved in synaptic vesicle exocytosis (McMahon & Sudhof, 1995). Several studies showed that SNAP-25 is not only concentrated at synapses and in transport vesicles but also in the axonal membrane (Garcia et al. 1995; Tao-Cheng et al. 2000). Using SNAP-25 antibodies, our study shows for the first time that even rats have putative palisade endings associated with their global layer 'non-twitch' muscle fibres, implying that palisade endings may be present universally in mammalian eye muscles.

## Methods

All experimental procedures conformed to the state and university regulations on Laboratory Animal Care, including the Principles of Laboratory Animal Care (NIH Publication 85-23, Revised 1985), and were approved by their Animal Care Officers and Institutional Animal Care and Use Committees.

Paraformaldehyde-fixed eye muscles were obtained from macaque monkey and three rats. The animals were killed with an overdose of nembutal (80 mg kg<sup>-1</sup> body weight) and transcardially perfused with 0.9% saline (35 °C) followed by 4% paraformaldehyde in 0.1 M phosphate buffer (PB; pH 7.4) and 10% sucrose in 0.1 M PB (pH 7.4). Then, the eyes were removed from the orbits and the eye muscles were carefully dissected and equilibrated in 20 and 30% sucrose in 0.1 M PB for 3 days. Additional unfixed eye muscles were obtained from sheep. Human muscle specimens were removed during optical surgery, post-fixed in 4% PB-buffered paraformaldehyde, and equilibrated in 10, 20 and 30% sucrose. Fixed monkey and unfixed sheep eye muscles were shock frozen in isopentane (−60 °C) and kept at −20 °C until cutting. Rat and human eye muscles were directly frozen in the cryostat microtome (MICROM HM 560). All eye muscles were cut longitudinally at 20 µm and thaw-mounted onto glass slides (Superfrost Plus).

Prior to immunohistochemistry, sheep eye muscles were fixed for 5 min in 4% paraformaldehyde in 0.1 M PB. SNAP-25 immunoreactivity was revealed with the monoclonal mouse antibody SMI81 (Sternberger Monoclonals Inc.).

### Single peroxidase staining of SNAP-25

All sections were pretreated with 3% H<sub>2</sub>O<sub>2</sub>/10% methanol in 0.1 M PB, pH 7.4, for 15 min to suppress endogenous peroxidase activity and then thoroughly washed. For the detection of SNAP-25 immunoreactivity, sections were blocked with 5% horse serum in 0.1 M PB, pH 7.4, containing 0.3% Triton X-100 for 1 h and subsequently processed with mouse anti-SNAP-25 antibodies (1 : 5000) overnight at room temperature. After several buffer washes the sections were treated with biotinylated horse antimouse antibody (1 : 200; Alexis) for 1 h at room temperature, washed and incubated in extravidin-horseradish peroxidase (1 : 1000; Sigma) for 1 h. Diaminobenzidine served as chromogen for the

detection of SNAP-25 immunoreactivity. Some sections were counterstained with hemalaun (0.1%).

### Double and triple fluorescence labelling

In order to verify that SNAP-25 is present in both nerve fibres and terminals, double immunofluorescence staining was performed on monkey and rat eye muscles using SNAP-25 antibodies combined with either anti-synaptophysin or anti-neurofilament-M (NF-M).

First the eye muscle sections were blocked with 5% normal donkey serum in 0.1 M PB, pH 7.4, containing 0.3% Triton X-100 for 1 h. Then, the sections were processed with a mixture of mouse anti-SNAP-25 (1 : 1000) and either rabbit anti-synaptophysin (1 : 100; Synaptic Systems) or rabbit anti-NF-M (1 : 1000; Chemicon) overnight. For visualization of the applied antibodies, the sections were then reacted with a mixture of fluorochrome-tagged secondary antibodies from donkey, namely Alexa 488-anti-rabbit (1 : 200; Molecular Probes) and Cy<sup>3</sup>-anti-mouse (1 : 200; Dianova) for 2 h.

For the identification of putative palisade endings in rat extraocular muscles, longitudinal sections of 17 eye muscles were processed for the detection of SNAP-25 combined with  $\alpha$ -bungarotoxin binding, and staining for synaptophysin or myosin heavy chain slow twitch. After blocking with 5% normal donkey serum in 0.1 M PB, pH 7.4, containing 0.3% Triton X-100 for 1 h, the sections were first treated with mouse anti-SNAP-25 (1 : 1000) overnight, followed by a 2-h incubation of Alexa 488-tagged donkey anti-mouse (1 : 200; Molecular Probes) secondary antibody. After extensive rinsing in 0.1 M PB, pH 7.4, the sections were then processed with mouse anti-myosin heavy chain slow-twitch (1 : 100; Novocastra) or rabbit anti-synaptophysin (1 : 100) overnight, followed by a 2-h incubation of Cy<sup>5</sup>-tagged donkey anti-mouse or donkey anti-rabbit (1 : 150; Dianova) secondary antibody. After washing in 0.1 M PB, the sections were then treated with Cy<sup>3</sup>-tagged  $\alpha$ -bungarotoxin (1 : 200, Molecular Probes) for 30 min at room temperature and rinsed in 0.1 M PB.

All fluorochrome-stained sections were coverslipped with GEL/MOUNT permanent aqueous mounting medium (Biomedica) and stored in the dark at 4 °C.

### Analysis

Images of bright-field photographs were digitalized by using the 3-CCD videocamera (Hamamatsu; C5810)

mounted on a Leica DMRB microscope. The images were captured on a computer with Adobe Photoshop 5 software. Sharpness, contrast and brightness were adjusted to reflect the appearance of the labelling seen through the microscope.

### Confocal microscopy and image processing

Fluorescence-stained eye muscle sections were imaged with a Leica TCS NT and a Leica TCS SP2 laser-scanning confocal fluorescence microscope (Leica, Heidelberg, Germany). Images were taken with a 40 $\times$  oil objective, NA 1.4, at a resolution of approximately 200 nm per pixel. Dual or triple channel imaging of Cy<sup>2</sup>/Alexa 488, Cy<sup>3</sup> and Cy<sup>5</sup> fluorescence were sequentially recorded at 488 nm excitation/525–550 nm emission, 543 nm excitation/555–620 nm emission, and 633 nm excitation/650–750 nm emission, respectively. Z-series were collected from 0.5–1  $\mu$ m optical sections taken through the specimen. Image stacks were processed using Metamorph 6.1 (Universal Imaging Inc., USA). Brightness and contrast were enhanced as required, and maximum intensity projections were generated for visualization.

All pictures were arranged and labelled with drawing software (CorelDraw 8 and 11; Corel).

## Results

SNAP-25 immunolabelling is used to stain neural structures in the extraocular muscles of monkey, human, sheep and rat. It is shown here to stain motor nerves and endplates, sensory fibres and terminals, autonomic innervation of blood vessels, and palisade endings at the myotendinous junction.

### Motor innervation

The motor nerves are completely visualized with the SNAP-25 antibody stain, from their entry into the extraocular muscle up to the fine ramifications where they yield the nerve terminals of 'en plaque' endings on the twitch muscle fibres (Fig. 1A,D). This was verified with double labelling of the 'en plaque' endings with synaptophysin antibodies (Fig. 1E). In all of these endings SNAP-25 and synaptophysin immunoreactivity were always co-localized (Fig. 1D–F). In contrast to

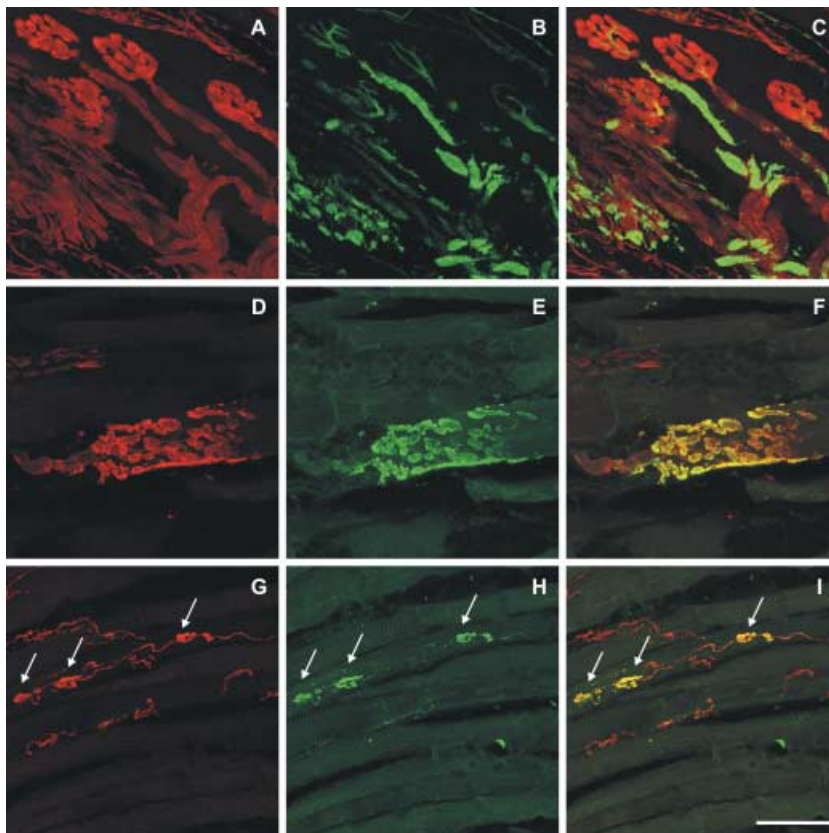


**Fig. 1** Laser scanning photomicrographs of longitudinal sections of extraocular eye muscles. (A–C) Double immunofluorescence labelling of a rat inferior rectus muscle with antibodies for SNAP-25 (red) and NF-M (green). A motor nerve is entering the eye muscle and branches into several 'en plaque' endings. SNAP-25 antibodies visualize both the nerve fibres and the 'en plaque' endings (A) whereas NF-M immunoreactivity is present only in the majority of the nerve fibres (B). This is clearly shown in the overlay of both markers in C. (D–I) Double immunofluorescence labelling of a monkey inferior rectus muscle with antibodies for SNAP-25 (red) and synaptophysin (green). Detailed view of an 'en plaque' ending on a twitch muscle fibre (D–F) and 'en grappe' endings (arrows) on a multiply innervated muscle fibre (G–I). In both types of endings, SNAP-25 and synaptophysin immunoreactivity clearly outline the morphology of these endings and are co-localized in all terminals, as indicated in the overlays (F,I). Note that the motor nerve giving rise to the 'en grappe' endings lacks synaptophysin and is only visualized with SNAP-25 antibodies (H,I). Scale bar, 50  $\mu$ m.

SNAP-25 (red fluorescence), which clearly visualizes both nerves and terminals, NF-M (green fluorescence) is only present in the nerve branches (Fig. 1B,C).

The motor nerve and the small 'en grappe' motor endplates along the length of multiply innervated muscle fibres were strongly labelled with SNAP-25 antibodies (Fig. 1G,I). All 'en grappe' endplates were double labelled for synaptophysin and SNAP-25 (Fig. 1H,I).

### Sensory innervation

In order to test the ability of SNAP-25 to label sensory nerves and their terminals, sheep eye muscles, which contain muscle spindles, were stained with SNAP-25 antibody. Muscle spindles were easily identified in van Giesson stains by the collagen fibre capsule. The sensory annulospiral endings on the equatorial region of the intrafusal fibre of muscle spindles were fully labelled with SNAP-25 antibodies (Fig. 2A).

### Autonomic innervation

Blood vessels within the extraocular muscle are innervated by a network of fine varicose nerves which are clearly SNAP-25 positive (Fig. 2B).

### Palisade endings

Only palisade endings in which the supplying axon could be seen to enter the muscle fibre from the distal tendon were analysed in this study. Because staining for SNAP-25 labels both nerve fibres and terminals of motor and sensory axons, it could be used for the complete visualization of palisade endings at the myotendinous junction. In Fig. 2(C), the palisade ending in a human eye muscle is visualized to its full extent with SNAP-25 antibodies. The reconstruction of the double labelled monkey palisade ending shows the red fluorescence of SNAP-25 positive afferent axon and cuff of terminals around the tip of a muscle fibre (Fig. 3A). In

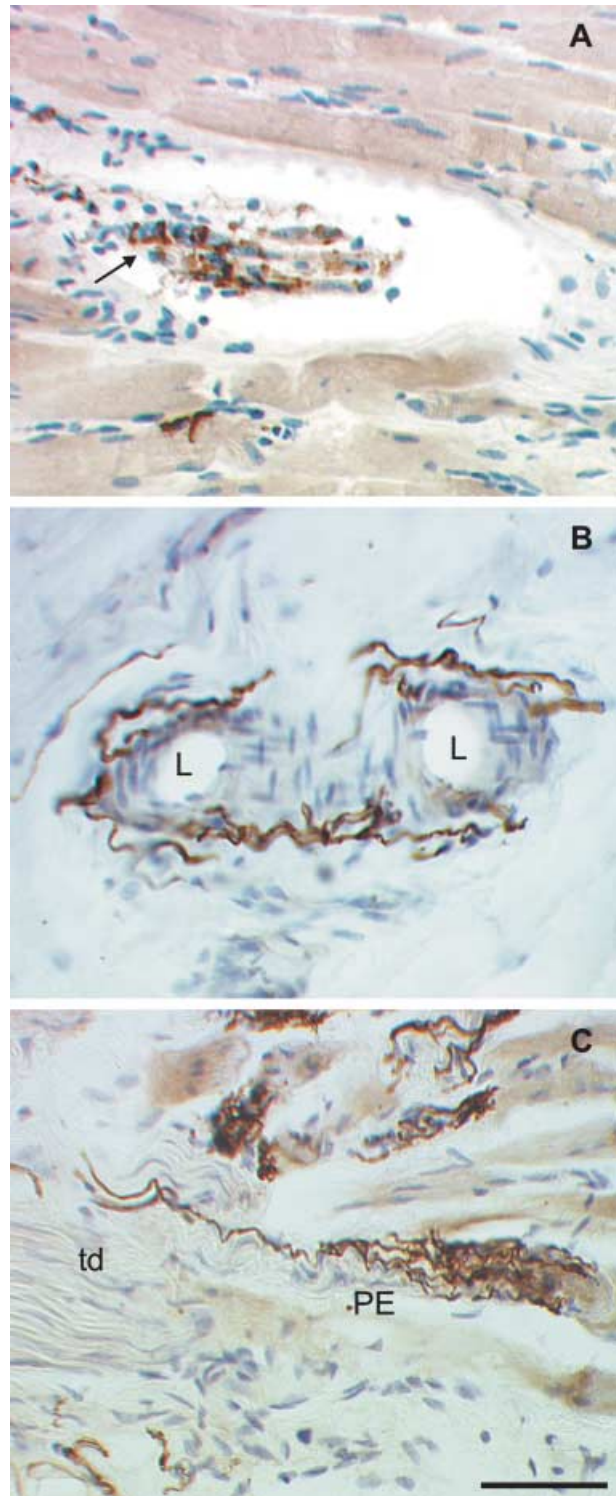


**Fig. 2** Photomicrographs of neural structures in longitudinal sections of sheep and human extraocular eye muscles labelled with SNAP-25 antibodies and counterstained with hemalaun. (A) Identified muscle spindle in a sheep inferior rectus muscle. With SNAP-25 immunolabelling, a nerve fibre which enters the collagenous capsule is visualized. On the intrafusal muscle fibres an annulospiral ending which winds around the fibres is clearly SNAP-25 positive (arrow). (B) Blood vessels in the tendon of a human extraocular muscle. Using SNAP-25

antibodies, a fine network of varicose nerve fibres surrounding the lumen (L) of the vessels could be identified. (C) A palisade ending at the myotendinous junction of a human extraocular eye muscle. SNAP-25 antibodies completely label the palisade ending (PE), the axon which enters from the tendon (td) as well as the bunch of branches and small terminals which terminate on a muscle fibre. Scale bar, 50  $\mu$ m.

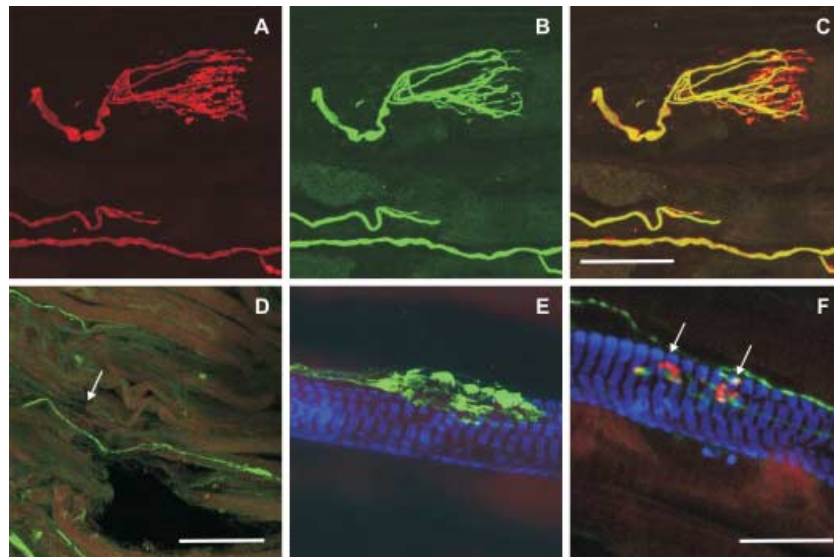


**Fig. 3** Laser scanning photomicrographs of longitudinal sections of extraocular eye muscles. (A–C) Double immunofluorescence labelling of a palisade ending at the myotendinous junction of a monkey inferior rectus muscle with antibodies for SNAP-25 (red) and NF-M (green). The afferent axon and the bunch of axonal branches are both visible in the SNAP-25 (A) stain and the NF-M (B) stain. In contrast, the cuff of terminals lacks NF-M immunoreactivity and can only be identified with SNAP-25 antibodies (B), which is clearly demonstrated in the overlay of both markers in C. (D–F) Double (D) or triple (E,F) immunofluorescence labelling of a rat inferior rectus muscle with antibodies for SNAP-25 (green), myosin heavy chain slow-twitch (MHC<sub>slow-twitch</sub>; blue) and additional applied  $\alpha$ -bungarotoxin (red). Panels D–F show overlays of the applied markers. (D) At the myotendinous junction (tendon left, muscle right), a putative palisade ending is identified with SNAP-25 antibodies. A nerve fibre enters from the distal tendon (arrow) and forms a clump of terminals on a muscle fibre. At higher magnification, a similar clump of terminals of the putative palisade ending in a different section can be clearly identified as several individual terminals, which form neuromuscular contacts on an MHC slow-twitch positive multiply innervated muscle fibre (E). In the same section, two  $\alpha$ -bungarotoxin and SNAP-25 positive 'en grappe' endings (arrows) on an MHC slow-twitch-positive multiply innervated muscle fibre are clearly visible (F). Note that in contrast to these 'en grappe' endings, the terminals of the putative palisade endings in D and E do not show red any  $\alpha$ -bungarotoxin binding. Scale bars: 50  $\mu$ m (A–C), 200  $\mu$ m (D), 20  $\mu$ m (E,F).

contrast, NF-M immunoreactivity (green fluorescence) is present only in the axonal branches and not in the terminals (Fig. 3B,C).

The study of 17 rat extraocular muscles stained with SNAP-25 antibodies showed a more widespread network of neural structures at the distal tip of the muscle and the adjacent tendon compared with in monkey or human. Some of these could be identified as 'en grappe' endplates on muscle fibres, whereas others were associated with blood vessels and connective tissue. In addition, axons could be traced from the distal tendon, and were found to terminate in close proximity to the muscle fibre tips, where the global layer inserts into the sclera (Blumer et al. 2001b; Miller et al. 2003). These axons were of a larger calibre than the fine nerves innervating blood vessels. In spite of the difficulty in obtaining intact myotendinous junctions in rat eye muscles, 27 such structures were found and they varied in their morphology from a fine network to a compact clump of terminals (Fig. 3D,E). A review of the spectrum of terminals is beyond the scope of this paper. Here,

one such terminal is selected as an example, and used to illustrate some of the histochemical properties of structures at the myotendinous junction of the rat eye muscles.

Nineteen of the presumed palisade endings were tested for  $\alpha$ -bungarotoxin binding, and all but one were completely negative, implying the absence of motor endplates. In contrast, a control labelling of 'en grappe' endplates on a multiply innervated muscle fibre in the same section shows clear  $\alpha$ -bungarotoxin binding (Fig. 3F). Additional staining with antibodies for synaptophysin on ten of the bungarotoxin-negative terminals verified the presence of synapses. In the few terminals in which  $\alpha$ -bungarotoxin binding is present, it was assumed to be due to the presence of 'en grappe' endplates from a distally projecting motor nerve adjacent to the presumed palisade ending.

Palisade endings are always associated with multiply innervated muscle fibres of the global layer (Alvarado-Mallart & Pincon Raymond, 1979). In order to support our assumption that the terminals at the myotendinous junction of the rat eye muscles share the same

properties of palisade endings we combined the SNAP-25 staining with immunolabelling for the myosin heavy chain slow-twitch isoform, which is only expressed in the multiply innervated muscle fibres according to several authors (Kranjc et al. 2001; Rubinstein & Hoh, 2001; Kjellgren et al. 2003; D. Porter, personal communication). We found that the putative palisade endings in rat were always attached to a myosin heavy chain slow-twitch-positive, multiply innervated muscle fibre (Fig. 3E,F).

The putative palisade endings terminate in close proximity (about 200  $\mu\text{m}$ ) to the distal tip of the muscle fibre, but do not show the typical palisade-like branching seen in monkeys (Fig. 3). No neurotendinous terminals were found in the rat experiments. Accordingly, in this light microscopic study, all terminals appear to contact the muscle fibres.

## Discussion

The staining properties of antibodies against the synaptosomal associated protein SNAP-25 enabled us to stain both motor and sensory nerve axons and terminals in extraocular muscles. In particular, palisade endings and their terminals could be reliably visualized in human and monkey, and for the first time putative palisade endings are described in rat. In many previous studies silver staining methods were used to identify palisade endings (Dogiel, 1906; Alvarado-Mallart & Pincon Raymond, 1979; Richmond et al. 1984). The visualization of palisade endings using SNAP-25 antibodies is at least as good as with the silver staining techniques, and it avoids their major disadvantages. (1) Silver stains cannot be combined with immunohistochemical stains, (2) the technique is complex and not easy to reproduce (3) as stated by some authors (Richmond et al. 1984), some structures may remain unstained. Looking for alternative stainings to SNAP-25 immunolabelling, there are at least two other antibodies which visualize both nerve fibres and terminals and can also be combined with other immunohistochemical techniques: neurocalcin and protein gene product 9.5 (PGP 9.5). Neurocalcin is a member of the EF-hand family of calcium-binding proteins and stains myelinated axons and motor nerve endings in extraocular muscles (Junttila et al. 1995). However, this antibody is not commercially available. PGP 9.5 is a cytoplasmatic neuronal protein identified as a ubiquitin carboxyl-terminal hydrolase (Wilkinson et al. 1989) and has also been used to stain

palisade endings. But up to now, the PGP 9.5 stainings of palisade endings have not yielded the high-resolution morphology seen here with SNAP-25 immunolabelling (Lukas et al. 2000).

The morphology of rat palisade endings varies and appeared to be less elaborate in comparison with the highly branched terminals in monkey and human, but they always showed typical properties of palisade endings, in that they (1) are innervated by a nerve arising from the tendon (Fig. 3D), and (2) terminate on a multiply innervated muscle fibre at the myotendinous junction of the global layer (Fig. 3E) (Dogiel, 1906; Richmond et al. 1984; Ruskell, 1999). The structures in Fig. 3(D,E) represent only one type of ending with a rather compact clump of terminals. In spite of the fact that the appearance of this structure is so unlike a palisade, we assume it to be homologous to a palisade ending, because of its other attributes.

In addition, the rat putative palisade endings were shown to contain synaptophysin immunoreactivity, proving the presence of synapses at their terminals. The presence of rudimentary palisade endings in rats may not be surprising, because rats are not highly visual animals and would not be expected to have well-developed receptors in their oculomotor system.

The function of palisade endings is still controversial, and current studies have attributed both motor and sensory properties to them. We combined the staining for SNAP-25 in palisade endings with the classical proof for the presence of motor endplates, the binding of  $\alpha$ -bungarotoxin (Anderson & Cohen, 1974), and found no evidence for motor endplates at the terminals of rat palisade endings. According to Alvarado-Mallart & Pincon Raymond (1979) and Lukas et al. (2000), a defining feature of palisade endings is that they form mainly neurotendinous contacts, whereas neuromuscular contacts were rare. An exception to this was found in the rabbit, where Blumer et al. (2001b) showed that palisade endings form exclusively myoneural contacts. In our analysis of the putative palisade endings of the rat we only found neuromuscular contacts, implying a similarity to the rabbit. Exclusive neuromuscular contacts combined with  $\alpha$ -bungarotoxin positive terminals led Blumer et al. (2001b) to assume that rabbit palisade endings are motor and may act as effectors. However, the rat putative palisade endings never bind  $\alpha$ -bungarotoxin, implicating a sensory function. It is hard to believe that these contradictions are due to species differences; and a possible explanation has been put

forward by Lukas et al. (2000). They suggest that palisade endings are proprio-effectors with mixed sensory and motor properties.

The presence of palisade-like endings in rat opens up the possibility that they are a universal feature of all eye muscles, whereas the occurrence of muscle spindles and Golgi tendon organs is not. Several authors have suggested that palisade endings could be the source of sensory afferent signals (Ruskell, 1999; Donaldson, 2000; Steinbach, 2000; Weir et al. 2000; Büttner-Ennever et al. 2002). The ultrastructural morphology of palisade endings in cat, rhesus monkey and sheep has been shown to be typical of a sensory structure (Ruskell, 1978; Alvarado-Mallart & Pincon Raymond, 1979; Blumer et al. 1998). However, Blumer et al. (2001b), Lukas et al. (2000), and Konakci et al. (2005) show that in rabbit, and to a minor extent in human and in cat, palisade terminals exhibit motor-terminal-like properties. The problem is compounded by the conflicting evidence for the location of the cell soma of the palisade ending. If the palisade endings are sensory, their cell body should lie in the trigeminal ganglion or in the mesencephalic trigeminal nucleus; by contrast, if the endings are of a motor origin then they would have cell bodies associated with the motor nuclei of the extraocular muscles. Tozer & Sherrington (1910) as well as Sas & Scháb (1952) provided evidence for their location in the oculomotor nerve or nucleus, a result more compatible with a motor role for the palisade endings (Gentle & Ruskell, 1997; Ruskell, 1999), whereas the results of other studies point to the trigeminal ganglion as the location of palisade ending soma (Billig et al. 1997), and imply a sensory function.

The work of Gordon Ruskell has revived the interest in palisade endings, but their function still remains unclear. We have shown that the synaptosomal associated protein SNAP-25 is a useful marker for studying their properties. Finally, our demonstration that palisade-like endings occur in the extraocular muscles of the rat implies that palisade endings may be a general feature of mammalian eye muscles, unlike extraocular proprioceptors such as muscle spindles and Golgi tendon organs.

## Acknowledgements

This study was sponsored by a grant from the Deutsche Forschungsgemeinschaft (Ho 1639/4-1; GRK 267). We also thank Christine Glombik for her technical

assistance, Ahmed Messoudi for his expertise and Professor Lange for his continual support.

## References

- Abuel-Atta AA, DeSantis M, Wong A (1997) Encapsulated sensory receptors within intraorbital skeletal muscles of a camel. *Anat. Rec.* **247**, 189–198.
- Alvarado-Mallart RM, Pincon Raymond M (1979) The palisade endings of cat extraocular muscles: a light and electron microscope study. *Tissue Cell* **11**, 567–584.
- Anderson MJ, Cohen MW (1974) Fluorescent staining of acetylcholine receptors in vertebrate skeletal muscle. *J. Physiol.* **237**, 385–400.
- Billig I, Buisseret-Delmas C, Buisseret P (1997) Identification of nerve endings in cat extraocular muscles. *Anat. Rec.* **248**, 566–575.
- Blumer R, Lukas JR, Wasicky R, Mayr R (1998) Presence and structure of innervated myotendinous cylinders in sheep extraocular muscle. *Neurosci. Lett.* **248**, 49–52.
- Blumer R, Wasicky R, Brugger PC, Hoetzenecker W, Wicke WL, Lukas JR (2001a) Number, distribution, and morphologic particularities of encapsulated proprioceptors in pig extraocular muscles. *Invest. Ophthalmol. Vis. Sci.* **42**, 3085–3094.
- Blumer R, Wasicky R, Hötzenecker W, Lukas JR (2001b) Presence and structure of innervated myotendinous cylinders in rabbit extraocular muscle. *Exp. Eye Res.* **73**, 787–796.
- Blumer R, Konakci KZ, Brugger PC, et al. (2003) Muscle spindles and Golgi tendon organs in bovine calf extraocular muscle studied by means of double-fluorescent labeling, electron microscopy, and three-dimensional reconstruction. *Exp. Eye Res.* **77**, 447–462.
- Büttner-Ennever JA, Horn AKE, Graf W, Ugolini G (2002) Modern concepts of brainstem anatomy. *Ann. NY Acad. Sci.* **956**, 75–84.
- Büttner-Ennever JA, Eberhorn A, Horn AKE (2003) Motor and sensory innervation of extraocular eye muscles. *Ann. NY Acad. Sci.* **1004**, 40–49.
- Cooper S, Daniel PM (1949) Muscle spindles in human extrinsic eye muscles. *Brain* **72**, 1–24.
- Demer JL (2002) The orbital pulley system: a revolution in concepts of orbital anatomy. *Ann. NY Acad. Sci.* **956**, 17–32.
- Dogiel AS (1906) Die Endigungen der sensiblen Nerven in den Augenmuskeln und deren Sehnen beim Menschen und den Säugetieren. *Arch. Mikrosk. Anat.* **68**, 501–526.
- Donaldson IML, Long AC (1980) Interactions between extraocular proprioceptive and visual signals in the superior colliculus of the cat. *J. Physiol.* **298**, 85–110.
- Donaldson IML (2000) The functions of the proprioceptors of the eye muscles. *Phil. Trans. R. Soc. Lond. [Biol.]* **355**, 1685–1754.
- Fiorentini A, Maffei L (1977) Instability of the eye in the dark and proprioception. *Nature* **269**, 330–331.
- Garcia EP, McPherson PS, Chillocote TJ, Takei K, De Camilli P (1995) rb-Sec1A and B colocalize with syntaxin 1 and SNAP-25 throughout the axon, but are not in a stable complex with syntaxin. *J. Cell Biol.* **129**, 105–120.
- Gentle A, Ruskell GL (1997) Pathway of the primary afferent nerve fibres serving proprioception in monkey extraocular muscles. *Ophthalmol. Physiol. Opt.* **17**, 225–231.

- Harker DW** (1972) The structure and innervation of sheep superior rectus and levator palpebrae extraocular eye muscles. II: Muscle spindles. *Invest. Ophthalmol. Vis. Sci.* **11**, 970–979.
- Junttila T, Koistinaho J, Rechart L, Hidaka H, Okazaki K, Pelto-Huikko M** (1995) Localization of neurocalcin-like immunoreactivity in rat cranial motoneurons and spinal cord interneurons. *Neurosci. Lett.* **183**, 100–103.
- Kato T** (1938) Über histologische Untersuchungen der Augenmuskeln von Menschen und Säugetieren. *Okajimas Folia Anat. Jap.* **16**, 131–145.
- Keller EL, Robinson DA** (1972) Abducens unit behavior in the monkey during vergence movements. *Vision Res.* **12**, 369–382.
- Kjellgren D, Thornell L-E, Andersen J, Pedrosa-Domellöf F** (2003) Myosin heavy chain isoforms in human extraocular muscles. *Invest. Ophthalmol. Vis. Sci.* **44**, 1419–1425.
- Konakci KZ, Streicher J, Hoetzenecker W, Blumer MJF** (2005) Molecular characteristics suggest an effector function of palisade endings in extra-ocular muscles. *Invest. Ophthalmol. Vis. Sci.* **46**, 155–165.
- Kranjc BS, Sketelj J, Albis AD, Ambroz M, Erzen I** (2001) Fibre types and myosin heavy chain expression in the ocular medial rectus muscle of the adult rat. *J. Muscle Res. Cell Motil.* **21**, 753–761.
- Lukas JR, Aigner M, Blumer R, Heinzl H, Mayr R** (1994) Number and distribution of neuromuscular spindles in human extraocular muscles. *Invest. Ophthalmol. Vis. Sci.* **35**, 4317–4327.
- Lukas JR, Blumer R, Denk M, Baumgartner I, Neuhuber W, Mayr R** (2000) Innervated myotendinous cylinders in human extraocular muscles. *Invest. Ophthalmol. Vis. Sci.* **41**, 2422–2431.
- Maffei L, Fiorentini A** (1976) Asymmetry of motility of the eyes and change of binocular properties of cortical cells in adult cats. *Brain Res.* **105**, 73–78.
- Maier A, DeSantis M, Eldred E** (1974) The occurrence of muscle spindles in extraocular muscles of various vertebrates. *J. Morphol.* **143**, 397–408.
- McMahon HT, Sudhof TC** (1995) Synaptic core complex of synaptobrevin, syntaxin, and SNAP-25 forms high affinity alpha-SNAP binding site. *J. Biol. Chem.* **270**, 2213–2217.
- Miller JM, Demer JL, Poukens V, Pavlovski DS, Nguyen HN, Rossi EA** (2003) Extraocular connective tissue architecture. *J. Vis.* **3**, 240–251.
- Pachter BR** (1984) Rat extraocular muscle. 3. Histochemical variability along the length of multiply-innervated fibers of the orbital surface layer. *Histochemistry* **80**, 535–538.
- Pettorossi VE, Ferraresi A, Draicchio F, et al.** (1995) Extraocular muscle proprioception and eye position. *Acta Otolaryngol. (Stockholm)* **115**, 137–140.
- Porter JD, Poukens V, Baker RS, Demer JL** (1996) Structure-function correlations in the human medial rectus extraocular muscle pulleys. *Invest. Ophthalmol. Vis. Sci.* **37**, 468–472.
- Richmond FJR, Johnston WSW, Baker RS, Steinbach MJ** (1984) Palisade endings in human extraocular muscle. *Invest. Ophthalmol. Vis. Sci.* **25**, 471–476.
- Rubinstein NA, Hoh JF** (2001) The distribution of myosin heavy chain isoforms among rat extraocular muscle fiber types. *Invest. Ophthalmol. Vis. Sci.* **41**, 3391–3398.
- Ruskell GL** (1978) The fine structure of innervated myotendinous cylinders in extraocular muscles in rhesus monkey. *J. Neurocytol.* **7**, 693–708.
- Ruskell GL** (1999) Extraocular muscle proprioceptors and proprioception. *Prog. Retin Eye Res.* **18**, 269–291.
- Sas J, Scháb R** (1952) Die sogenannten 'Palisaden-Endigungen' der Augenmuskeln. *Acta Morph. Acad. Sci. (Hungary)* **2**, 259–266.
- Spencer RF, Porter JD** (1988) Structural organization of the extraocular muscles. In *Neuroanatomy of the Oculomotor System* (ed. Büttner-Ennever JA), pp. 33–79. Amsterdam: Elsevier.
- Steinbach MJ** (2000) The palisade ending: an afferent source for eye position information in humans. In *Advances in Strabismus Research. Basic and Clinical Aspects* (eds Lennerstrand G, Ygge J, Laurent T), pp. 33–42. London: Portland Press.
- Tao-Cheng J-H, Du J, McBain CJ** (2000) Snap-25 is polarized to axons and abundant along the axolemma: an immunogold study of intact neurons. *J. Neurocytol.* **29**, 67–77.
- Tozer FM, Sherrington CS** (1910) Receptors and afferents of the third, fourth and sixth cranial nerves. *Proc. R. Soc. London Ser.* **82**, 451–457.
- Weir CR, Knox PC, Dutton GN** (2000) Does extraocular muscle proprioception influence oculomotor control? *Br. J. Ophthalmol.* **84**, 1071–1074.
- Wiedenmann B, Franke WW** (1985) Identification and localization of synaptophysin, an integral membrane glycoprotein of Mr 38 000 characteristic of presynaptic vesicles. *Cell* **41**, 1017–1028.
- Wilkinson KD, Lee KM, Deshpande S, Duerksen-Hughes P, Boss JM, Pohl J** (1989) The neuron-specific protein PGP 9.5 is an ubiquitin carboxyl-terminal hydrolase. *Science* **246**, 670–673.

## Discussion

In monkeys SIF and MIF motoneurons of extraocular muscles were identified by tracer injections into the belly or the distal myotendinous junction of the medial or lateral rectus muscle. For the characterization of both motoneuron types, the tracer visualization was combined with the detection of four histochemical markers: perineuronal nets, non-phosphorylated neurofilaments, parvalbumin and cytochrome oxidase. The experiments revealed that the MIF motoneurons in the periphery of the motonuclei do not contain non-phosphorylated neurofilaments or parvalbumin and lack perineuronal nets. In contrast, SIF motoneurons intensively express all markers. Cytochrome oxidase immunostaining was found in both motoneuron populations. Another population of motoneurons with 'MIF properties' was identified within the boundaries of the abducens nucleus, but not labelled by distal muscle injections. They could represent the motoneurons innervating MIFs in the orbital layer of lateral rectus muscle. In addition to the histochemical differences, the MIF motoneurons are on average significantly smaller in size than the SIF motoneurons.

Analogous to the study in monkey, the SIF and MIF motoneurons of rats were identified with tracer injections into the belly or the distal myotendinous junction of the medial and lateral rectus muscle and further characterized using immunohistochemical methods. For the first time both motoneuron populations were identified in the rat. As in the monkey, the MIF motoneurons lie for the greater part separated from the SIF motoneurons and are different in size and molecular components: the smaller MIF motoneurons lack non-phosphorylated neurofilaments and perineuronal nets, both definite markers of the larger SIF motoneurons.

A possible proprioceptive control of eye movements requires the presence of proprioceptive structures. The palisade endings, representing the best candidate for an EOM-proprioceptor, were analysed using antibodies against the synaptosomal associated protein of 25kDA, SNAP-25. With this method palisade ending-like structures were identified for the first time

in the extraocular muscles of the rat. Furthermore the rat palisade endings show characteristics of a sensory structure and thereby supporting their role in proprioception.

Hence the results of this work further strengthen the presence of a dual motor innervation to control the extraocular eye muscles, at least in all mammals. As described in the studies on monkey the premotor innervation of MIF and SIF motoneurons shows clear differences (Büttner-Ennever et al., 2002; Wasicky et al., 2004). Accordingly, the MIF motoneurons are associated with premotor areas for vergence and gaze holding, but in contrast to SIF motoneurons, *not* with premotor areas generating saccades or VOR. The functional difference between these motoneurons is supported by their molecular equipment. SIF motoneurons contain parvalbumin and perineuronal nets, both markers of highly active neurons (Blümcke and Celio, 1992; Brückner et al., 1993; Horn et al., 2003). This is supported by recording studies from lateral rectus motoneurons in monkey which demonstrated that most abducens motoneurons had maximal burst firing rates of 300-400 Hz, some of which could reach rates as high as 800 Hz (Fuchs and Luschei, 1971; Fuchs et al., 1988) therefore requiring a remarkable high level of metabolic activity. In contrast the MIF motoneurons lack parvalbumin and perineuronal nets. Electrophysiological data of MIF motoneurons is sparse, though their characteristics may be deduced from studies in frog and cat, where non-twitch units (innervating the global MIF) were described and shown to fire tonically (Dieringer and Precht, 1986), lack tetanic fusion frequency, and are extreme fatigue resistant (Morgan and Proske, 1984; Shall and Goldberg, 1992).

In summary, the overall characteristics of the MIF motoneurons underline the assumption that their contribution to the rotation of the globe is of minor importance.

One hypothesis is that the global MIF in the EOM are a giant fusiform fibre and, together with the palisade endings, form an enormous inverted muscle spindle (Robinson, personal

communications). This structure may now act as a proprioceptive apparatus which sends sensory information used for fine alignment of the eye to the brain. Looking at the literature, there are lots of contradictory reports on the issue of extraocular proprioception. First: no stretch reflex could be recorded if the eye was pulled (Keller and Robinson, 1971); second: cutting the ophthalmic nerves in monkey to sensory denervate the EOM hardly affected saccades (Guthrie et al., 1983), smooth pursuit, vestibular responses, conjugacy, adaptation and ocular alignment (Lewis et al., 2001); third: the presence of eye muscle proprioceptors varies between species, and, while in rats proprioceptors appear not to be present at all (Ruskell, 1999; Donaldson, 2000), proprioception was regarded to be absent in the extraocular eye muscles.

On the other hand, there is much more evidence supporting EOM proprioception. For example, spatial localisation in humans can be altered by either pulling eye muscles (Lewis and Zee, 1993) or by strabismus surgery (Steinbach and Smith, 1981). Stretching eye muscles in animals evokes responses in the superior colliculus (Donaldson and Long, 1980), the cerebellum and the visual cortex (Donaldson, 2000). Anatomical tracing studies have demonstrated projections through the trigeminal ganglion, and the spinal trigeminal nucleus (Porter, 1986; Ogasawara et al., 1987; Buisseret-Delmas and Buisseret, 1990; Buisseret, 1995). Physiological evidence has been presented for the existence of proprioceptive signals in many areas of the central nervous system, including the superior colliculus, the lateral geniculate body, the vestibular nuclei, prepositus hypoglossi nucleus, the cerebellum as well as areas of the cerebral cortex (Ruskell, 1999; Donaldson, 2000). Cutting the ophthalmic nerve (deafferentation) causes fixation instability in cat (Maffei and Fiorentini, 1976), reduction in stereoacuity in cat (Fiorentini and Maffei, 1977) and deviation of eye position in lambs (Pettorossi et al., 1995). Ultimately and significantly, the eye muscles in all mammal species examined so far including the rat (Eberhorn et al., 2005) indeed contain proprioceptive end-organs: if not muscle spindles or Golgi tendon organs, then palisade

endings. Of these three receptors, only the palisade endings seem to be present in all mammal species (Büttner-Ennever et al., 2003; Eberhorn et al., 2005) and, together with their opportune position at the distal tip of the global layer MIF, are the best candidate to monitor EOM activity.

With the assumption that eye movements in fact underlie proprioceptive control (and that palisade endings subserve a sensory function), a hypothetical sensory feedback pathway could be described, which designates the global MIF motoneurons to act like gamma motoneurons and adjust the tension on the palisade endings to modulate the afferent proprioceptive signal used for fine alignment of the eye (see figure 5). This proprioceptive signal is possibly provided to the spinal trigeminal nucleus (SpV), though this pathway has not yet been satisfactorily demonstrated. From SpV, a sensory signal is sent to the superior colliculus (SC), which may come from EOM proprioceptors (Porter, 1986). The inputs on the global MIF motoneurons originate from premotor areas associated with vergence, gaze holding, and in addition from the central mesencephalic reticular formation (cMRF). The cMRF, which has already been suggested as a structure carrying sensory information to the oculomotor system (Moschovakis et al., 1996), is powerfully interconnected with the SC (Chen and May, 2000). The SC, or at least its rostral part, was proposed to carry a positional error network, which rather provides a position signal than a motor signal (Krauzlis et al., 2000; Basso et al., 2000). Assuming that the global MIF motoneuron premotor inputs interact in the SC would make the SC an interface which may be influenced by descending afferents from higher brain centres and may further modulate the alignment signal (positional error) at this level.

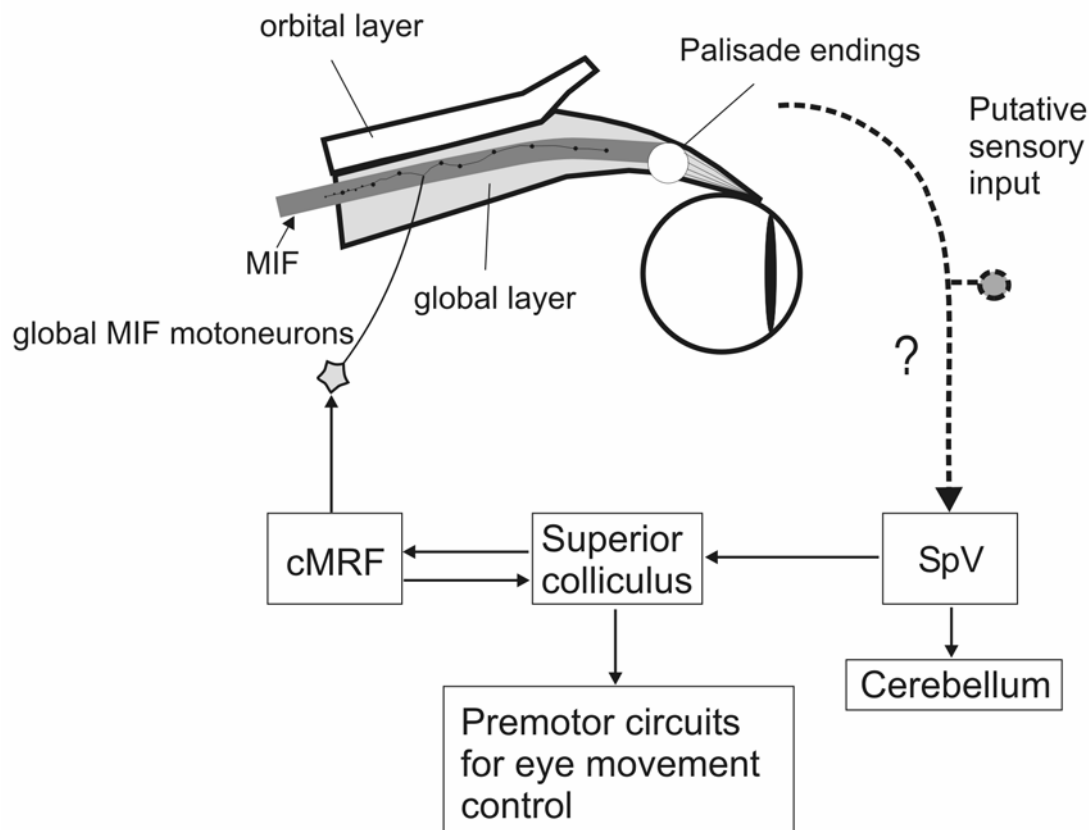


Figure 5: Sensory feedback hypothesis. The palisade endings monitor globe movements and could provide a putative proprioceptive signal to the, perhaps to the spinal trigeminal nucleus (SpV). The SpV sends a sensory signal to the superior colliculus which itself is tightly interconnected with the cMRF (central mesencephalic reticular formation). This structure could now provide a sensory signal to the MIF motoneurons innervating the global MIF. If the superior colliculus acts as an interface between sensory and motor signals, it could relay SpV signals concerning extraocular muscle tension back to the global MIF motoneurons via the cMRF.

Summarized, the results of this PhD project strongly support the hypothesis of a dual motor innervation of eye muscles and present some good evidence that this concept is a common feature at least of all mammals. The debate about the presence or absence of proprioceptive control of eye movement gains some ground on the pro-side, since the previously reported lack of an ubiquitous proprioceptor is now compounded by finding that palisade endings are present in all mammalian eye muscles so far investigated. On the other hand, there are still many open questions. Beginning with palisade endings, their proprioceptive function will still remain on debate since the cell bodies innervating these structures are not yet identified. In

addition, in some species the palisade endings show morphologic and molecular characteristics of motor terminals, which contradicts their role in proprioception. Some preliminary data in our lab additionally support the sensory character of palisade endings in rat, since no such structure was labelled after anterograde tracing from the oculomotor nucleus. Since the rat shows a similar organization of MIF and SIF motoneurons in its oculomotor nuclei compared to the monkey, a study of the differences in premotor inputs on both motoneuron types in rats could help to understand their basic functional significance.

## **Final considerations**

The identification of an extraocular motoneuron as SIF or MIF motoneuron solely on the basis of immunohistochemical differences gives now the opportunity to analyse their localization in other animals, including humans. The detailed localization of both motoneuron types within the oculomotor nuclei together with their easy identification may now help to correlate better the electrophysiological data with the type of motoneuron recorded from and therefore gather more information on the firing characteristics of MIF motoneurons. After single cell recordings, the motoneuron can be dye labelled and subsequently immunostained for ChAT and NF-NPs and thus be identified as MIF or SIF motoneuron. With the knowledge of the overall distribution of both motoneuron types, extracellular recordings can now be placed at positions where only SIF or MIF motoneurons are prevailing.

The search for palisade endings in rat with SNAP-25 antibodies revealed that this protein is an excellent marker for the visualization of nerve tissue. It enabled us to show the complete innervation of the EOM, motor, sensory, and autonomic, with only one single antibody. The staining results were outstanding in a variety of animal species (man, monkey, rat, sheep) and tissue (eye muscle, limb muscle, muscles of the middle ear), and in a wide range of used fixatives, even in fresh unfixated tissue. Thus SNAP-25 immunolabelling may be a powerful tool to analyse possible functional changes in the innervation of EOM caused by oculomotor diseases or surgery (including experimental surgeries) in the oculomotor system.

## Literature cited

Abuel-Atta AA, De Santis M, and Wong A. 1997. Encapsulated sensory receptors within intraorbital skeletal muscles of a camel. *Anat Rec* 242:189-198.

Akagi Y. 1978. The localization of the motor neurons innervating the extraocular muscles in the oculomotor nuclei of the cat and rabbit, using horseradish peroxidase. *J Comp Neurol* 181:745-761.

Alvarado-Mallart RM and Pincon Raymond M. 1979. The palisade endings of cat extraocular muscles: a light and electron microscope study. *Tissue Cell* 11:567-584.

Basso MA, Krauzlis RJ, and Wurtz RH. 2000. Activation and inactivation of rostral superior colliculus neurons during smooth-pursuit eye movements in monkeys. *J Neurophysiol* 84:892-908.

Billig I, Buisseret -Delmas C, and Buisseret P. 1997. Identification of nerve endings in cat extraocular muscles. *Anat Rec* 248:566-575.

Blümcke I and Celio MR. 1992. Parvalbumin and calbindin D-28k immunoreactivities coexist within cytochrome oxidase-rich compartments of squirrel monkey area 18. *Exp Brain Res* 92:39-45.

Blumer R, Konakci KZ, Brugger PC, Blumer MJF, Moser D, Schoefer C, Lukas J-R, and Streicher J. 2003. Muscle spindles and Golgi tendon organs in bovine calf extraocular muscle studied by means of double-fluorescent labeling, electron microscopy, and three-dimensional reconstruction. *Exp Eye Res* 77:447-462.

Blumer R, Lukas JR, Wasicky R, and Mayr R. 1998. Presence and structure of innervated myotendinous cylinders in sheep extraocular muscle. *Neurosci Lett* 248:49-52.

Blumer R, Lukas JR, Wasicky R, and Mayr R. 2000. Presence and morphological variability of golgi tendon organs in the distal portion of sheep extraocular muscle. *Anat rec* 258:359-368.

Blumer R, Wasicky R, Hötzenecker W, and Lukas JR. 2001. Presence and structure of innervated myotendinous cylinders in rabbit extraocular muscle. *Exp Eye Res* 73:787-796.

Briggs MM and Schachat F. 2002. The superfast extraocular myosin (MYH13) is localized to the innervation zone in both the global and orbital layers of rabbit extraocular muscle. *The Journal of Experimental Biology* 205:3133-3142.

Brooke MH, Kaiser KK. 1970 Muscle fiber types: how many and what kind? *Arch Neurol.* 23:369-79

Brückner G, Brauer K, Härtig W, Wolff JR, Rickmann MJ, Derouiche A, Delpech B, Girard D, Oertel WH, and Reichenbach A. 1993. Perineuronal nets provide a polyanionic, glia-associated form of microenvironment around certain neurons in many parts of the rat brain. *Glia* 8:3183-3200.

Bruenech JR and Ruskell GL. 2001. Muscle spindles in extraocular muscles of human infants. *Cell Tissue Res* 169:388-394.

Buisseret -Delmas C and Buisseret P. 1990.entral projections of extraocular muscle afferents in the cat. *Neurosci Let* 109:48-53.

Buisseret P. 1995. Influence of extraocular muscle proprioception on vision. *Physiological Rev* 75:323-338.

Büttner U and Büttner-Ennever JA. 1988. Present concepts of oculomotor organization. In Büttner-Ennever JA, editor. *Neuroanatomy of the oculomotor system*. Amsterdam, New York, Oxford: Elsevier. p 3-32.

Büttner U, Helmchen C, and Büttner-Ennever JA. 1995. The localizing value of nystagmus in brainstem disorders. *Neuro-Ophthalm* 15:283-290.

Büttner-Ennever JA. 1992. Paramedian tract cell groups: A review of connectivity and oculomotor function. In Shimazu H and Shinoda Y, editors. *Vestibular and brain stem control of eye, head and body movements*. Tokyo, Basel: Japan Scientific Societies Press, Karger. p 323-330.

Büttner-Ennever JA and Akert K. 1981. Medial rectus subgroups of the oculomotor nucleus and their abducens internuclear input in the monkey. *J Comp Neurol* 197:17-27.

Büttner-Ennever JA, Eberhorn AC, and Horn AKE. 2003. Motor and sensory innervation of extraocular eye muscles. *Ann N Y Acad Sci*.

Büttner-Ennever JA, Horn AKE, Graf W, and Ugolini G. 2002. Modern concepts of brainstem anatomy. *Ann N Y Acad Sci* 956:75-84.

Büttner-Ennever JA, Horn AKE, Scherberger H, and D'Ascanio P. 2001. Motoneurons of twitch and nontwitch extraocular muscle fibers in the abducens, trochlear, and oculomotor nuclei of monkeys. *J Comp Neurol* 438:318-335.

Büttner-Ennever JA, Horn AKE, and Schmidtke K. 1989. Cell groups of the medial longitudinal fasciculus and paramedian tracts. *Rev Neurol (Paris)* 145:533-539.

Burke RE. 1981 Motor units: anatomy, physiology, and functional organization. In: VB Brooks (Ed.), *Handbook of Physiology, Section 1: The Nervous System Volume II. Motor Control, Part 1*, American Physiological Society, Bethesda: 345-422

Carry MR, O'Keefe K, and Ringel SP. 1982. Histochemistry of mouse extraocular muscle. *Anat Embryol* 164:403-412.

Chen B and May PJ. 2000. The feedback circuit connecting the superior colliculus and central mesencephalic reticular formation: a direct morphological demonstration. *Exp Brain Res* 131:10-21.

Cheng G and Porter JD. 2002. Transcriptional profile of rat extraocular muscle by serial analysis of gene expression. *Invest Ophthalmol Vis Sci* 43:1048-1058.

Chiarandini DJ and Jacoby J. 1987. Dependence of tonic tension on extracellular calcium in rat extraocular muscle. *Amer J Physiol* 253:C375-C383.

Cilimbaris PA. 1910a. Histologische Untersuchungen über die Muskelspindeln der Augenmuskeln. In Hertwig O and Waldeyer W, editors. Berlin: p 692-747.

- Cilimbaris PA. 1910b. Histologische Untersuchungen über die Muskelspindeln der Augenmuskeln. *Archiv für mikroskopische Anatomie und Entwicklungsgeschichte* 75:692-747.
- Cohen B. 1974. The vestibulo-ocular reflex arc. In Kornhuber HH, editor. *Handbook of Sensory Physiology*. New York: Springer. p 477-540.
- Collins CC. 1975 The human oculomotor control system, in Lennerstrand G, Bach-y-Rita P (Eds.): *Basic Mechanisms of Ocular Motility and their Clinical Implications*. New York, Pergamon Press: 145-180
- Daunicht WJ. 1983. Proprioception in extraocular muscles of the rat. *Brain Res* 278:291-294.
- Daunicht WJ, Jaworski E, and Eckmiller R. 1985. Afferent innervation of extraocular muscles in the rat studied by retrograde and anterograde horseradish peroxidase transport. *Neurosci Lett* 56:143-148.
- Dean P. 1996. Motor unit recruitment in a distribution model of extraocular muscle. *J Neurophysiol* 76:727-742.
- Delgado-Garcia JM. 2000. Why move the eyes if we can move the head? *Brain Res Bull* 52:475-482.
- Demer JL. 2002. The orbital pulley system: A revolution in concepts of orbital anatomy. *Ann N Y Acad Sci* 956:17-32.
- Demer JL, Miller JM, Poukens V, Vinters HV, Glasgow BJ. 1995 Evidence for fibromuscular pulleys of the recti extraocular muscles. *Invest Ophthalmol Vis Sci*. 36:1125-36.
- Demer JL, Poukens V, Miller JM, Micevych P. 1997 Innervation of extraocular pulley smooth muscle in monkeys and humans. *Invest Ophthalmol Vis Sci*. 38:1774-85
- Demer JL, Yeul Oh S, and Poukens V. 2000. Evidence for active control of rectus extrocular muscle pulleys. *Invest Ophthal Vis Sci* 41:1280-1290.
- Dieringer N and Precht W. 1986. Functional organization of eye velocity and eye position signals in abducens motoneurons of the frog. *J Comp Physiol* 158:179-194
- Dimitrova DM, Shall MS, Goldberg SJ. 2003 Stimulation-evoked eye movements with and without the lateral rectus muscle pulley. *J Neurophysiol*. 90:3809-15
- Dogiel AS. 1906. Die Endigungen der sensiblen Nerven in den Augenmuskeln und deren Sehnen beim Menschen und den Säugetieren. *Archiv für mikroskopische Anatomie* 68:501-526.
- Donaldson IML. 2000. The functions of the proprioceptors of the eye muscles. *Philos Trans R Soc Lond [Biol]* 355:1685-1754.
- Donaldson IML and Long AC. 1980. Interactions between extraocular proprioceptive and visual signals in the superior colliculus of the cat. *J Physiol* 298:85-110.

- Eberhorn AC, Horn AKE, Eberhorn N, Fischer P, Boergen K-P, and Büttner-Ennever JA. 2005. Palisade endings in extraocular eye muscles revealed by SNAP-25 immunoreactivity. *J Anat* 205:307-315.
- Evinger C. 1988. Extraocular motor nuclei: location, morphology and afferents. In Büttner-Ennever JA, editor. *Neuroanatomy of the oculomotor system*. Amsterdam; New York; Oxford: Elsevier. p 81-117.
- Evinger C, Graf WM, and Baker R. 1987. Extra- and intracellular HRP analysis of the organization of extraocular motoneurons and internuclear neurons in the guinea pig and rabbit. *J Comp Neurol* 262:429-445.
- Ezure K and Graf WM. 1984. A quantitative analysis of the spatial organization of the vestibulo-ocular reflexes in lateral- and frontal-eyed animals. I. Orientation of semicircular canals and extraocular muscles. *Neurosci* 12:85-93.
- Fernand VSV and Hess A. 1969. The occurrence, structure and innervation of slow and twitch muscle fibres in the tensor tympani and stapedius of the cat. *J Physiol* 200:547-554.
- Fink WH. 1953. The development of the extrinsic muscles of the eye. *Am J Ophthalmol* 36:10-23.
- Fiorentini A and Maffei L. 1977. Instability of the eye in the dark and proprioception. *Nature* 269:330-331.
- Fischer MD, Corospe JR, Felder E, Bogdanovich S, Pedrosa-Domellöf F, Ahima RS, Rubinstein NA, Hoffman RP, and Khurana TS. 2002. Expression profiling reveals metabolic and structural components of extraocular muscles. *Physiol Genom* 9:71-84.
- Fuchs AF, Kaneko CR, and Scudder CA. 1985. Brainstem control of saccadic eye movements. *Annu Rev Neurosci* 8:307-337.
- Fuchs AF and Luschei ES. 1971. Development of isometric tension in simian extraocular muscle. *J Physiol* 219:155-166.
- Fuchs AF, Scudder CA, and Kaneko CR. 1988. Discharge patterns and recruitment order of identified motoneurons and internuclear neurons in the monkey abducens nucleus. *J Neurophysiol* 60:1874-1895.
- Fuller JH. 1985. Eye and head movements in the pigmented rat. *Vision Res.* 25:1121-1128
- Gacek RR. 1974. Localization of neurons supplying the extraocular muscles in the kitten using horseradish peroxidase. *Exp Neurol* 44:381-403.
- Gentle A and Ruskell GL. 1997. Pathway of the primary afferent nerve fibres serving proprioception in monkey extraocular muscles. *Ophthalm Physiol Opt* 17:225-231.
- Glicksman MA. 1980. Localization of motoneurons controlling the extraocular muscles of the rat. *Brain Res* 188:53-62.
- Gomez-Segade LA and Labandeira-Garcia JL. 1983. Location and quantitative analysis of the motoneurons innervating the extraocular muscles of the guinea-pig, using horseradish

peroxidase (HRP) and double or triple labelling with fluorescent substances. *J Hirnforsch* 24:613-626.

Grossman GE, Leigh RJ, Abel LA, Lanska DJ, Thurston SE. 1988 Frequency and velocity of rotational head perturbations during locomotion. *Exp Brain Res*.70:470-6

Guthrie BL, Porter JD, and Sparks DL. 1983. Corollary discharge provides accurate eye position information to the oculomotor system. *Science* 221:1193-1195.

Hanson J, Lennerstrand G, and Nichols KC. 1980. The postnatal development of the inferior oblique muscle of the cat. III. Fiber sizes and histochemical properties. *Acta Physiol Scand* 108:61-71.

Harker DW. 1972a. The structure and innervation of sheep superior rectus and levator palpebrae extraocular eye muscles. II: Muscle spindles. *Invest Ophthalmol Vis Sci* 11:970-979.

Harker DW. 1972b. The structure and innervation of sheep superior rectus and levator palpebrae extraocular muscles. *Invest Ophthalmol* 11:970-979.

Hensen V, Völckers C. 1878 Über den Ursprung der Accomodationsnerven. *V. Graefe's Arch. F. Ophthalmol.* 24:1-26

Highstein, SM. 1977. Abducens and oculomotor internuclear neurons: relation to gaze. In: R. Baker and A. Berthoz (Eds.), *Control of Gaze by Brainstem Neurons*, Elsevier/North Holland, New York:153-162

Horn AKE, Helmchen C, and Wahle P. 2003. GABAergic neurons in the rostral mesencephalon of the Macaque monkey that control vertical eye movements. *Ann N Y Acad Sci* 1:1-10.

Isomura G. 1981. Comparative anatomy of the extrinsic ocular muscles in vertebrates. *Anat Anz* 150:498-515.

Jacoby J, Chiarandini DJ, and Stefani E. 1989. Electrical properties and innervation of fibers in the orbital layer of rat extraocular muscles. *J Neurophysiol* 61:116-125.

Jacoby J, Ko K, Weiss C, and Rushbrook JI. 1990. Systematic variation in myosin expression along extraocular muscle fibres of the adult rat. *J Muscle Res Cell Motil* 11:25-40.

Jampel RS. 1967 Multiple motor systems in the extraocular muscles of man. *Invest Ophthalmol.* 6:288-93

Kato T. 1938. Über histologische Untersuchungen der Augenmuskeln von Menschen und Säugetieren. *Okajimas Folia Anat Jap* 16:131-145.

Keller EL and Robinson DA. 1971. Absence of a stretch reflex in extraocular muscles of the monkey. *J Neurophysiol* 34:908-919.

Keller EL and Robinson DA. 1972. Abducens unit behavior in the monkey during vergence movements. *Vision Res* 12:369-382.

Khanna S, Cheng G, Gong B, Mustari MJ, and Porter JD. 2004. Genome-wide transcriptional profiles are consistent with functional specialization of the extraocular muscle layers. *Invest Ophthalmol* 45:3055-3066.

Khanna S, Merriam AP, Gong B, Leahy P, Porter JD. 2003 Comprehensive expression profiling by muscle tissue class and identification of the molecular niche of extraocular muscle. *FASEB J*. 17:1370-2

Khanna S and Porter JD. 2001. Evidence for rectus extraocular muscle pulleys in rodents. *Invest Ophthalmol Vis Sci* 42:1986-1992.

Khanna S, Richmonds CR, Kaminski H, and Porter JD. 2003. Molecular organization of the extraocular muscle neuromuscular junction: partial conservation of and divergence from the skeletal muscle prototype. *Invest Ophthalmol Vis Sci* 44:1918-1926.

Konakci KZ, Streicher J, Hoetzenecker W, Blumer MJ, Lukas JR, Blumer R. 2005 Molecular characteristics suggest an effector function of palisade endings in extraocular muscles. *Invest Ophthalmol Vis Sci*. 46:155-65

Krauzlis RJ, Basso MA, and Wurtz RH. 2000. Discharge properties of neurons in the rostral superior colliculus of the monkey during smooth-pursuit eye movements. *J Neurophysiol* 84:876-891.

Labandeira-Garcia JL, Gomez-Segade LA, and Nunez JMS. 1983. Localisation of motoneurons supplying the extra-ocular muscles of the rat using horseradish peroxidase and fluorescent double labelling. *J Anat* 137:247-261.

Langer TP, Fuchs AF, Scudder CA, and Chubb MC. 1985. Afferents to the flocculus of the cerebellum in the rhesus macaque as revealed by retrograde transport of horseradish peroxidase. *J Comp Neurol* 235:1-25.

Langer T, Kaneko CRS, Scudder CA, and Fuchs AF. 1986. Afferents to the abducens nucleus in the monkey and cat. *J Comp Neurol* 245:379-400.

Leigh RJ and Zee DS. 1991. *The neurology of eye movements*. Philadelphia: F.A.Davis Company.

Leigh RJ and Zee DS. 1999. *The neurology of eye movements*. New York; Oxford: Oxford University press.

Lewis RF, Zee D, Hayman MR, and Tamargo RJ. 2001. Oculomotor function in the rhesus monkey after deafferentation of the extraocular muscles. *Exp Brain Res* 141:349-358.

Lewis RF and Zee DS. 1993. Abnormal spatial localization with trigeminal-oculomotor synkinesis. *Brain* 116:1105-1118.

Ling L, Fuchs AF, Phillips JO, and Freedman EG. 1999. Apparent dissociation between saccadic eye movements and the firing patterns of premotor neurons and motoneurons. *J Neurophysiol* 82:2808-2811.

Lukas JR, Blumer R, Denk M, Baumgartner I, Neuhuber W, and Mayr R. 2000. Innervated myotendinous cylinders in human extraocular muscles. *Invest Ophthalmol Vis Sci* 41:2422-2431.

- Maffei L and Fiorentini A. 1976. Asymmetry of motility of the eyes and change of binocular properties of cortical cells in adults cats. *Brain Res* 105:73-78.
- Maier A, DeSantis M, and Eldred. 1974. The occurrence of muscle spindles in extraocular muscles of various vertebrates. *J Morph* 143:397-408.
- Mayr R, Gottschall J, Gruber H, and Neuhuber W. 1975. Internal structure of cat extraocular muscle. *Anat Embryol* 148:25-34.
- McCrea RA, Strassman A, and Highstein SM. 1986. Morphology and physiology of abducens motoneurons and internuclear neurons intracellularly injected with horseradish peroxidase in alert squirrel monkey. *The Journal of Comparative Neurology* 243:291-308.
- McLoon LK, Rios L, and Wirtschafter JD. Complex three-dimensional patterns of myosin isoform expression: differences between and within specific extraocular muscles. *Journal of Muscle Research and Cell Motility* 20, 771-783. 1999.
- Miles FA. 1998 The neural processing of 3-D visual information: evidence from eye movements. *Eur J Neurosci.* 10:811-22
- Miller JM. 1989. Functional anatomy of normal human rectus muscles. *Vision Res* 29:223-240.
- Miller JM, Bockisch CJ, and Pavlovski DS. 2001. Missing lateral rectus force and absence of medial rectus co-contraction in ocular convergence. *J Neurophysiol* 87, 2421-2433.
- Miller JM, Demer JL, Poukens V, Pavlovski DS, Nguyen HN, and Rossi EA. 2003. Extraocular connective tissue architecture. *Journal of Vision* 3:240-251.
- Miyazaki S. 1985. Bilateral innervation of the superior oblique muscle by the trochlear nucleus. *Brain Res* 348:52-56.
- Moore GE, Schachat FH. 1985 Molecular heterogeneity of histochemical fibre types: a comparison of fast fibres. *J Muscle Res Cell Motil.* 6:513-24
- Morgan DL and Proske U. 1984. Vertebrate slow muscle: its structure, pattern of innervation, and mechanical properties. *Physiol Rev* 64:103-138.
- Moschovakis AK, Scudder CA, and Highstein SM. 1996. The microscopic anatomy and physiology of the mammalian saccadic system. *Prog Neurobiol* 50:133.
- Murphy EH, Garone M, Tashayyod D, and Baker RB. 1986. Innervation of extraocular muscles in the rabbit. *J Comp Neurol* 254:78-90.
- Naito H, Tanimura K, Taga N, and Hosoya Y. 1974. Microelectrode study on the subnuclei of the oculomotor nucleus in the cat. *Brain Res* 81:215-231.
- Namba T, Nakamura T, and Grob D. 1968a. Motor nerve endings in human extraocular muscle. *Neurology* 18:403-407
- Nelson JS, Goldberg SJ, and McClung JR. 1986. Motoneuron electrophysiological and muscle contractile properties of superior oblique motor units in cat. *J Neurophysiol* 55:715-726.

- Oda K. 1986. Motor innervation and acetylcholine receptor distribution of human extraocular muscle fibres. *J Neurol Sci* 74:125-133.
- Ogasawara K, Onodera S, Shiwa T, Ninomiya S, and Tazawa Y. 1987. Projections of extraocular muscle primary afferent neurons to the trigeminal sensory complex in the cat as studied with the transganglionic transport of horseradish peroxidase. *Neurosci Lett* 73:242-246.
- Ogata T. 1988. Structure of motor endplates in the different fiber types of vertebrate skeletal muscles. *Arch Histol Cytol* 51:385-424.
- Oh SY, Poukens V, and Demer JL. 2001. Quantitative analysis of rectus extraocular layers in monkey and humans. *Invest Ophthalmol Vis Sci* 42:10-16.
- Pachter BR. 1983. Rat extraocular muscle. 1. Three dimensional cytoarchitecture, component fibre populations and innervation. *J Anat* 137:143-159.
- Pachter BR. 1984. Rat extraocular muscle. 3. Histochemical variability along the length of multiply-innervated fibers of the orbital surface layer. *Histochem* 80:535-538.
- Pachter BR and Colbjornsen C. 1983. Rat extraocular muscle. 2. Histochemical fibre types. *J Anat* 137:161-170.
- Pettorossi VE, Ferraresi A, Draicchio F, and et al. 1995. Extraocular muscle proprioception and eye position. *Acta Otolaryngol (Stockh)* 115:137-140.
- Pierobon-Bormioli SP, Sartore S, Vitadello M, and Schiaffino S. 1980 'Slow' myosins in vertebrate skeletal muscle. An immunofluorescence study. *J Cell Biol* 85:672-681
- Pierobon-Bormioli SP, Sartore S, Dalla Libera L, Vitadello M, and Schiaffino S. 1981 'Fast' isomyosins and fibre types in mammalian skeletal muscle. *J Histochem Cytochem* 29:1179-1188
- Porter JD. 1986. Brainstem terminations of extraocular muscle primary afferent neurons in the monkey. *J Comp Neurol* 247:133-143.
- Porter JD, Baker RS, Ragusa RJ, and Brueckner JK. 1995. Extraocular muscles: basic and clinical aspects of structure and function. *Surv Ophthalmol* 39:451-484.
- Porter JD, Guthrie BL, and Sparks DL. 1983. Innervation of monkey extraocular muscles: localization of sensory and motor neurons by retrograde transport of horseradish peroxidase. *J Comp Neurol* 218:208-219.
- Porter JD, Khanna S, Kaminski HJ, Rao JS, Merriam AP, Richmonds CR, Leahy P, Li J, and Andrade FH. Extraocular muscle is defined by a fundamentally distinct gene expression profile. *Proc.Natl.Acad.Sci.* 98(21), 12062-12067. 2001.
- Reichmann H and Srihari T. 1983. Enzyme activities, histochemistry and myosin light chain pattern in extraocular muscles of rabbit. *Histochemistry* 78:111-120.
- Ringel SP, Wilson WB, Barden MT, and Kaiser KK. 1978a. Histochemistry of human extraocular muscle. *Arch Ophthalmol* 96:1067-1072.

- Ringel SP, Engel WK, Bender AN, Peters ND, Yee RD. 1978b Histochemistry and acetylcholine receptor distribution in normal and denervated monkey extraocular muscles. *Neurology*. 28:55-63.
- Rubinstein NA and Hoh JF. 2001. The distribution of myosin heavy chain isoforms among rat extraocular muscle fiber types. *Invest Ophthalmol Vis Sci* 41:3391-3398.
- Ruskell GL. 1978. The fine structure of innervated myotendinous cylinders in extraocular muscles in rhesus monkey. *J Neurocytol* 7:693-708.
- Ruskell GL. 1999. Extraocular muscle proprioceptors and proprioception. *Prog Retin Eye Res* 18:269-291.
- Sanes JR, Lichtman JW. 1999 Development of the vertebrate neuromuscular junction. *Annu Rev Neurosci*. 22:389-442
- Sas J and Schab R. 1952. Die sogenannten "Palisaden-Endigungen" der Augenmuskeln. *Acta Morph Acad Sci (Hungary)* 2:259-266.
- Schiaffino S, Hanzlikova V, and Pierobon S. 1970 Relations between structure and function in rat skeletal muscle fibers. *J Cell Biol* 47:107-119
- Scott AB and Collins CC. 1973. Division of labor in human extraocular muscle. *Arch Ophthalmol* 90:319-322.
- Sevel D. 1986. The origins and insertions of the extraocular muscles: development, histologic features, and clinical significance. *Trans Am Ophthalmol Soc* 24:488-526.
- Shall MS, Goldberg SJ. 1992. Extraocular motor units - type classification and motoneuron stimulation frequency-muscle unit force relationships. *Brain Res* 587: 291-300.
- Siebeck R, Kruger P. 1955 Die histologische Struktur der äußeren Augenmuskeln als Ausdruck ihrer Funktion. *Graefes Arch. Ophthalmol* 156:637-652
- Simpson JI and Graf WM. 1981. Eye-muscle geometry and compensatory eye movements in lateral-eyed and frontal-eyed animals. *Ann N Y Acad Sci* 374:20-30.
- Spencer RF, Baker R, and McCrea RA. 1980. Localization and morphology of cat retractor bulbi motoneurons. *J Neurophysiol* 43:754-770.
- Spencer RF and Porter JD. 1981. Innervation and structure of extraocular muscles in the monkey in comparison to those of the cat. *J Comp Neurol* 198:649-665.
- Spencer RF and Porter JD. 1988. Structural organization of the extraocular muscles. In Büttner-Ennever JA, editor. *Neuroanatomy of the oculomotor system*. Amsterdam; New York; Oxford; Elsevier. p 33-79.
- Steinbach M and Smith D. 1981. Spatial localization after strabismus surgery: evidence for inflow. *Science* 213:1407-1409.
- Tozer FM and Sherrington CS. 1970. Receptors and afferents of the third, fourth and sixth cranial nerves. *Proc R Soc London Ser* 82:451-457.

Warwick R. 1953. Representation of the extraocular muscles in the oculomotor nuclei of the monkey. *J Comp Neurol* 98:449-495.

Wasicky R, Horn AKE, and Büttner-Ennever JA. 2004. Twitch and non-twitch motoneuron subgroups of the medial rectus muscle in the oculomotor nucleus of monkeys receive different afferent projections. *J Comp Neurol* 479:117-129.

Wasicky R, Zhya-Ghazvini F, Blumer R, Lukas JR, and Mayr R. 2000. Muscle fiber types of human extraocular muscles: a histochemical and immunohistochemical study. *Invest Ophthalmol Vis Sci* 41:980-990.

Weir CR, Knox PC, and Dutton GN. 2000. Does extraocular muscle proprioception influence oculomotor control? *Br J Ophthalmol* 84:1071-1074.

Wieczorek DF, Periasamy M, Butler Browne GS, Whalen RG, and Nadal Ginard B. 1985. Co-expression of multiple myosin heavy chain genes, in addition to a tissue-specific one, in extraocular musculature. *J Cell Biol* 101:618-629.

## **Acknowledgements**

I would like to thank Prof. Jean Büttner-Ennever for giving me the opportunity to perform my PhD thesis in her laboratory, and for always being supportive in all kinds of scientific, academic and non-academic concerns. Likewise, I am especially grateful to my supervisor PD Dr. Anja Horn-Bochtler for all her scientific advice and support, for always having a 'free minute' for me, for her patience and for her overall friendship. Moreover, I am thankful to Ahmed Messoudi for his scientific and technical support and for his friendship. Being a member of this group was at all times enjoyable.

I am very thankful to Prof. Ulrich Büttner, who enrolled me in the graduate program "Gradiertenkolleg GRK 267". Special thanks go to Dr. Isolde von Bülow for supporting me throughout my time as a PhD student.

Many thanks to PD Dr. Mark Hübener and Dr. Albrecht Kossel for their scientific support as members of my thesis committee.

I am very thankful to my wife Nicola Eberhorn not only for her excellent work with the confocal microscope for the collaboration for the SNAP-25 paper but also for her patience, love and understanding.

Thanks to Ulrich Nuding for his helpful comments in image analysis and for the scientific beer at the right moment.

Thanks to my coworkers on some parts of my publications Patricia Ardeleanu, Dr. Petra Fischer and Prof. Klaus-Peter Boergen.

Last, but not least, thanks to my parents and my family.

This work was financially supported by the DFG Forschungsgemeinschaft

## Curriculum Vitae

### Anschrift

beruflich:  
Anatomisches Institut Lehrstuhl III  
Ludwig Maximilians Universität  
Pettenkoferstrasse 11  
80336 München  
Tel: +49-89-51604880  
Email: andreas.eberhorn@med.uni-muenchen.de

privat:  
Kurfürstenstrasse 21  
80801 München  
Deutschland  
Tel: +49-89-27774898

### Geburtsdatum und -ort

17.03.1975, in Garmisch-Partenkirchen

### Familienstand

Verheiratet mit Nicola, geborene Tobisch  
1 Sohn: Luis Jacob Eberhorn, geb. 08.02.2005

### Akademische Ausbildung

- 01/2002-heute      Biologische Doktorarbeit am Anatomischen Institut, LMU-München  
(Arbeitsgruppenleiter: Prof. J.A. Büttner-Ennever, Betreuer: Dr. habil.  
Anja Horn-Bochtler); Stipendiat im Graduiertenkolleg GRK 267  
„Sensorische Interaktion in biologischen und technischen System“
- 01/2000-10/2000      Diplomarbeit/Zulassungsarbeit am Anatomischen Institut, LMU-  
München  
(Arbeitsgruppenleiter: Prof. Jean Büttner-Ennever, Betreuer: Dr. habil.  
Anja Horn-Bochtler)
- 10/1995-11/2001      Studium Lehramt für Biologie und Chemie Gymnasium, LMU-  
München; erweitertes Studium in Biologie, Hauptfach Neurobiologie
- 09/1985-07/1994      Werdenfels-Gymnasium, Garmisch-Partenkirchen

### Abschlüsse

- 11/2001      Staatsexamen in Biologie und Chemie, LMU-München
- 07/1994      Abitur, Werdenfels-Gymnasium, Garmisch-Partenkirchen

### Lehrerfahrung

- 02/2005      Betreuung des Großpraktikums „Funktionelle Anatomie des  
Säugergehirns“
- 03/2004-heute      Vorträge zu neurobiologischen und philosophischen Themen an den  
Volkshochschulen München und Gilching
- 05/2004      Lehrauftrag „Hirnmorphologisches Seminar“ am Anatomischen Institut,  
LMU-München
- 03/2004      Betreuung des Großpraktikums „Funktionelle Anatomie des  
Säugergehirns“
- 06/2002      Lehrauftrag: „Seminar Anatomie“ am Anatomischen Institut, LMU-  
München

- 01/2002 Betreuung des Großpraktikums: „Funktionelle Anatomie der Augenbewegungen beim Säuger“
- 01/2002-heute Anleitung von Studenten der Biologie und Medizin zur wissenschaftlichen Arbeit

### **Weitere wissenschaftliche Erfahrungen**

- 09/2003 Versuchstierkundlicher Kurs des TIZ-Bifo München mit Zertifikat erfolgreich abgeschlossen.
- 05/2003 DFG Workshop: Funktionelle Genanalyse in komplexen neuronalen Geweben
- 06/2002 Kurs: Grundlagen der Biosignalverarbeitung mit MATLAB
- 02/2002 Kurs: Wissenschaftsjournalismus an der Akademie der Bayerischen Presse
- 07/-09/1999 Labor-Rotation, Zoologische Fakultät, Neurobiologie, LMU-München
- 09/-09/1999 Studentische Hilfskraft im Anatomischen Institut, LMU-München

### **Publikationen**

- **Eberhorn AC**, Ardeleanu P, Büttner-Ennever JA, Horn AKE: Motoneurons of multiply-innervated muscle fibres in extraocular muscles have different histochemical properties than motoneurons of singly-innervated muscle fibres. J Comp Neurol 2005(accepted)
- **Eberhorn AC**, Horn AKE, Eberhorn N, Fischer P, Boergen K-P, Büttner-Ennever JA: Palisade endings in extraocular eye muscles revealed by SNAP-25 immunoreactivity. J Anat 2005, 206:307-315
- **Eberhorn AC**, Horn AKE, Fischer P, Büttner-Ennever JA: Proprioception and Palisade endings in extraocular eye muscles. Ann N Y Acad Sci 2005 (in press)
- **Eberhorn AC**, Horn AK, Messoudi A, Büttner-Ennever JA: Twitch and Non-Twitch Motoneurons of Extraocular Muscles Have Different Histochemical Properties. Ann N Y Acad Sci. 2003 Oct;1004:414-417
- Büttner-Ennever JA, **Eberhorn AC**, Horn AK: Motor and sensory innervation of extraocular eye muscles. Ann N Y Acad Sci. 2003 Oct;1004:40-9

## **Ehrenwörtliche Versicherung:**

Ich versichere hiermit ehrenwörtlich, dass meine Dissertation mit dem Titel  
„An investigation of the sensory and motor innervation of extraocular muscles in monkey and  
rat with combined tract-tracing and immunofluorescence methods: evidence for a dual motor  
innervation as common concept in mammals.“  
von mir selbständig, ohne unerlaubte Beihilfe angefertigt ist. Wörtlich oder inhaltlich  
übernommene Stellen sind als solche gekennzeichnet.

München, den 17.03.2005



Andreas Eberhorn